Composite Laminates Made by Automated Fiber Placement of Dry Fibers and Vacuum Assisted Resin Transfer Molding

NORVAN GHARABEGI

A thesis

in

The Department

of

Mechanical, Industrial & Aerospace Engineering

Presented in Partial fulfillment of the requirements

for the Degree of Master of Applied Science

(Mechanical Engineering)

Concordia University

Montreal, Quebec, Canada

March 2018

CONCORDIA UNIVERSITY

School of Graduate Studies

This is to certify that the thesis prepared

By: Norvan Gharabegi

Entitled: Composite Laminates Made by Automated Fiber Placement of Dry Fibers and Vacuum Assisted Resin Transfer Molding

and submitted in partial fulfillment of the requirements for the degree of

Master of Applied Science

Complies with the regulations of this University and meets the accepted standards with respect to originality and quality.

Signed by the final examining committee:

_____ Examiner, External

Dr. Catharine Marsden

_____ Examiner

Dr. Martin Pugh

_____ Co-Supervisor

Dr. Suong V. Hoa

_____ Co-Supervisor

Dr. Mehdi Hojjati

Approved by:

_____

Dr. Sivakumar Narayanswamy, MASc Program Director

Department of Mechanical, Industrial & Aerospace Engineering

_____

Dr. Amir Asif, Dean

Faculty of Engineering and Computer Science

Date: _____

Abstract

Composite Laminates Made by Automated Fiber Placement of Dry Fibers and Vacuum Assisted Resin Transfer Molding

Norvan Gharabegi

Automation in production is crucial to increase productivity, reduce costs, reduce waste, and to enhance repeatability. Automation in the aerospace industry is being adopted by large original equipment manufacturers in order to meet increasing demands with the use of Automated Fiber Placement (AFP) or Automated Tape Laying (ATP) machines. These machines process conventional pre-impregnated materials which are then processed using large autoclaves. The use of AFP or ATL systems for large structures such as wing skins or fuselages have proven to be effective compared to traditional methods. Autoclave curing systems force manufacturers to invest large amounts of capital and operational costs associated to autoclaves. Out-of-autoclave (OOA) prepreg materials have been developed in order to remove the need for autoclave, however processing these types of materials require longer cure times and extensive debulking, which counters productivity. Dry fiber tapes have been developed by materials suppliers that can be processed using AFP/ATL equipment to manufacture dry preforms. These dry preforms can then be impregnated using a variety of resin transfer molding methods. This work focuses on developing a process window for dry automated fiber placement (DAFP) using an AFP machine equipped with a hot gas torch, impregnation of dry fiber preform using vacuum assisted resin transfer molding (VARTM), and evaluating the laminates quality and mechanical properties. Properties determined show to be in the realms of autoclave curing and OOA curing systems presently qualified in the aerospace industry. In addition, a cost analysis shows DAFP VARTM to be a competitive method of production comparing to current material systems.

Acknowledgements

I express my greatest gratitude to both my academic supervisors, Dr. Suong V. Hoa and Dr. Mehdi Hojjati, for their invaluable guidance and support throughout my studies, and for giving the opportunity to explore my curiosity both scientifically and professionally.

I would also like to thank the NSERC Industrial Research Chair in Automated Composites Manufacturing and its industrial partners Bombardier Aerospace and Bell Helicopter Textron Canada Ltd. for giving me the opportunity to work on a research project that is industrially relevant.

I am very grateful for the support from the CONCOM technical staff. Notably the efforts of Dr. Iosif Daniel Rosca, Mr. Heng Wang, and Mr. Jeffery Fortin-Simpson for their guidance and expertise in manufacturing and testing specimens.

A special thanks to Dr. Robert Fews, for the discussions in his office, and his invaluable mentorship and wisdom that has given me strength throughout my undergraduate and graduate studies.

I would like to thank the entire Materials & Processes team at Bell Helicopter Textron Canada for supporting my studies during the beginnings of my professional career. Thank you to Felix Bednar for planting the seed from which brought rise to the subject of this dissertation. Thank you to Pierre Doyon for support and help in the M&P Labs to manufacture and test specimens. And thank you to Pierre Beaulieu, for accepting me as his student, supporting my topic of research, and giving me the opportunity to work alongside him and the entire M&P team.

Finally, I thank my sister, mother, and father for their countless sacrifices and love throughout my life. For never stopping to push me to become a better and stronger person, for making me realise that nothing is impossible, and shaping me to the person I am today. Without my family, there would be no one to thank. My character, my thoughts, my drive, and my achievements I owe to you.

Table of Contents

List of Figures viii

List of Tables xii

Abbreviations xiii

Chapter 1 - Introduction 1

1.1. Introduction to AFP Manufacturing 2

1.1.1 Types of AFP Machines 6

1.2. Introduction of Out-of-Autoclave Systems 7

1.2.1. Out of Autoclave Prepregs 7

1.2.2. Non-Crimp Fabrics 8

1.2.3. Resin Transfer Molding 11

Chapter 2 - Literature Review 13

2.1. Mitsubishi 13

2.2. AUTOW 14

2.3. Permeability of Preforms 16

2.4. Mechanical Performance of DAFP Infused Laminates 19

2.5. Evaluation of Material Systems for DAFP 21

2.6. Potential Cost Savings using AFP 23

2.7. Motivation 25

2.8. Objectives 25

Chapter 3 - Materials and Methods 26

3.1. Material Selection 26

3.1.1. Hexcel Hi-Tape 26
3.1.2. Cytec PRISM EP2400 28
3.2. Dry Preform Manufacturing 30
3.2.1. Automated Fiber Placement Process 30
3.2.2. Building Process Window for DAFP 32
3.2.3. Dry Fiber Processing Challenges 34
3.2.4. Tailored Preform Gaps 42
3.2.5. Hot VARTM Process 43
3.3. Quality Control 49
3.3.1. Resin Viscosity 49
3.3.2. Differential Scanning Calorimetry (DSC) 52
3.3.3. Microscopic Evaluation 55
Chapter 4 - Testing, Results and Discussion 61
4.1. Evaluation of VARTM Flow Front 61
4.1.1. Conventional Preforms 62
4.1.2. Preforms with Gaps 65
4.1.3. Discussion 69
4.2. Mechanical Characterization 70
4.2.1. Tensile Testing (0°) 71
4.2.2. Tensile Testing (90°) 73
4.2.3. Short Beam Shear (0°) 75
4.2.4. Compression Testing (0°) 77
4.2.5. Open Hole Tensile Testing 80
4.2.6. Open Hole Compression Testing 82

4.2.7. Summary of Mechanical Test Results 84
4.3. Mechanical Performance Compared to Conventional Aerospace Material Systems 85
4.3.1. Selection of Carbon/Epoxy System Baselines 85
4.3.2. DAFP VARTM vs. Autoclave Prepreg 87
4.3.3. DAFP VARTM vs. OOA Prepreg 88
4.3.4. Discussion 89
Chapter 5 - Cost Analysis 91
5.1. Cost modeling 91
5.1.1. Assumptions 92
5.1.2. Overall Costs 95
5.2. Cost Comparison 97
Chapter 6 - Conclusion & Outlook 99
6.1. Conclusion 99
6.2. Outlook 101
Chapter 7 - Contributions 102
References 104

List of Figures

Figure 1.1: Publication on Automated Manufacturing using AFP and ATL from the 1970s [7]... 3

Figure 1.2: Estimated 2013-2022 Market for Aerospace Composite Structures [8] 4

Figure 1.3: Types of AFP Systems a) Vertical AFP Gantry [10] b) Robotic arm AFP with removable head [11] c) Horizontal AFP Gantry [12] d) Robotic arm AFP with removable head on rails [13] 6

Figure 1.4: Schematic of EVaC introduced into OOA prepregs [15] 8

Figure 1.5: Example of Different NCF types [18] 9

Figure 1.6: Bombardier Aerospace C Series Wing Skin made using NCF and RTM [21] 10

Figure 1.7: Schematic of the RTM Process [23] 11

Figure 1.8: Schematic of the VARTM Process [23] 12

Figure 2.1: A-VARTM used to manufacture stringer panels [25] 13

Figure 2.2: Example of Fraying and binder build-up from AUTOW 15

Figure 2.3: Manufacturing of sine-wave dry preform with AFP and VARTM infusion of preform 15

Figure 2.4: Fiber architecture of dry fiber preform (left), woven fabric (center), bi-axial NCF (left) [31] 17

Figure 2.5: Schematic illustration of the DFP process (left), fiber placement head during DFP process (right) [31] 18

Figure 2.6: Mechanical Performance of Hexcel HiTape with RTM6 Resin vs. Conventional Prepreg [31] 19

Figure 2.7: Automated Dry Fiber Placement System (a) Creel, (b) Tape Delivery System, and (c) Temperature Controlled Tape [32] 20

Figure 2.8: Skethes of Dry Fiber Materials [33] 22

Figure 2.9: Schematic of Hercules 7-axis AFP Machine [34] 23
Figure 2.10: Hand Layup versus AFP manufacturing of Aft Stiffened Skin [34] 24
Figure 3.1: Hexcel HiTape dry carbon slit tape 27
Figure 3.2: Typical Cure Cycle for EP200 Resin System 30
Figure 3.3: ADC AFP Machine with Thermoset Head at Concordia University 31
Figure 3.4: AFP processing schematic 31
Figure 3.5: Nip-point Temperature of AFP using HGT 33
Figure 3.6: Example of 6"x6" $[0]_2$ preform 35
Figure 3.7: Schematic of HGT Nozzle at Roller 35
Figure 3.8: 6" by 6" [0/0/90/45] preform manufactured using AFP 36
Figure 3.9: Example of a Roll-up defect during AFP manufacturing 37
Figure 3.10: OEM placement of air-knife 38
Figure 3.11: Example of side view of staggered preform 39
Figure 3.12: Example side view of a Taped down preform 39
Figure 3.13: Schematic showing an example of induced gap between a band of tows 42
Figure 3.14: Prepared Preform for Infusion 44
Figure 3.15: Laminate after Bagging and application of Vacuum 45
Figure 3.16: Radius Engineering External Degassing System 46
Figure 3.17: Schematic of the VARTM process 47
Figure 3.18: Example of Infusion Process completed before Ramping up to Final Cure 48
Figure 3.19: Cytec PRSIM EP2400 Viscosity versus Temperature Properties [36] 49
Figure 3.20: Brookfield Viscometer Used for Resin Viscosity Evaluation 50
Figure 3.21: Comparison of Tested Resin Viscosity and Manufacture Resin Viscosity Data 51
Figure 3.22: Example of TA Instruments DSC Q200 machine 53

Figure 3.23: Heat Cool Heat cycle of Quasi 24ply laminate 54
Figure 3.24: Specimen and Equipment used for Microscopic Analysis 56
Figure 3.25: Stitched Image from [0/90]4S sample using 5X Magnification 57
Figure 3.26: Stitched Image from [0/90]4S sample using 10X Magnification 57
Figure 3.27: Image Capture Threshold set to Zero 58
Figure 3.28: Image Capture Threshold set to 0-85, Porosity Highlighted in Red 58
Figure 3.29: Image Capture of Fibers and Resin, default Threshold 0-255 59
Figure 3.30: Image Capture of Fibers and Resin, Threshold set to 150-255 59
Figure 4.1: Cascading Effect during VARTM Infusion 62
Figure 4.2: 16ply Quasi Preform after Infusion with Flow Front Markings 63
Figure 4.3: Flow Front Distance vs. Time plot for $[45/-45/0/90]_{2S}$ preform 64
Figure 4.4: Flow Front vs. Time for all conventional preforms 65
Figure 4.5: Flow front observed of 8ply unidirectional preform with 4mm gaps 66
Figure 4.6: Flow front observed of 8ply cross-ply preform with 4mm gaps 67
Figure 4.7: Comparison of Flow Front vs. Time between Conventional and Gapped Preforms . 68
Figure 4.8: Tensile 0° Specimen 71
Figure 4.9: Example of Load vs. Displacement for Tensile 0° Specimen 72
Figure 4.10: Tensile 90° Specimen 73
Figure 4.11: Example of Stress vs. Strain Curve of Tensile 90° Sample 74
Figure 4.12: Short Beam Shear 0° Specimen 75
Figure 4.13: Example of Load vs. Displacement of ILSS 0° Specimen 76
Figure 4.14: Specimen in ASTM D6641 CLC Fixture 77
Figure 4.15: Example of Stress vs. Strain Curve of Compression $[0/90]_{4S}$ Specimen 79
Figure 4.16: Open Hole Tensile Test Specimen 80

Figure 4.17: Example of Load vs. Displacement of OHT Specimen 81

Figure 4.18: Open Hole Compression Specimen..... 82

Figure 4.19: Example of Load vs. Displacement of OHC Specimen 83

Figure 4.20: Normalized Mechanical Data Comparison of DAFP VARTM to Hexply 8552 Autoclave Prepreg..... 87

Figure 4.21: Normalized Mechanical Data Comparison of DAFP VARTM to Cytec's 5320-1 OOA Prepreg 88

Figure 4.22: Example of Waviness Observed in Dry Preform Tows 90

List of Tables

Table 1: Advantages of AFP/ATL Process over Conventional Hand Layup 5

Table 2: Mechanical Performance of HiTape infused with RTM6 and EP2400 [32] 21

Table 3: Overview of different available dry fiber materials [33] 22

Table 4: List of different fault types observed during automated fiber placement [33] 22

Table 5: Typical Properties for 6K tow of Hexcel IM7 Carbon Fiber [35] 27

Table 6: Cytec EP2400 Neat Resin Properties [36] 29

Table 7: AFP Parameter to Achieve Required Nip-Point Temperatures for DAFP Processing 34

Table 8: AFP Processing Parameters 41

Table 9: List of dry fiber preforms manufactured for VARTM infusion 41

Table 10: Test Matrix for Tailored Gapped Preforms 42

Table 11: List of Tailored Preforms Manufactured for VARTM Infusion 43

Table 12: Tg Results from DSC 55

Table 13: Results from Microscopic Evaluation of Fiber Volume Content, and Porosity 60

Table 14: Summary of Tests Performed and their Details 70

Table 15: Summary of all Mechanical Testing Data 84

Table 16: Equipment Overhead Costs 93

Table 17: Consumable Costs 93

Table 18: AFP Processing and Bagging Times 94

Table 19: Cure Cycle Times 95

Table 20: Cost Breakdown 96

Abbreviations

ADC	Automated Dynamics Corporation
AFP	Automated Fiber Placement
ASTM	American Society for Testing Materials
ATL	Automated Taple Laying
ATP	Automated Tape Placement
BF	Back-out Factor
CLC	Combined Loading Compression
COV	Coefficient of Variation
DAFP	Dry Automated Fiber Placement
DAQ	Data Acquisition
DMA	Dynamic Mechanical Analysis
DSC	Differential Scanning Calorimetry
EVaC	Engineered Vacuum Channel
FAA	Federal Aviation Administration
HGT	Hot Gas Torch
ILSS	Interlaminar Short beam Shear
MH	Man Hours
NCAMP	National Center for Advanced Materials Performance
NCF	Non-crimp Fabric
OEM	Original Equipment Manufacturer

OHC	Open Hole Compression
OHT	Open Hole Tension
OOA	Out-of-Autoclave
RTM	Resin Transfer Molding
SBS	Short Shear Beam
SLPM	Standard Liters Per Minute
TMA	Thermomechanical Analysis
VARTM	Vacuum Assisted Resin Transfer Molding
VBO	Vacuum Bag Only

Chapter 1 - Introduction

The increasing demands of composites materials for primary structural applications in the field of aerospace, automotive, nautical, and wind energy bring a rise to the need of increasing productivity, reducing costs, reducing waste, and to enhance repeatability in manufacturing [1]. Traditional methods of composite manufacturing such as wet-layup or hand layup of pre-impregnated (prepreg) carbon or glass fabrics require skilled technicians and laborious work. The nature of traditional composite manufacturing inhibits significant advancements to be made. Automated composite manufacturing methods, such as Automated Fiber Placement (AFP) or Automated Tape Laying (ATP) machines, are methods of production that can address many of the needs of industry, which was not capable with traditional methods. Conventional pre-impregnated (prepreg) systems are now offered in standardized tape sizing formats to allow for automation of the process. Notable examples of present day aerospace structures manufactured by AFP are wing skins and spars for Airbus A350 XWB [2], and Boeing 787 and 777X [3]. These examples mentioned use carbon/epoxy prepregs that are laid onto a mold using automated equipment, and then cured in large autoclaves.

Volume of composites structures is projected to increase in all realms of production; aerospace, automotive, nautical, wind energy etc. With that said, Original Equipment Manufacturers (OEM) and material suppliers are on the continuous look-out to develop new materials and methods that can meet the increase in production volumes, while reducing overall costs, retaining quality and performance comparable to prepreg systems. Such processes that have been developed are Resin Transfer Molding (RTM), Out-of-Autoclave (OOA) materials, Vacuum Assisted Resin Transfer Molding (VARTM), and Controlled Atmospheric Pressure Resin Infusion (CAPRI) [4]. These processes although very different from one another, share a similar goal, to eliminate the

requirement of autoclave curing. Autoclaves are large capital investments for manufacturers, and have significant operational associated costs [5].

A new type of material has been developed by materials suppliers, which can be paired with automated manufacturing technology. Dry fiber tapes are designed to be processed with common AFP or ATL equipment. The result is the ability to manufacture dry fiber preforms using automation. The dry fiber preforms can then be impregnated with a variety of RTM processes. These processes do not require high capital investment for an autoclave, have lower energy consumption, lower tooling costs, and lower material costs when compared to conventional prepreg systems [6]. Incorporating the benefits of automated dry fiber preform manufacturing with RTM processing, high performance materials can be created that can compete with conventional prepreg systems.

This dissertation focuses on evaluating the manufacturing feasibility and mechanical performance of Dry Automated Fiber Placement (DAFP) and VARTM infused laminates, and compares them to current autoclave curing and OOA curing prepreg systems used in aerospace.

1.1. Introduction to AFP Manufacturing

In many industries, production automation plays a crucial role of meeting increasing demands, quality, repeatability and reduction of costs. Composite manufacturing, although still labour intensive to this day, is implementing higher levels of automation. It has been shown that interest and research in automated composite manufacturing dates from the 1960s, beginning with automated filament winding systems, and AFP/ATL systems from the 1970s [7]. Figure 1.1 shows an overview of the amount of archived publications on automated composite manufacturing throughout the years.

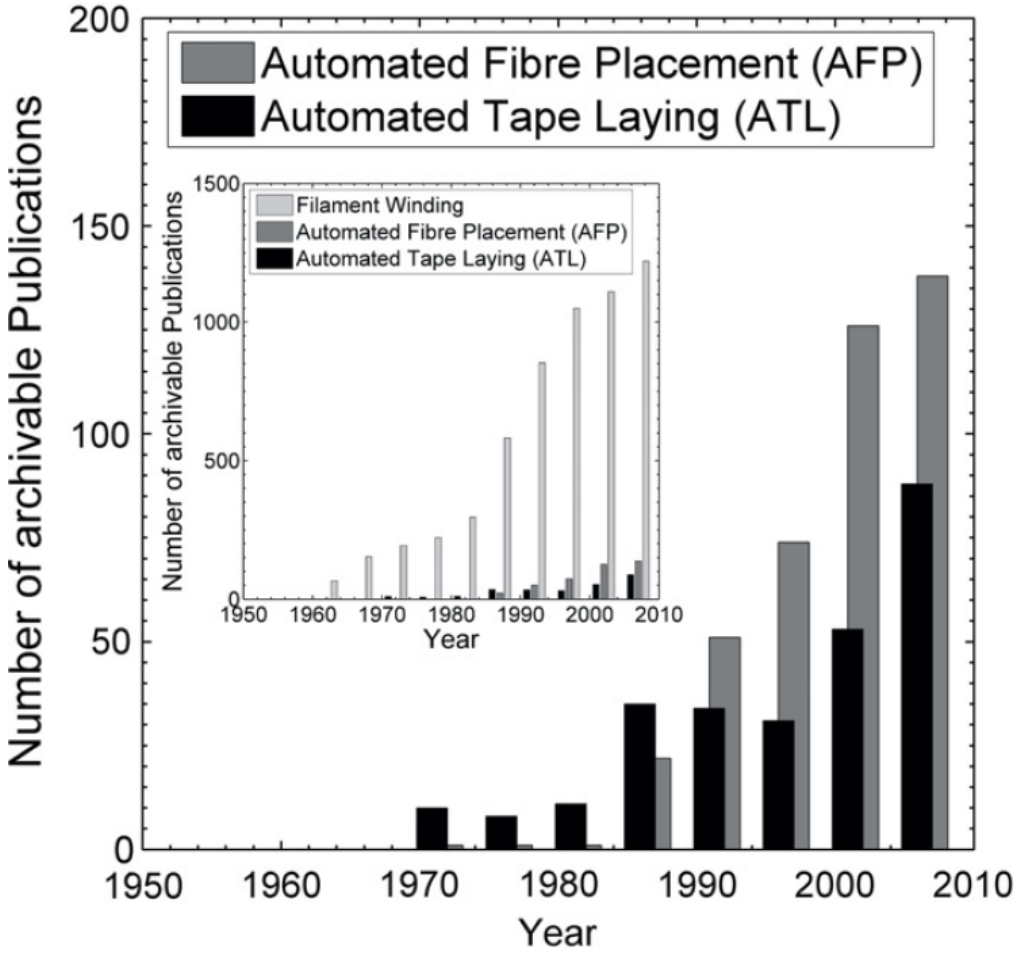

Figure 1.1: Publication on Automated Manufacturing using AFP and ATL from the 1970s [7]

The increase of technical publications over the years demonstrates that there is demand to further develop knowledge of this technology and increase automation in composite manufacturing.

In aerospace, the commercial aircraft industry has shown to be the largest producer of composite structures, as seen in Figure 1.2. In addition, multiple market studies have shown that the industry shows no signs of slowing down. New fleets of aircrafts are becoming more composite intensive, in the search to reduce aircraft weight, which in turn increases performance, and reduce operational costs.

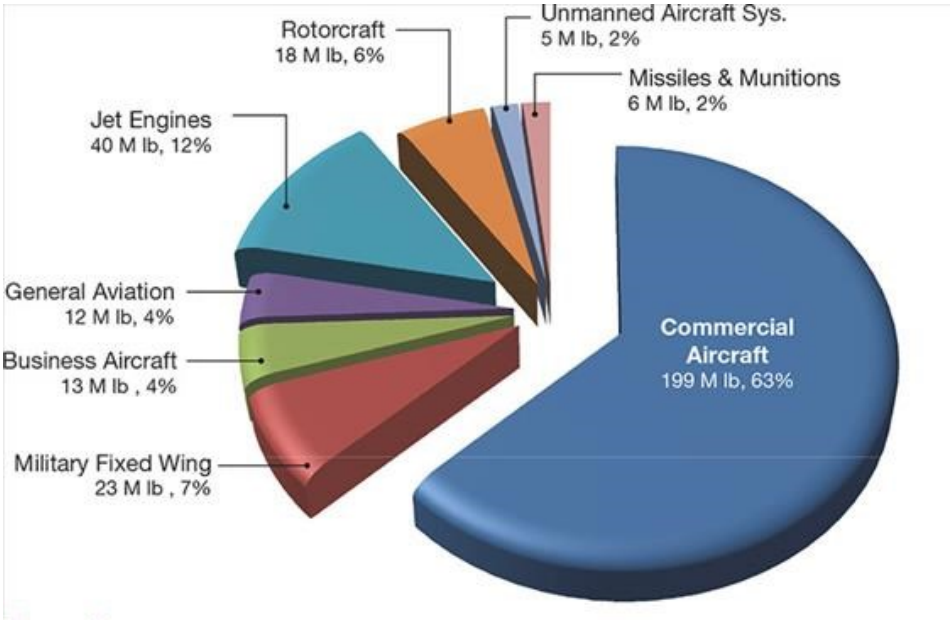

Figure 1.2: Estimated 2013-2022 Market for Aerospace Composite Structures [8]

Automated composite manufacturing plays a crucial role for large aerospace OEMs (Original Equipment Manufacturers) such as Airbus and Boeing in order to meet demands, as well as improve the overall performance of their products. Table 1 summarises a few of the key advantages of AFP/ATL manufacturing over traditional hand layup methods.

Table 1: Advantages of AFP/ATL Process over Conventional Hand Layup

Reduced manufacturing time	AFP/ATL laydown rates have been shown to reach 30lbs/hr, whereas the most skilled operators using conventional hand layup can reach laydown rates of 2.5lbs/hr [9]. Laydown rates are linked with mold complexity; structures such as fuselages, blades and wing skins are examples where AFP/ATL excels in productivity.
Reduced operational costs	With significant increase in laydown rates, time required to place material into mold is decreased. In addition amount of operators required for layup is less, all of which result in a reduction of operational costs.
Reduce amount of scrap	Scrap material using traditional hand layup methods can reach up to 20%. AFP/ATL has shown to be capable of reducing scraps to less than 5%, this further reduces costs and wastes.
Integration of larger structures	Utilizing automation and smart tooling methods, large structures incorporating multiple components such as fuselage, frames and stringers can be cured together at once. This in turn reduces the required amount of fasteners and rivets needed to mate structures together, reducing overall costs and weight.
Improve quality & uniformity	Automation allows control of all parameters during layup, and can therefore be repeatable. This improves quality and uniformity of each part, unlike hand layup method which can be different from one operator to another.
Steered Fibers	With AFP/ATL, new possibilities arise by steering fibers during the laydown of a ply, which is not possible to control using traditional hand layup method. Structures can have plies that are tailored to the design requirements, improving mechanical performance and reducing overall weight.

1.1.1 Types of AFP Machines

AFP systems are generally designed with gantry, robotic arm, rotating tool, or a combination of systems. The style of AFP is dependent on the customers' requirements, relating to part design and application. Figure 1.3 shows examples of AFP systems that are used in today's automated composite manufacturing industry.

a) b) c) d)

Figure 1.3: Types of AFP Systems a) Vertical AFP Gantry [10] b) Robotic arm AFP with removable head [11] c) Horizontal AFP Gantry [12] d) Robotic arm AFP with removable head on rails [13]

1.2. Introduction of Out-of-Autoclave Systems

Manufacturing of composite materials without the use of an autoclave are referred to as OOA systems. This section briefly describes types of OOA systems that are used in aerospace such as OOA prepregs, non-crimp fabrics, and resin transfer molding.

1.2.1. Out of Autoclave Prepregs

OOA prepregs are stored, treated and handled identically to conventional prepreg materials. Its difference comes to curing process. OOA can be cured using vacuum pressure alone, requiring no additional pressure. This alleviates the need to invest in large autoclaves, special tooling and high operational costs associated with autoclaves. This allows manufacturers to save significant costs associated with conventional prepreg manufacturing.

Early generations of OOA prepregs, also designated as Vacuum Bag Only (VBO) prepregs, were introduced in the mid-1990s. These prepregs were cheaper because of low temperature curing using vacuum pressure only, but did not have high mechanical properties and cycle times were too long to be used for large scale productions [14]. Today, OOA prepregs have significantly advanced and suppliers such as Cytec (now Solvay), Hexcel, and Toray offer a line of OOA prepregs systems that can be comparable to conventional primary structural prepregs. An example of an OOA prepreg system that is qualified in the aerospace industry is Cytec's 5320-1 OOA system. The key to attaining high performing OOA prepregs is to evacuate any entrapped air or volatiles that are introduced during the lay-up process. As OOA prepregs do not have autoclave pressure to assist the removal of these volatiles, Engineered Vacuum Channels (EVaC) are introduced during the manufacturing stage of OOA prepregs. These channels create a network of pathways that facilitate gases to escape during the cure cycle. During the cure, resin flows into these channels creating a low void laminate [15]. Schematic of the EVaCs found in OOA prepreg materials is shown in Figure 1.4.

Figure 1.4: Schematic of EVaC introduced into OOA prepregs [15]

In order for OOA prepregs to successfully cure without the aid of any external pressure, the resin systems used are engineered to have lower viscosity compared to tradition resin systems. The need to modify the resin systems rheology can be explained by examining equation (1) which denotes Darcy's Law in one dimension. Darcy velocity is a superficial fluid velocity and is denoted as u. This velocity is directly proportional to the fluid viscosity, the materials permeability K, and the pressure gradient ∇p [16].

$$u = -\frac{1}{\mu} K \nabla p \tag{1}$$

As OOA prepreg systems are processed without the use of any external pressure, the pressure gradient is far less than that of autoclave curing systems. Therefore resin system must be tailored to the process in order to be capable successfully wet-out the prepreg fibers during the cure cycle.

1.2.2. Non-Crimp Fabrics

Fabrics come in many types of fibers, woven patterns, and thicknesses. Non-Crimp Fabrics (NFCs) are different from conventional woven fabrics as they are made up of unidirectional fibers that are stitched and held together. This stitching, typically polyester yarn, prevents crimping or undulations that may lead to loss in mechanical performance in finished laminate

[17]. Advantages of NCF over conventional fabrics are improved mechanical properties, through thickness impregnation, and drapability [18] [19].

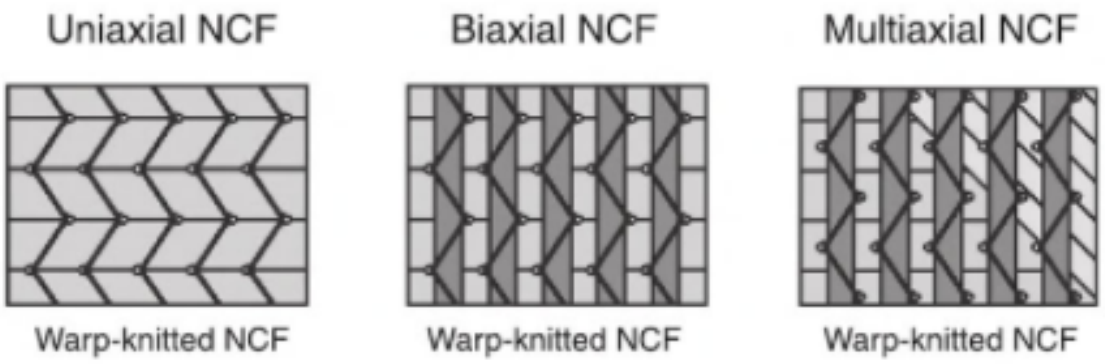

Figure 1.5: Example of Different NCF types [18]

As with conventional fabrics, NCFs require to be infused with resin in order to create a final laminate. This can be performed in many forms of Resin Transfer Molding (RTM) that suit the needs of the customer. Traditionally in aerospace, primary structural applications have been reserved to prepreg systems. However, recent advancements in NCF and RTM technology have driven aerospace manufactures to give these technologies a second look. A notable mention of NCFs currently used in aerospace, and the first commercial aircraft wing to use dry fiber composites versus prepreg, is Bombardier Aerospace's C Series program [20].

a) Operators placing NCF into mold

b) Final resin infused wing skin

Figure 1.6: Bombardier Aerospace C Series Wing Skin made using NCF and RTM [21]

The C Series program wing skin and spars are manufactured using a patented Resin Transfer Infusion (RTI) process. This process uses a one sided mold where NCFs are laid to create the preform. The placed preform is vacuum bagged, resin is injected into the preform, and then finally cured [22]. Figure 1.6 shows operators laying NCF onto mold, and final laminate wing skin after the RTI process.

1.2.3. Resin Transfer Molding

Resin Transfer Molding (RTM) process is a cost-effective fabrication for relatively high volume production of polymer composites. Conventional RTM process involves a dry preform inserted and compacted into a closed mold. A thermosetting resin is then injected into the mold, impregnating the fibers and filling the remaining areas, and cures inside the mold [23]. Injection pressure within the closed mold is generally in the range of 100psi [16]. A schematic of the RTM process is shown in Figure 1.7.

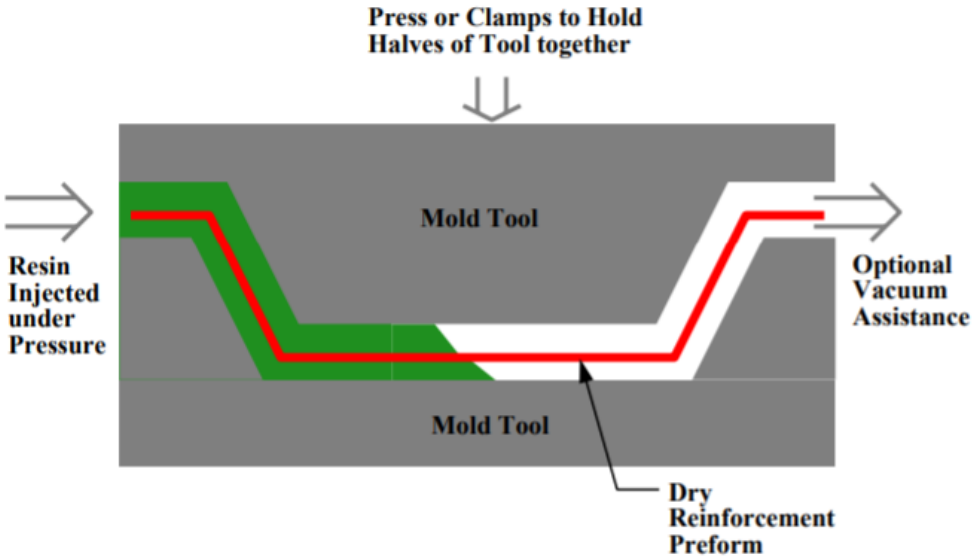

Figure 1.7: Schematic of the RTM Process [23]

Advantages of the RTM process are that it does not require the use of autoclave, is capable of achieving high fiber volume fractions, can produce complex shapes, and the injection step lasts within the order of minutes. The disadvantage of RTM process is the capital investment and expertise required to design and manufacture a closed mold tooling. This becomes a greater issue when designing larger complex parts. For large composite parts used in the aerospace industry, such as fuselage or wing skins, RTM is not a feasible method for production.

VARTM is a process developed as a variant of the Resin Transfer Molding (RTM) process. A schematic of the VARTM process is shown in Figure 1.8. Whereas RTM uses closed mold tooling, VARTM replaces the need of upper half tooling with vacuum bag. This significantly reduces overall costs and design requirements associated with tooling. Without the need for upper half tooling, the production of larger composite panels suitable for aerospace is possible. In addition, the need for only one (lower) tool side greatly simplifies tool design. Vacuum is used to drive resin into the dry preform, as well as remove air and volatiles. As a vacuum is created within the bag, atmospheric pressure provides compaction. As injection pressure is relatively low compared to RTM a flow mesh, also known as distribution media, is used to improve resin flow and injection times. The flow mesh is a highly porous plastic mesh that is placed on top of the fiber preform. The mesh acts as a lower resistance path, and during infusion the resin initially flows along the top of the fiber preform and them impregnates the preform in the through-thickness direction [24]. Without the use of a flow mesh, large structures such as wing skins would not be feasible to manufacture using VARTM.

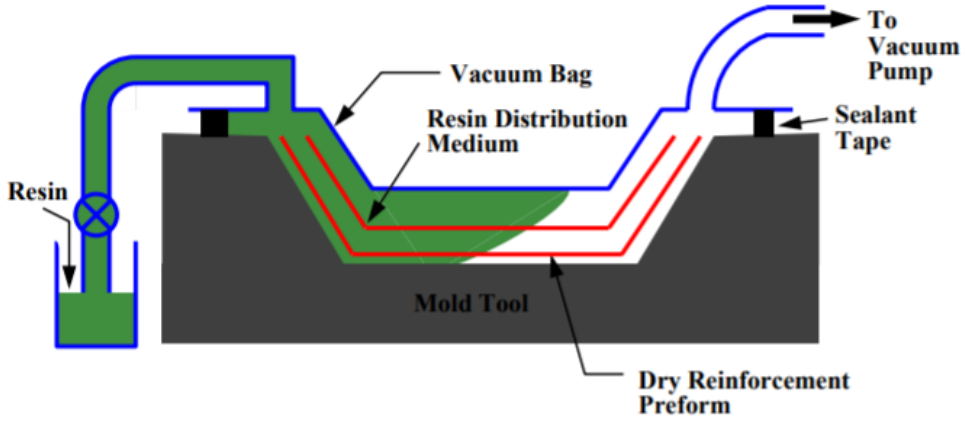

Figure 1.8: Schematic of the VARTM Process [23]

The advantages of VARTM are lower costs associated to manufacturing and designing tooling, ability to manufacture large composite parts, reduced capital and operational costs associated with autoclaves, and reduced raw materials costs.

Chapter 2 - Literature Review

This chapter is to overview key advancements that have been made in VARTM infusion, dry automated fiber placement technology, permeability of dry preforms, mechanical evaluation of DAFP VARTM laminates, and potential cost savings using AFP manufacturing. In addition, overall thesis motivation and objectives are outlined.

2.1. Mitsubishi

A study performed by Mitsubishi Heavy Industries and Toray Industries published in 2005 investigated the feasibility VARTM infusion to manufacture primary composite structures of an aircraft [25]. The Advanced-VARTM (A-VARTM) technique was developed using NCF and thermosetting epoxy resin system. Large scale stringer panels were manufactured, as well as I-beams and were loaded in compression till failure in order to evaluate their mechanical performance. The stringer panel consisted of a pre-infused skin, and co-bonded infused stringers.

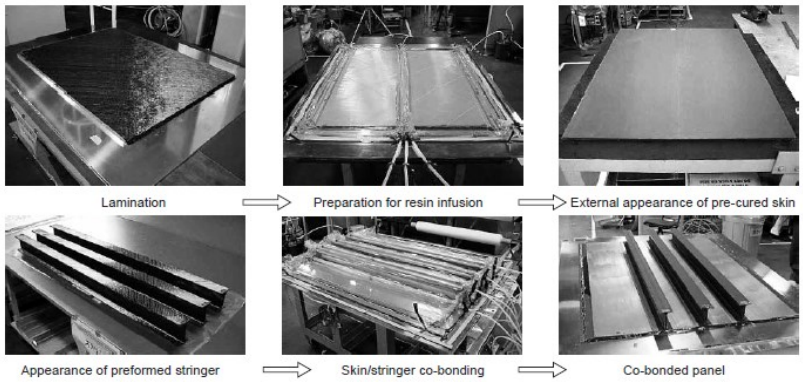

Figure 2.1: A-VARTM used to manufacture stringer panels [25]

The results of the study shows that A-VARTM manufactured structures have sufficient mechanical properties to be utilized as primary structural applications in comparison to conventional prepreg materials. However the preforms are manufactured by conventional hand-layup method. For simplicity, the stringer panels were manufactured using flat skin panels, and stringers of constant cross-sections. The potentials of automation were not investigated, but the study shows that infusion techniques can be adapted to aerospace applications of primary structures.

2.2. AUTOW

Initiated in 2007, the Automated Preform Fabrication by Dry Tow Placement (AUTOW) project stems from a European Union (EU) collaborative effort involving multiple industrial and research partners such as Dassault, EADS, Innovations works, Hexcel Reinforcements ONERA, Catholic University of Leuven, University of Stuttgart IFB, TU Delft, VZLU, Israel Aerospace Industries and Keilmann Sondermaschinenbau KSL. This consortium was managed and lead by the Netherlands Aerospace Center NLR [26]. This type of project is a first of its kind and has paved the way for automated dry fiber manufacturing technology.

This project was first to address the new challenges faced in dry fiber automation, as well as lead the development of dry fiber materials. Traditional AFP machines were not designed for depositing dry fiber tows and needed to be modified. Issues such as fraying during deposition, fraying at the compaction roller, and winding of tows were common problems [27]. Once necessary modifications to AFP machinery were addressed material development and characterization was performed. Initial dry tow fibers were processed with binder powder. However to improve material performance Hexcel proposed and incorporated thermoplastic veils. This became the material of choice for dry fiber processing, and material suppliers have followed to manufacture dry fiber material in similar concept. Flat preforms were successfully manufactured with AFP and flat laminates were manufactured using Resin Transfer Molding

(RTM) and inspected using Non Destructive Inspection (NDI) method of C-Scan. The successful manufacturing of laminates and quality showed promising results.

Figure 2.2: Example of Fraying and binder build-up from AUTOW

Full scale validation was performed by manufacturing sine-wave rib beam, which is representative of a rib section that would be found within a business jet wing. The general dimension of the sine-wave rib was 1.37m by 0.4m in length and height respectively. The conclusion of the full scale validation showed a decrease in overall weight of over 10%, when compared to a conventional aluminum I-beam component, whilst being able to withstand ultimate bending loads.

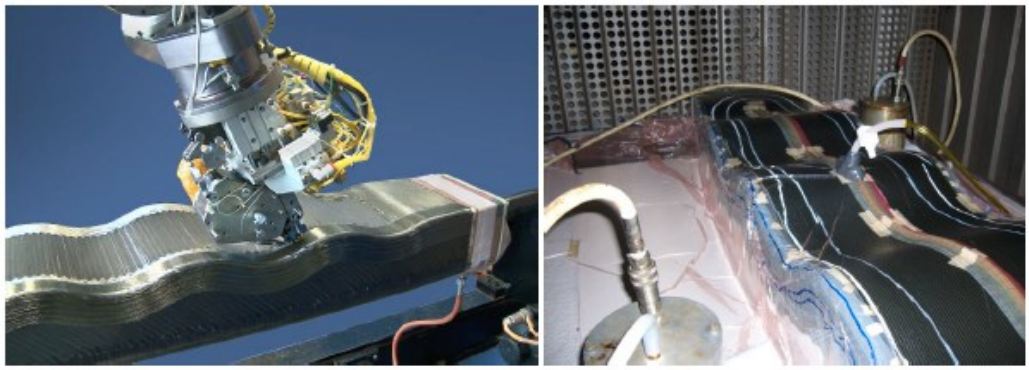

Figure 2.3: Manufacturing of sine-wave dry preform with AFP and VARTM infusion of preform

The AUTOW project has shown the feasibility of automated dry fiber placement and has laid the ground work of this technology. Due to this success, significant amount of research and collaborative work in automated dry fiber placement have continued such as the ADVanced Intergrated TAil Cone (ADVITAC) project funded by the European Commission research and development program [28]. However due to these research programs being large consortiums of industry leaders and research centers, detailed works and publications are very limited.

2.3. Permeability of Preforms

The permeability of a preform describes the capability of a porous, in our case fibrous, material to let fluid flow through it [29]. The unique advantage that DAFP can offer is the tailoring of preforms in order to improve permeability. This can be done by creating open channels within the preform, which would allow resin to flow and impregnate the fibers more easily. Tailoring a preform with unique gaps or overlaps would not be possible using traditional woven fabrics or NCFs. Increasing permeability has to potential to reduce processing time related to RTM and increase productivity. Fraunhofer Institute of Chemical Technology ICT investigated the out-of-plane as well as in plane permeability of dry fiber preforms and NCF. In addition, the effects of induced gaps in dry fiber preforms were explored. This research has shown that implementing gaps within the preform shows an increase of permeability in the order of 1-2 magnitudes when compared to traditional dry preforms manufactured from NFCs, as well as reach up to a 65% reduction in impregnation times [30]. The effects of increasing gaps in dry fiber preforms in turn reduce the overall fiber volume content of preforms, and the final infused laminate. Therefore, when designing dry fiber preforms with gaps induced to potentially reduce processing time, the influences on mechanical properties of the overall laminate should be taken into consideration.

In addition to work presented above, work published by [31] focuses on the maximization of out-of-plane permeability of dry preforms manufactured by dry fiber placement. Dry fiber preform out-of-plane permeability is typically in the range of 1E-15 m^2 - 5E-14 m^2 which 1-2 orders of magnitude lower than conventional textiles, such as NCFs [31]. This makes preforms made by dry automated fiber placement less capable in secondary LCM operation, particularly those

which rely heavily on out-of-plane impregnation such as high pressure RTM. The cause of the lower out-of-plane thickness performance is due to the architecture of dry fiber preforms when manufactured using automation.

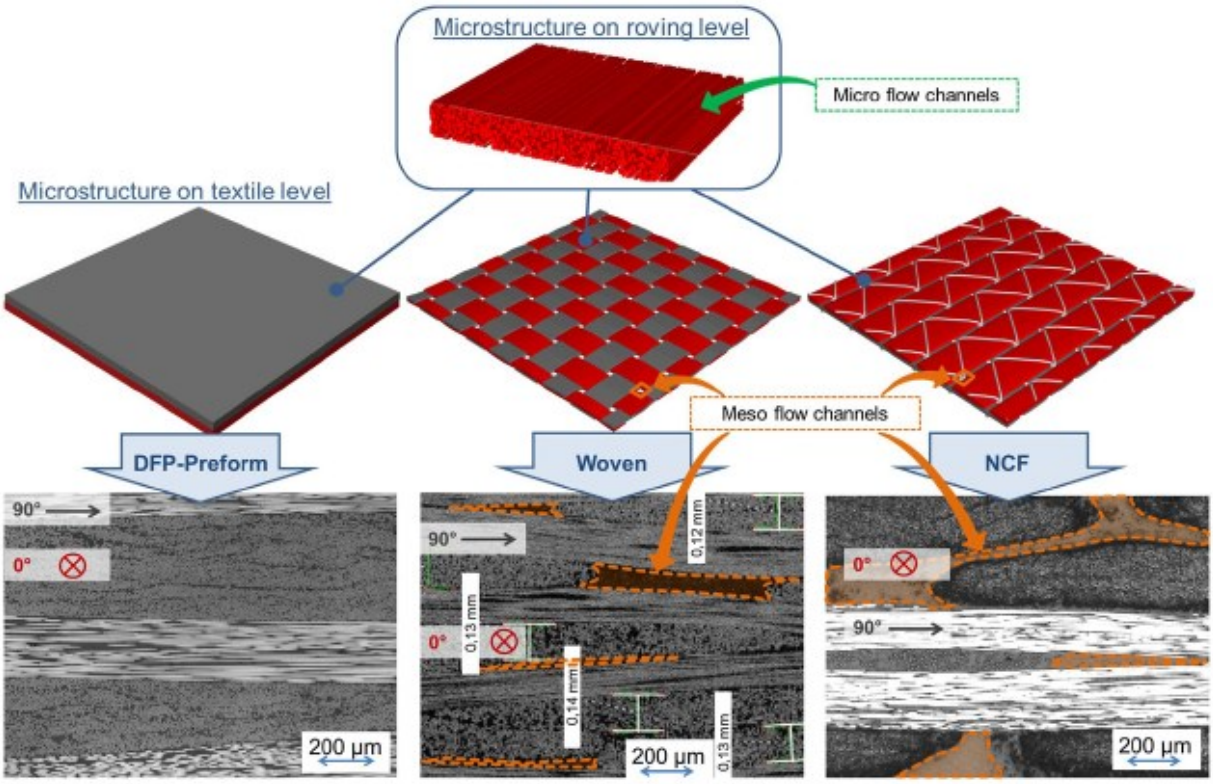

Figure 2.4: Fiber architecture of dry fiber preform (left), woven fabric (center), bi-axial NCF (left) [31]

The Figure 2.5 describes how dry fiber preforms do not have out-of-plane flow channels that are present in woven fabrics or NCFs. The lack of these channels are what cause lower permeability in the out-of-plane direction of dry fiber preforms. The study does not use commercially available semi-finished dry fiber material, rather an online binder application system is used to process standard dry rovings in-situ during fiber placement. Figure 2.5 shows system that was developed which applies binder material to the nip point during processing.

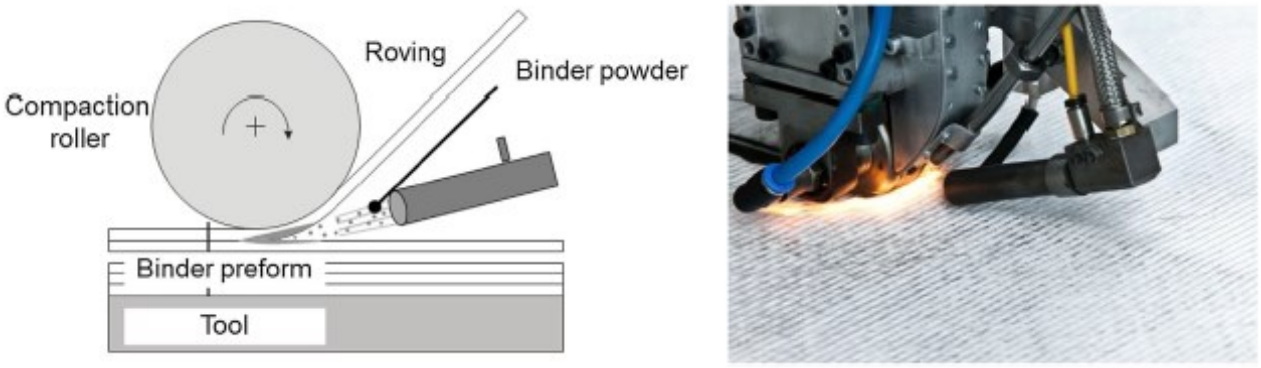

Figure 2.5: Schematic illustration of the DFP process (left), fiber placement head during DFP process (right) [31]

The developed system gives flexibility to process multiple different types of rovings with multiple binder solutions. The effects of multiple binder contents in terms of percent, binder practical sizing, layup sequence and secondary tufting treatment were studied to evaluate their effects on out-of-plane permeability. The conclusion of the works determined that the effects of binder amount or partical sizing had the least amount of impact on permeability results. Modification of layup sequence, simulating a woven fabric, had the ability of doubling permeability. Lastly tufting showed an increase in permeability of more than a factor of 30. However it should be taken into consideration that tufting is an additional operation added to the manufacturing process of the dry fiber preforms.

2.4. Mechanical Performance of DAFP Infused Laminates

Material supplier such a Hexcel provides a brief comparison of their dry fiber unidirectional tape, HiTape, designed for AFP manufacturing, infused with Hexcel's HexFlow RTM6 toughened epoxy resin system to conventional prepreg material mechanical properties.

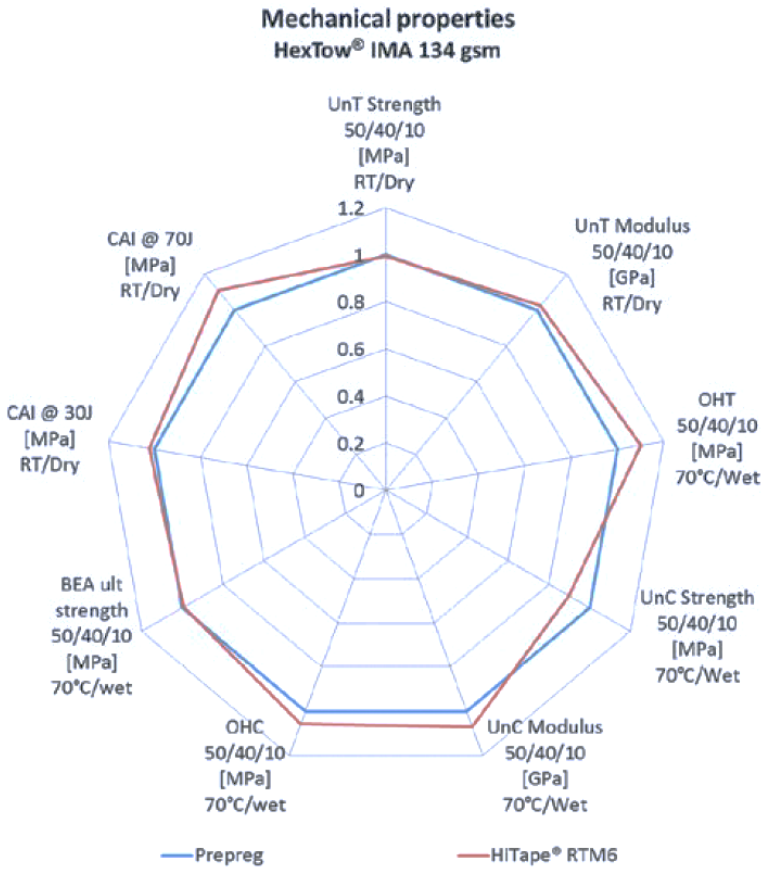

Figure 2.6: Mechanical Performance of Hexcel HiTape with RTM6 Resin vs. Conventional Prepreg [32]

Exact performance results are not provided, however the graph provided gives a general overview of the materials performance in different areas. It is important to note that the stacking sequence used in this comparison is 50/40/10 (50% ±45°, 40% 0°, and 10% 90°). In most of the properties presented in Figure 2.6, HiTape dry fiber tape infused with RTM6 resin system shows to be comparable to prepreg material. There is a knock-down of roughly 10% in Un-notched

Compression (UnC) strength tested at elevated temperature (70°C) and wet conditions. An increase in performance is seen in Open Hole Tension (OHT), Open Hole Compression (OHC), UnC modulus which are all tested in elevated temperature wet conditions, as well as Compression after Impact (CAI) tested in room temperature dry condition.

In addition to Hexcel's provided information, mechanical evaluation of DAFP infused laminates has been explored by Cranfield University and Coriolis Composites, in part for their involvements in the ADVITAC project [33]. Their joint published work describes an overview of the implementation of automated manufacturing to dry fiber preforms, in addition the investigation of improving damage tolerance with the use of through thickness reinforcements. In the research described, a Coriolis AFP machine coupled with a laser heating system is used to manufacture dry fiber preforms. Preforms are manufactured with different types of dry fiber tape, and infused with different RTM resin systems.

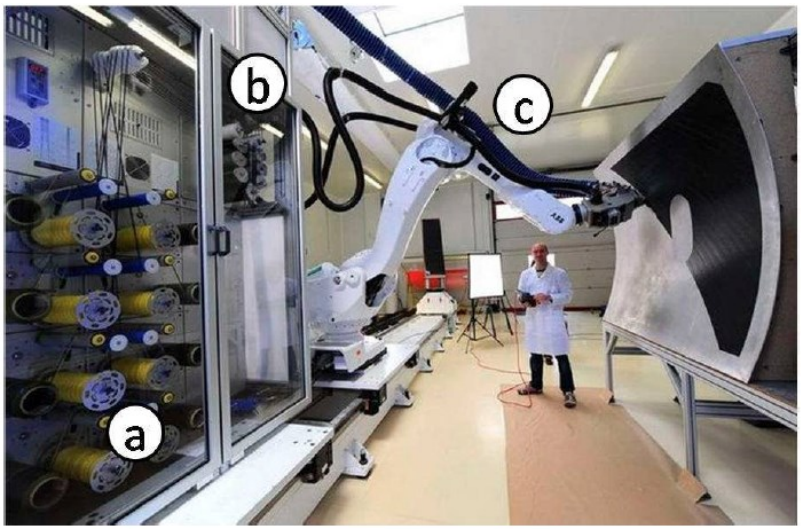

Figure 2.7: Automated Dry Fiber Placement System (a) Creel, (b) Tape Delivery System, and (c) Temperature Controlled Tape [33]

Tensile testing in the 0° and 90° orientations, as well as in-plane shear are performed on Hexcel AS7 12K dry carbon fibers infused using the VARTM process. The study infuses the Hexcel fiber preforms with two different epoxy resin systems; Hexcel's HexFlow RTM6 and Cytec's Prism EP2400. Table 2 gives a quantitative evaluation of HiTape's mechanical performance.

Results show to be comparable between resin systems; however Cytec's resin system performs notably better in transverse tensile strength and modulus.

Table 2: Mechanical Performance of HiTape infused with RTM6 and EP2400 [33]

Test	Property	Hexcel tape HexFlow RTM6	Hexcel tape Prism EP2400
Tensile 0°	Modulus [GPa]	142 ± 3	143 ± 7
	Strength [MPa]	2160 ± 100	2200 ± 190
	Ultimate strain [%]	1.44 ± 0.13	1.45 ± 0.05
Tensile 90°	Modulus [GPa]	7.2 ± 0.1	7.8 ± 0.3
	Strength [MPa]	33.3 ± 2.4	47.2 ± 7.9
	Ultimate strain [%]	0.46 ± 0.03	0.41 ± 0.28
In-plane shear	Modulus [GPa]	3.8 ± 0.3	4.1 ± 0.5
	Strength [MPa]	63 ± 1.3	61.6 ± 2.5

2.5. Evaluation of Material Systems for DAFP

As automated fiber placement of dry fibers is a newly developed manufacturing process and material suppliers have begun to develop material process. The subject of evaluating multiple material systems designed for dry fiber automated placement is performed in the works presented in [34]. The study presents the evaluation of 5 different commercially available material systems made for manufacturing of dry fiber preforms by means of automated manufacturing. The material systems used are not named, however classed alphabetically from A through E. The study evaluates the differences between each materials system in terms of its fiber type, tape type and binder compositions shown in Table 3.

Table 3: Overview of different available dry fiber materials [34]

	Definition	*Material* A	B	C	D	E
Carbon Fibre						
Fibre type		HS*	HT*	HT*	IM*	HS*
Nominal areal weight [g/m^2]		196	126	126	210	262
Tape type	Tow		✓	✓	✓	✓
	Slit tape	✓				
Binder						
Chemical composition	Epoxy based	✓	✓			
	Thermoplastic based			✓	✓	✓
Binder application	Veil	✓**			✓	
	Powder/spray	✓	✓	✓		✓

*HS = high strength; HT = high tenacity; IM = intermediate modulus
** carbon fibre veil including binder

The study also describes the notable visual differences between each material system. These differences can be associated to the methods and processes used by each supplier to manufacture their systems.

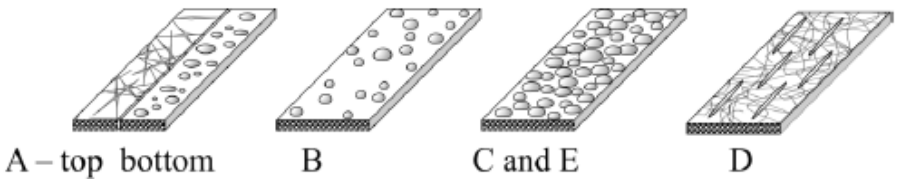

Figure 2.8: Skethes of Dry Fiber Materials [34]

Each material system is processed using a Coriolis Composites AFP machine with a 3 kW diode laser as heat source. During the manufacturing trials of all the material systems, a list of nine different types of flaws or defects, in this study coined as faults, are recorded during the automated fiber placement of preforms. The fault types are listed in Table 4

Table 4: List of different fault types observed during automated fiber placement [34]

Observed fault types		
fibre fluff	loose fibres on surface	shearing
binder residue inclusion	twisted tow	overlap
gap (>2 mm)	fibre folding	foreign inclusion

Some of the fault types described have been also identified by the works presented in [27]. These fault types are recorded and taken into consideration when evaluating materials systems in terms of AFP process ability. All preforms manufactured are infused with epoxy resin using VARTM. The manufactured laminates are evaluated using an analytical hierarchy process in terms of raw material characteristics, manufacturability using AFP, resin infusion processability, laminate characteristics and procurement. Material A evaluated was determined to be the best all-around material that met all requirements, however Materials D & E showed to be outperforming in the areas of AFP processing, resin impregnation and material costs.

2.6. Potential Cost Savings using AFP

The AFP manufacturing process has been evaluated and adopted by many large aerospace OEMs in order to meet their production demands, improve quality and repeatability, while significantly reducing overall costs. An example of such a study is Boeing's analysis of AFP manufacturing used to fabricate the Bell-Boeing V-22 composite aft fuselage [35]. The AFP machine used to manufacture the co-cured stiffened skin (skin and stringers) of the aft is manufactured by Hercules, a horizontal gantry fixed on rails. Figure 2.9 shows a schematic of this 7-axis machine.

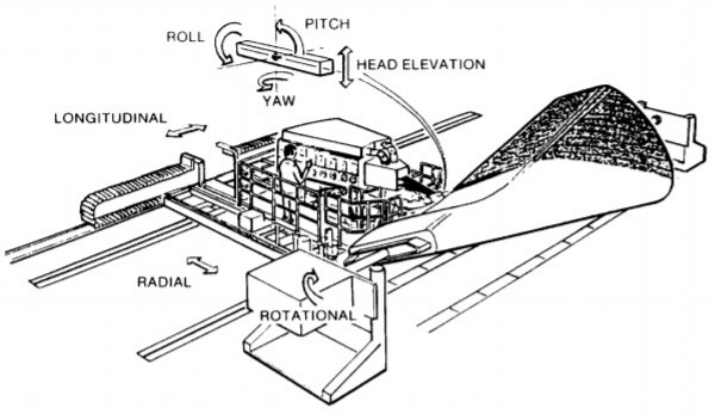

Figure 2.9: Schematic of Hercules 7-axis AFP Machine [35]

The study compares data from the production of the V-22 program, and uses conventional hand layup method as a baseline. The results of the study are shown in Figure 2.10 below.

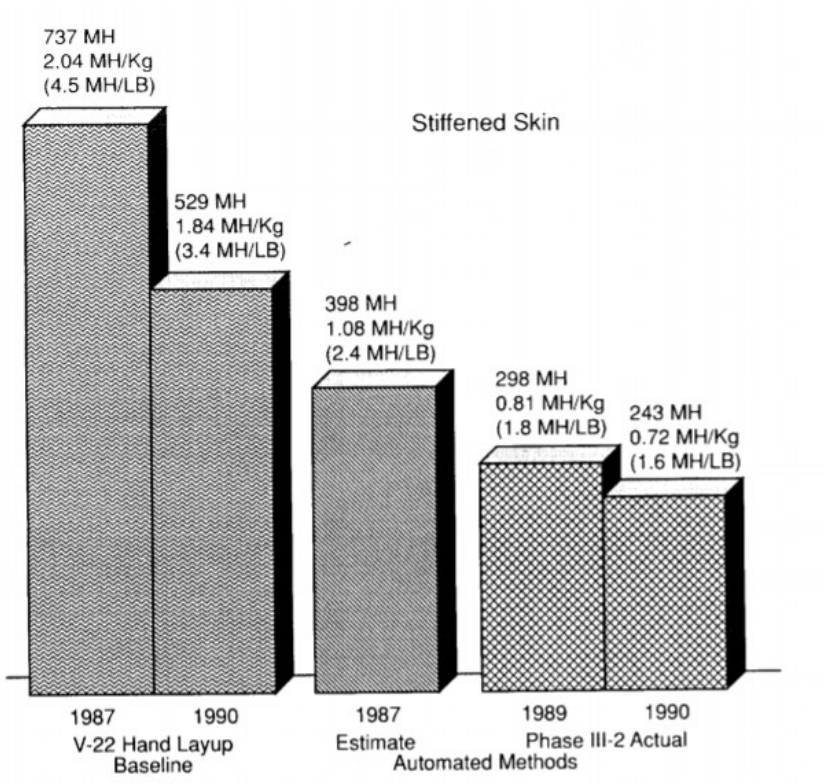

Figure 2.10: Hand Layup versus AFP manufacturing of Aft Stiffened Skin [35]

There were seven aft stiffened skins produced using hand layup. The hand layup process was optimized by reducing number of stiffeners, improved adhesive and copper shielding materials. This can be seen by the reduction of Man Hours (MH) from 737 to 529 per stiffened skin. These improvements were incorporated to the automated manufacturing of the aft stiffened skin, and the results show a significant reduction in operational costs. The improvements seen is the reduction of over half of the required MH associated to manufacturing one stiffened skin, compared to the optimized 529 MH hand layup baseline. The result has surpassed their initial estimates of operational cost savings. This is an indication of how AFP manufacturing utilized with smart tooling, incorporating multiple assemblies into one larger process, can result in significant advantages increasing out-put and reducing costs.

2.7. Motivation

The review from the above research and industrial trends show that automated dry fiber placement and VARTM infusion technologies is of significant interest to aerospace OEMs, and reached to point in which adoption to large scale manufacturing is feasible. Further understanding dry fiber preform manufacturing using AFP is of benefit to the industry; better understanding its manufacturing challenges, difficulties, and potential for new opportunities must be investigated in detail.

To date, although interest is shown within the aerospace industries and research consortiums, very little information is published on details of manufacturing methods and processes used, in addition to the lack of understanding of mechanical properties of DAFP VARTM laminates. This has given motivation to focus on a heavily experimental based dissertation. By focusing on the entire process, from DAFP manufacturing, VARTM infusion, and mechanical characterization, every step of the process can be recorded in detail, and evaluated.

In addition to evaluating the manufacturing process in its entirety, its effectivity and efficiency will be used to evaluate the potential cost savings using DAFP VARTM manufacturing compared to conventional manufacturing methods of composites in aerospace.

2.8. Objectives

- To create a detailed process window of manufacturing of dry fiber material using AFP, and identify challenges and mitigations using hot gas torch as heat source.
- Study the effects of tailored gaps on the VARTM process of DAFP manufactured preforms.
- Characterize DAFP VARTM laminate mechanical properties and baseline against comparable aerospace grade prepreg materials.
- Cost Analysis of the DAFP process versus traditional AFP manufacturing of autoclave and OOA prepreg materials.

Chapter 3 - Materials and Methods

This chapter describes the materials that have been selected in order to perform evaluation of DAFP VARTM, the manufacturing methods used to create dry fiber preforms using AFP, and the procedure of infusion using the VARTM process. In addition, methods used to inspect the quality of the laminate are also described.

3.1. Material Selection

3.1.1. Hexcel Hi-Tape

Materials used to create dry fiber preforms are Hexcel's HiTape IM7 carbon fibers. The material is supplied in 1 pound creels of ¼" (6.35mm) width 140 AFW IM7 carbon fibers. The dry slit tape has a thin thermoplastic veil on its surface to allow the dry tape to adhere and tack to another surface. In order to activate the thermoplastic binder, temperatures of 300-350°F (150-175°C) are required. The usual heat source for these materials is by laser or infrared systems. HGT as a heat source has been proven to be feasible, but poses challenges. These challenges are addressed further in section 3.2.3. The creel format in which the dry fiber is supplied can be seen in Figure 3.1. The general properties of Hexcel IM7 carbon fibers are listed in Table 5.

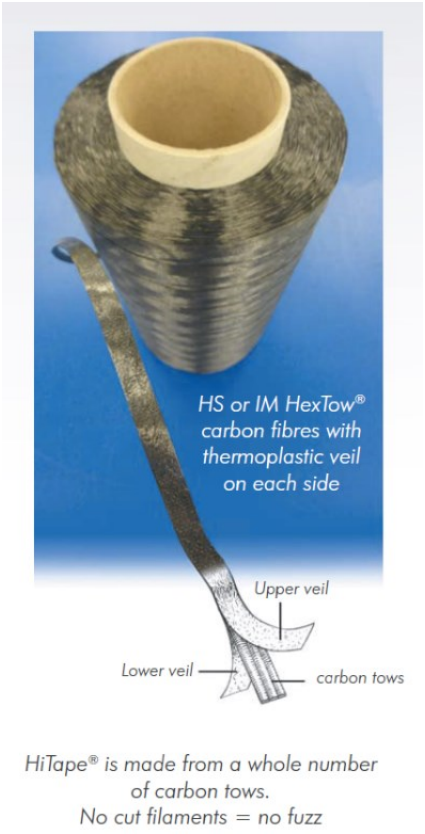

a) Dry fiber creel

b) Single ¼" (6.35mm) tow

Figure 3.1: Hexcel HiTape dry carbon slit tape

Table 5: Typical Properties for 6K tow of Hexcel IM7 Carbon Fiber [36]

Typical Fiber Properties	**U.S. Units**	**SI Units**
Tensile Strength	800 ksi	5,516 MPa
Tensile Modulus	40 Msi	276 GPa
Ultimate Elongation	1.9 %	1.9 %
Density	0.0643 lb/in^3	1.78 g/cm^3
Weight/Length	12.5 x 10^{-6} lb/in	0.223 g/m
Approximate Yield	6,674 ft/lb	4.48 m/g
Filament Diameter	0.203 mil	5.2 microns
Carbon Content	95.0%	95.0%

3.1.2. Cytec PRISM EP2400

The resin system used for VARTM infusion of the Hexcel's HiTape preforms is Cytec PRISM EP2400. This resin system is a single part, 180°C (356°F) curing, toughened liquid epoxy resin system designed for primary composite structures manufactured using VARTM or RTM. Standard supplier infusion and cure cycles were followed in order to cure the laminates, an example of the cure cycle is shown in Figure 3.2. Significant features and benefits of this of this resin system are listed below [37]. The neat resin properties can be found in Table 6.

- One-part toughened resin system specifically developed for ease of processing primary aircraft structures
- Suitable for processing via RTM, VaRTM, CAPRI
- Two-hour 180°C (356°F) cure giving service temperature of >120°C (>248°F)
- Exceptional "wet" Tg of 163°C (325°F)
- Injectable at 70°C (158°F)
- Wide processing window; 10 hours at <300cP at 100°C (212°F)
- <100cP initial injection viscosity
- Minimum viscosity of 20 cP at 120°C (248°F)
- Excellent compression strength and damage tolerance
- Compliance with FAR/JAR Flammability, Smoke and Toxicity
- High strain enhances fatigue and microcrack resistance
- Shelf-life >12 months at -18°C (0°F) and out-life >28 days at 22°C (72°F)
- Low reactivity; No special shipping requirements

Suggested applications

- Primary structure applications requiring superior toughness, low viscosity and extended pot-life
- Stringer Stiffened Box Covers
- Fuselage and Window Frames

- Pressure Bulkheads
- Passenger and Cargo Door Structures
- Engine Containment Cases
- Hinge/Brackets/Fittings

Table 6: Cytec EP2400 Neat Resin Properties [37]

Property	**Value**
Cured resin density, g/cm$_3$(lb/ft$_3$)	1.24 (77.4)
Tensile strength, MPa (ksi)	95 (13.8)
Tensile modulus GPa, (msi)	3.4 (0.49)
Tensile strain, %	7.2
Flexural strength, MPa (ksi)	164 (23.8)
Flexural modulus, GPa (msi)	3.6 (0.52)
Strain energy release, G_{IC}, J m^{-2}	279
Fracture toughness, K_{IC}, MPa m^{½}	0.96
CTE, x10-6 C-1	60.5
Tg, °C (°F)	179 (354)

It should be noted that the resin system was donated by industry to serve this dissertation. It is known that the resin batch has surpassed the OEMs designated shelf life, however due to significant costs and delayed lead times to acquire new product (6 months to 1 year) the donated resin system is used. For this reason properties of the resin are further evaluated in section 3.3.1.

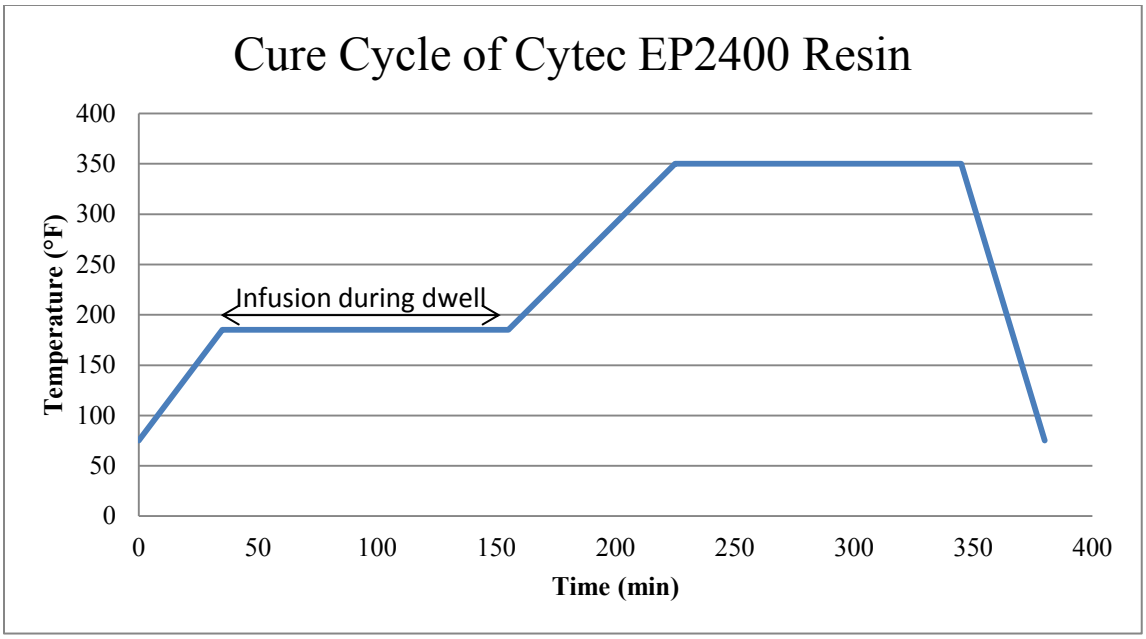

Figure 3.2: Typical Cure Cycle for EP200 Resin System

The first dwell of the cure cycle of the EP2400 resin system is intended for the infusion process. The resin system requires to be heated in order to attain lower viscosity to effectively infuse. The time of the first dwell during infusion is part geometry and complexity dependent. When the preform has been effectively infused, the cycle can proceed to the final dwell to cure the resin system.

3.2. Dry Preform Manufacturing

3.2.1. Automated Fiber Placement Process

In order to understand method of DAFP processing, it is important to understand how the AFP machine operates and its controllable parameters. The AFP machine used for this dissertation is manufactured by Automated Dynamics Corporation (ADC). It consists of a Kawasaki 6-axis robot arm fitted with an ADC designed thermoset deposition head, capable of up to 4 tow

placement of 0.25” (6.35mm) tows. The head lays on a mandrel, which is also rotatable. The heat source of the AFP is Hot Gas Torch (HGT). For the purpose of this study, a flat steel table of 4 feet by 3 feet is used as a tool laying surface.

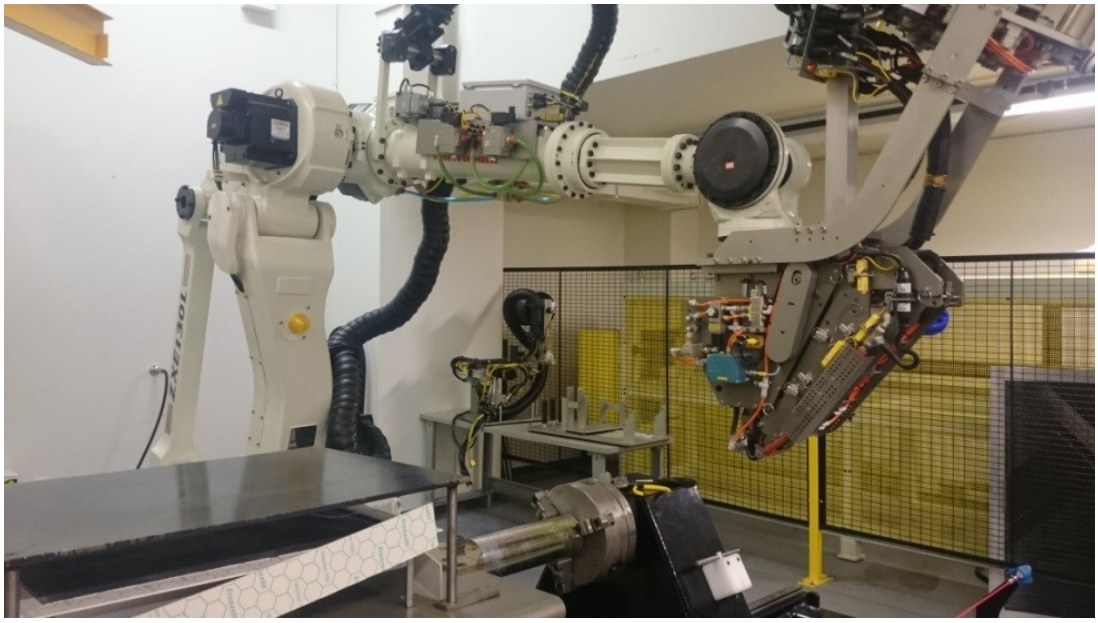

Figure 3.3: ADC AFP Machine with Thermoset Head at Concordia University

There are multiple parameters that can be controlled during the operation of the AFP. In Figure 3.4, a simplified schematic depicts the variables that are most critical when processing with AFP.

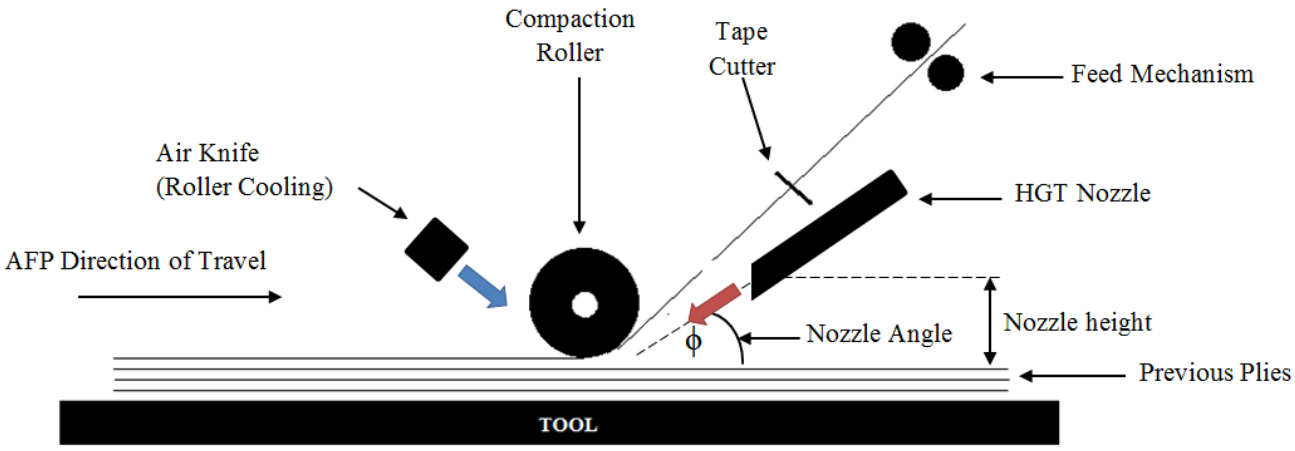

Figure 3.4: AFP processing schematic

The controllable parameters of the AFP and their details are shown below:

- AFP head cooling system: The thermoset head has an internal cooling system. This is particularly important for thermoset prepreg systems as it keeps internal tow feed mechanism cool, avoiding potential jamming and resin buildup.
- HGT nozzle exit temperature: Nozzle exit temperature is critical to heat incoming tows from feed mechanism to react and bind to tool surface and preform.
- HGT flow rate: The rate at which nitrogen gas flows through the HGT nozzle
- HGT nozzle height: height of HGT nozzle with respect to the tool/preform surface
- HGT nozzle angle: Angle in which the exit nozzle directs heated nitrogen to incoming tows/surface.
- Feed Rate: The speed in which the AFP head moves when laying tows, in terms of inches/minute.
- Compaction Pressure: The force at which the AFP applies to the compaction roller during lay-down of a course.
- Air Knife Flow rate: Flow of cool nitrogen gas which is used to cool the compaction roller during operation.
- Single or Multi tow placement: AFP is capable of processing 1 to 4 tows at once during a single pass.

3.2.2. Building Process Window for DAFP

Dry fiber manufactured using AFP is conventionally processed using a laser heating system. Advantages of laser heat sources are that the beam can be concentrated to a specific location and size, tighter process temperature control, and fast heat and cool down rates. As the AFP thermoset head from ADC is equipped with a HGT for heat source, the first hurdle to overcome was to confirm if HGT was capable of attaining the temperatures required to activate the

thermoplastic binder found in the dry tapes, while being a viable heat source to manufacture large multi-layered and multi-oriented preforms consistently.

The HGT temperature is a parameter controllable by the AFP system. The temperature is monitored by the AFP control system with a thermocouple placed within HGT nozzle tubing. The set AFP HGT temperature does not reflect the true nip-point temperature which the fibers are exposed to, as the thermocouple is located within the HGT piping just before the exit nozzle. Therefore in reality, there is a significant drop from set temperature to true temperature seen at the nip-point.

For this reason an evaluation of the true nip-point temperature with respect to HGT set parameters is performed. This involved having the AFP position itself on the tool surface, where an external thermocouple (Omega model 5TC-TT-K-36-36) is installed in the nip-point region on the tool surface. The thermocouple is plugged into a Data Acquisition (DAQ) system (Omega TC-08) where the temperature achieved at the tool surface is recorded. It was confirmed that the HGT is capable of reaching nip-point area temperatures of over 150°C, shown in Figure 3.5. The AFP parameters used when confirming this capability is shown in Table 7.

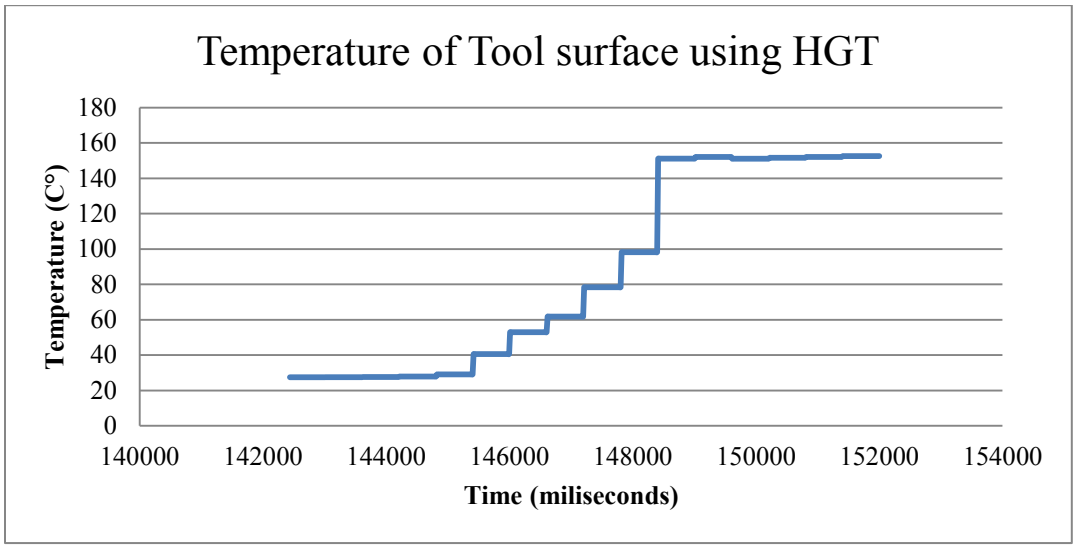

Figure 3.5: Nip-point Temperature of AFP using HGT

Table 7: AFP Parameter to Achieve Required Nip-Point Temperatures for DAFP Processing

AFP Parameter	
HGT temperature	330°C (626°F)
HGT flow rate	90 slpm[1]
HGT height	10 mm
HGT nozzle angle	45°

3.2.3. Dry Fiber Processing Challenges

As it was confirmed the HGT is capable of achieving temperatures required to activate the thermoplastic binder found in the dry slit tape, and building a process window for AFP processing can commence. At this stage, one creel of tape is mounted to the thermoset head, and passes are attempted using AFP parameter as described in Table 7, using a feed rate of 2 inches/second and compaction roller pressure of 70 lbf. The tool surface of the AFP is metallic; it was suggested by manufacturer to bag the tool surface using conventional vacuum bagging material with thick paper underneath the bag. The intent of the thick paper is to retain the heat at the surface, as a metallic surface will dissipate heat too quickly. The bagging material serves to hold the paper in place, is a good tacking surface, and allows for easy removal and transportation of completed preforms. As trials commenced, new challenges arose. The following describes these challenges in more depth, and what solutions were determined in order to mitigate.

[1] SLPM stands for Standard Liters Per Minute

Fraying

Preforms of 6” x 6” are laid in order to attempt multiple different processing scenarios. Figure 3.6 shows an example of a completed 2 ply preform. It can be seen that both beginnings and ends of the preform show dry fibers that are frayed. It is observed that this fraying is caused by the pressure of the exiting nitrogen gas from the HGT. These trials demonstrate that we are capable of creating small preforms, but the fragile nature of the dry fiber tows cause them to fray, in some cases even blow away, due to the HGT pressure.

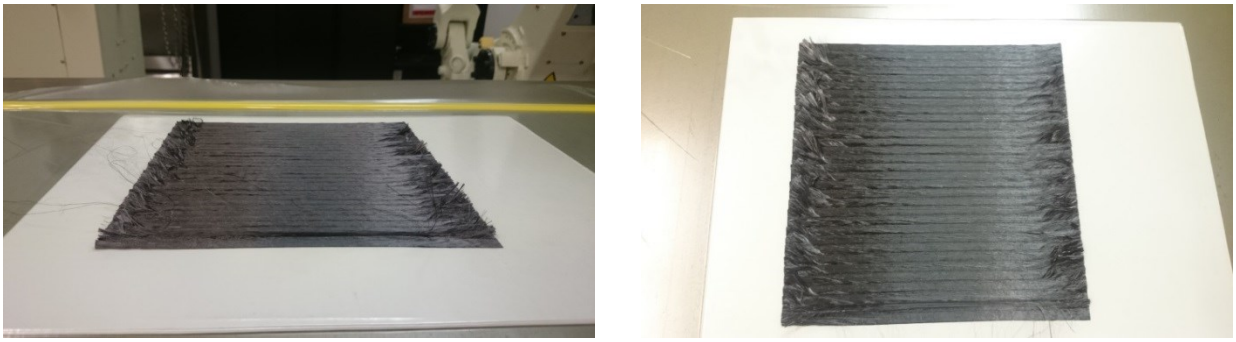

a) Side view b) Top view

Figure 3.6: Example of 6”x6” $[0]_2$ preform

In addition, due to the geometrical design of the exit nozzle, the heated nitrogen impacts the incoming tows at an angle, as depicted in the schematic of Figure 3.7. The angle of impact of heated nitrogen promotes fraying at beginnings, and ends of tows.

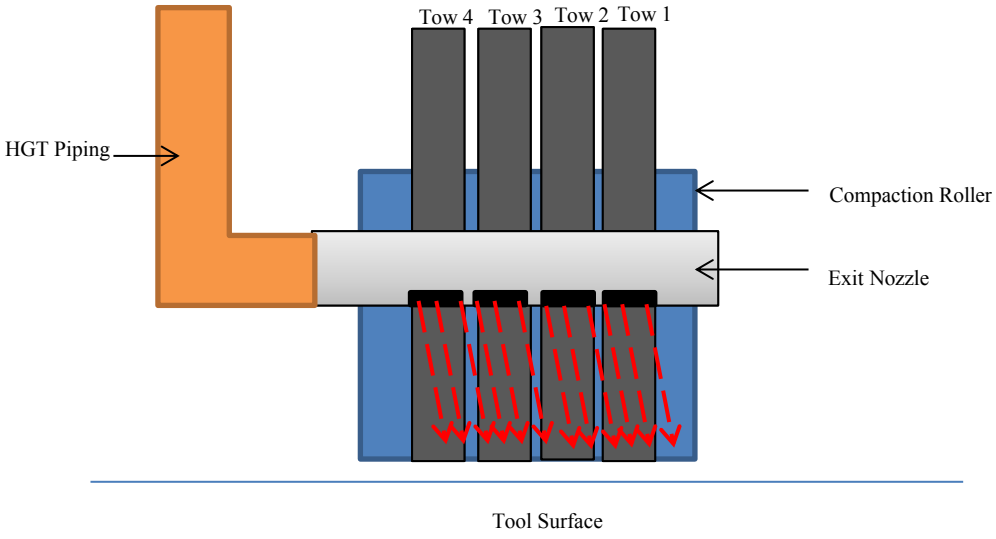

Figure 3.7: Schematic of HGT Nozzle at Roller

Before attempting to modify the AFP nozzle exit design, parameters such as nozzle flow rates are reduced. The AFP is capable of placing dry fiber tows and activating the thermoplastic binder at flow rates as low as 45 slpm. It was observed that lower flow rates become problematic in distributing heat to the surface. A consequence to reduced flow rates require the nozzle height to be placed closer to the tool surface, roughly 6mm. By significantly reducing flow rate and placing the exit nozzle closer to the tool surface, preform fraying is eliminated. A preform of 6" x 6" of [0/0/45/90] sequence is successfully manufactured without fraying as shown in Figure 3.8.

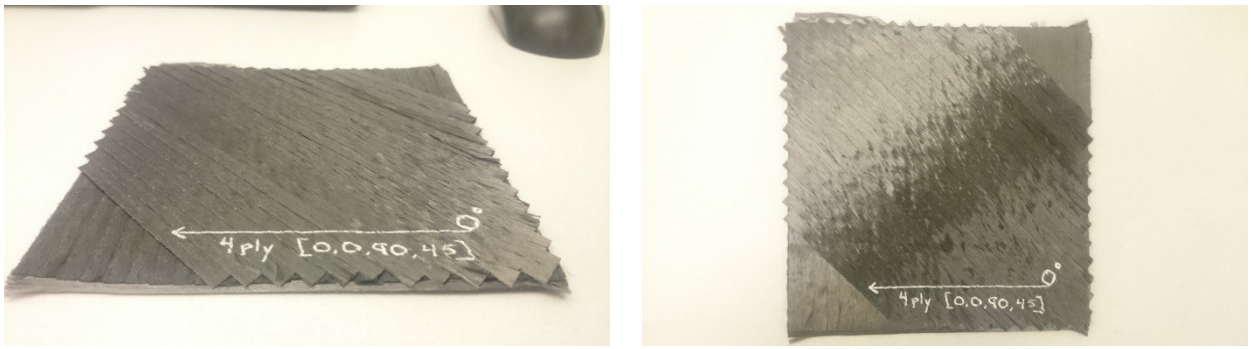

a) Side view b) Top view

Figure 3.8: 6" by 6" [0/0/90/45] preform manufactured using AFP

As the process window becomes more defined, larger preforms are manufactured that will be infused using VARTM. However, when scaling up preform size and the amount of plies, new difficulties begin to arise which affect the preform quality.

Roll-ups

During the manufacturing of an 8 layer preform, 12" x 22" of $[0/90]_{2S}$ stacking sequence, two new issues arise that have not been captured during previous trails and testing. The first issue occurs when dry fiber tows stick to the compaction roller's surface during a pass, rather than remaining on the tool surface. This phenomenon occurs only at the beginning of each pass, and is

termed as a roll-up. A roll-up is detrimental as dry fiber tows become entangled in the roller, and is capable of damaging and peeling tows of the preform that have been previously deposited.

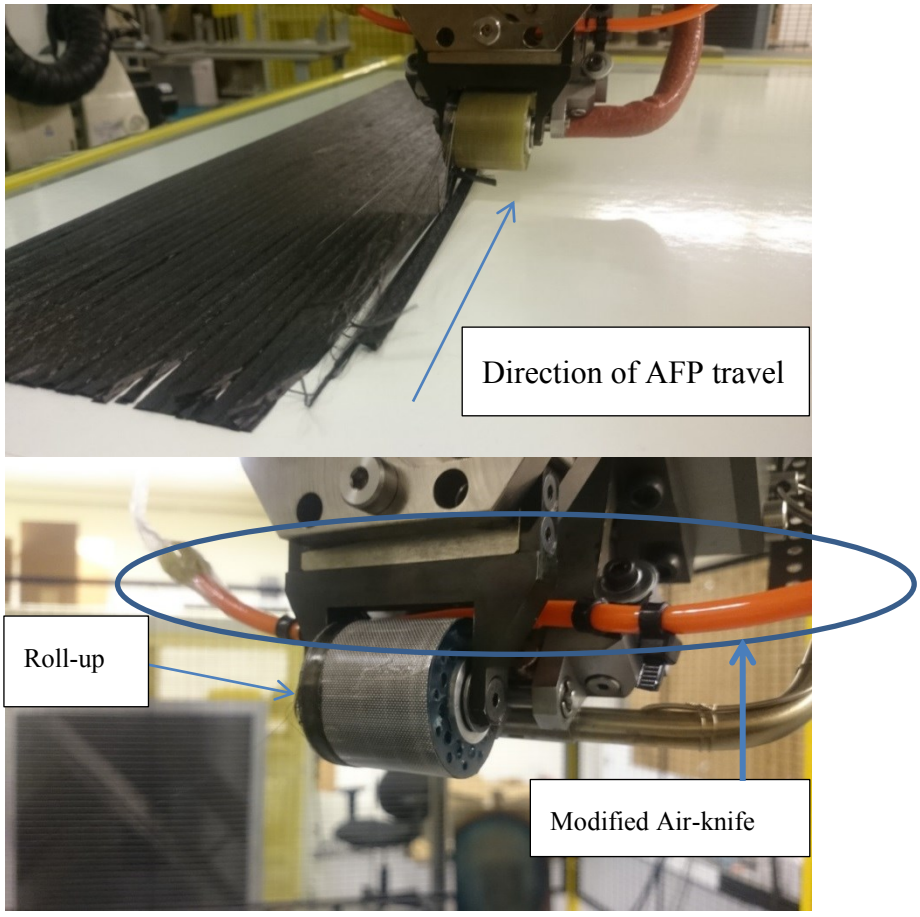

Figure 3.9: Example of a Roll-up defect during AFP manufacturing

The cause of roll-ups is associated to the roller retaining too much heat during AFP operation, causing thermoplastic binder of the dry tapes to activate and tack itself to the roller. This effect was not captured when testing smaller 6” x 6” preforms, as the AFP performed shorter passes. Larger preforms required longer and larger number of passes of the AFP which cause the compaction roller to absorb more heat causing roll-ups. The AFP thermoplastic head is equipped with an air-knife, an instrument which blows cool nitrogen gas behind the compaction roller during its operation. Utilizing the air-knife is critical to keep the roller cool to avoid roll-ups during longer operation. The air-knife mounted to the AFP head is shown in Figure 3.10. This gives rise to the second issue observed, due to its location and design a similar fraying effect of

the dry fiber tows is observed when applying the air-knife, as seen previously from the HGT. To counter this, a modification of relocating the position of the air-knife to an area in which its flow cannot affect the preform is achieved. This modification can be seen in Figure 3.9.

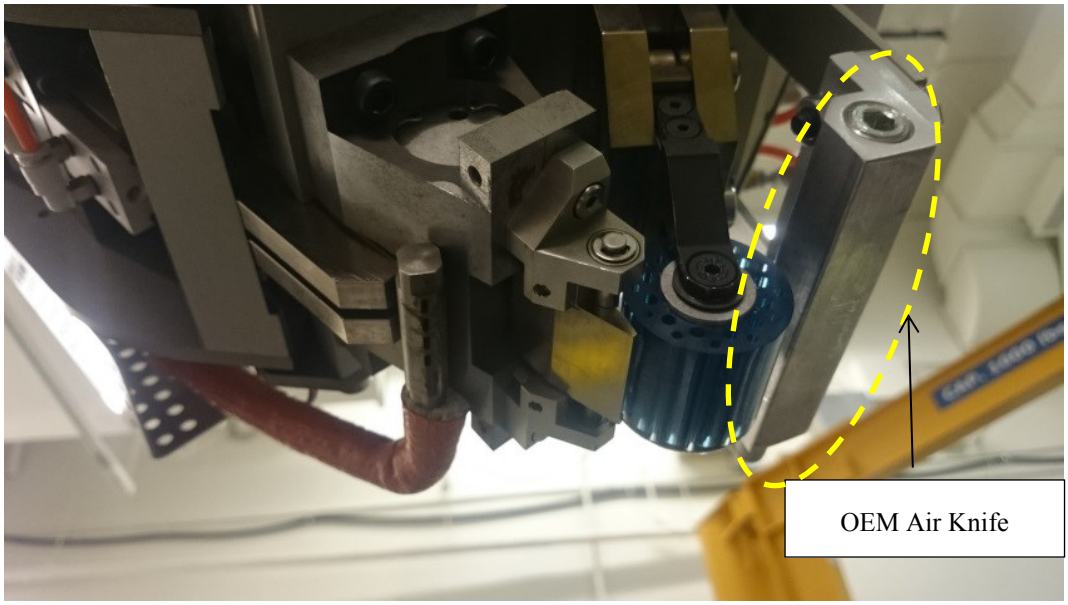

Figure 3.10: OEM placement of air-knife

By utilizing the air-knife modification and its placement, continuous operations is achieved without any occurrences of roll-ups.

Preform lifting

The first layer of preform manufacturing is the most critical to obtain a high quality preform. It serves as the foundation of all subsequent plies. In order for dry fiber tows to tack to the vacuum bagged surface, a slow feed rate is required to assure good adhesion of the first ply. A first ply feed rate of 1 inch/sec is found to be suitable, and is used for all preform manufacturing. Once the first ply has been successfully laid, feed rates can be significantly increased for all subsequent plies. This is because the incoming dry fiber tows are deposited on a surface of similar material, which also is coated with a thermoplastic veil. Speeds as high as 6 inch/sec have been achieved using our AFP. However, the ADC robotic arm is not designed for high feed rates

and as a result fiber placement accuracy is degraded, and jamming of the internal head feeding mechanism occurs. A feed rate of 4 inches/sec for subsequent plies is found to be suitable without significant degradation of accuracy, and no occurrences of tow jamming within the head feed mechanism.

These optimized parameters were implemented when creating larger preforms meant to be used for VARTM infusion. When surpassing 5-6 layers, preform lifting from the tool surface began to occur. The preform lifting is caused by the preform becoming more rigid as more plies are added, and the 1st ply's adhesion to the tool surface is not sufficiently strong to hold the preform down when building thicker laminates. This would cause the free edges of the first ply to begin to peel from the bagged surface on the tool. Once the preform edges begin to peel from the bagged tool surface, the quality of the preform degrades drastically over additional passes. There are two methods of manufacturing that have been shown to mitigate this issue. The first is to build a preform in a staggered sequence. For example, the first ply of the preform would be oversized, and subsequent plies would be built inwards of the first ply and offset continuously by 0.25". Figure 3.11 shows a cross-section schematic of what a staggered preform would look like. Once the preform is completed, any material remaining larger than the last ply is trimmed off.

Figure 3.11: Example of side view of staggered preform

The second method found to be suitable is to tape down the free edges of each ply using masking tape. The entire preform would be oversized by 0.5" in length and width. Once preform is completed, the masking and excess edges are trimmed off.

Figure 3.12: Example side view of a Taped down preform

The method of taping down preforms has proven to be the most simple and effective method of ensuring no preform lifting. It is a quick procedure to tape down edges, and far more simple to program building such a preform in AFP software. In addition, as preforms to be manufactured are up to 24plies thick, it significantly reduces the working area required, in turn reducing the amount of time needed to manufacture, as well as reduces the amount of excess required to be trimmed.

Multi-tow processing

The ADC AFP thermoset head is capable of up-to 4 tows placement at a time. During trialing it was shown that the AFP is capable 4 tows placement, utilizing its maximum laydown capability. However, for the first ply 3 tows placement was used, as the 4^{th} tow showed difficulty adhering to the bagged tools surface. This difficulty can be associated back to the HGT nozzle design not spreading its heat evenly around the roller.

Summary

In overview of the challenges and solutions determined to successfully process dry fiber preforms using AFP equipped with HGT as a heating source, Table 8 describes all the parameters that have been used to manufacture dry fiber preforms for infusion.

Table 8: AFP Processing Parameters

AFP Processing Parameters		
Parameters	1st Ply	All subsequent plies
Feed rate (inch/sec)	1	4
Multi-tow placement	3	4
Pressure (lbf)	70	70
HGT Temperature (°F)	350	350
HGT flow rate (slpm)	45	45
HGT nozzle height (mm)	6	6
HGT nozzle angle (deg)	57.5	57.5
Air-knife setting (valve turns)	6	6

In addition Table 9 lists all of the preforms successfully manufacturing using the optimized parameters.

Table 9: List of dry fiber preforms manufactured for VARTM infusion

Preforms Manufactured		
Layup Sequence	Preform Size (W x L)	Total Plies
$[0]_8$	12” x 24”	8
$[0]_{16}$	12” x 16”	16
$[0/90]_{2S}$	12” x 22”	8
$[0/90]_{4S}$	12” x 16”	16
$[45/-45/0/90]_{2S}$	12” x 22”	16
$[45/-45/0/90]_{3S}$	12” x 26”	24

3.2.4. Tailored Preform Gaps

Automated fiber placement allows for new possibilities of preform tailoring which would not be possible using traditional hand layup methods. Recent studies have shown that gaps can increase the permeability of the preform, which would reduce processing time, in turn reducing operational costs. The permeability of a dry fiber preform represents the amount of liquid, in our case epoxy resin, capable of flowing through. The higher the value of permeability, the easier the liquid can flow through. A part of this study is to evaluate the effects of gaps on preform permeability. Figure 3.13 shows a visual representation of a gap placed between two bands of a ply. For tailored preforms, all bands consist of four 0.25" (6.35mm) tows.

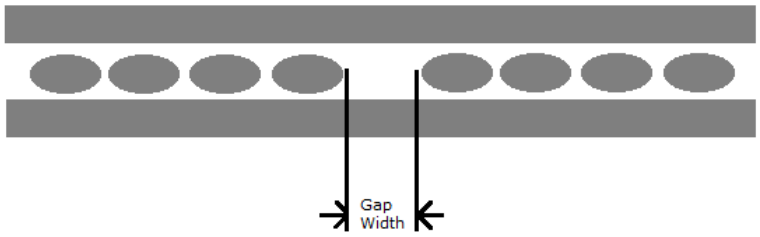

Figure 3.13: Schematic showing an example of induced gap between a band of tows

Fundamentally, gaps can act as 'resin highways' within the preform, allowing increase permeability and resin wet out. An initial test matrix is created in order to quantify the size and amount of gaps that will be induced in a preform for evaluation.

Table 10: Test Matrix for Tailored Gapped Preforms

Scenario	**A**	**B**	**C**
Size of Gap Width	1 mm	2 mm	4 mm

The gap size widths listed in the test matrix shown in Table 10 are arbitrarily chosen. AFP precision and industry limits to tow gaps are taken into consideration. Each scenario is to have a

preform manufactured in both unidirectional and cross-ply orientations. The importance of evaluating both unidirectional and cross-ply orientations is to confirm if channels within unidirectional preforms are not being blocked off during the AFP manufacturing process. Listed in Table 11 are preforms successfully manufactured with tailored gaps. It can be seen that the only Scenario C was evaluated from the initial test matrix. Its results and reasoning are later described in section 4.1, Evaluation of VARTM Flow Front.

Table 11: List of Tailored Preforms Manufactured for VARTM Infusion

Tailored Preforms Manufactured				
Layup Sequence	Preform Size (W x L)	Total Plies	Gap Width Size (mm)	Scenario
$[0]_8$	12” x 16”	8	4	C
$[0/90]_{2S}$	12” x 16”	8	4	C

3.2.5. Hot VARTM Process

The technique used to impregnate and cure dry fiber preforms manufactured by AFP is known as Hot VARTM. This process follows all the steps of VARTM, but is performed inside of an oven at elevated temperature rather than room temperature. Hot VARTM is performed as the Cytec EP2400 resin system requires an elevated infusion temperature. During the infusion at elevated temperature, time is given for resin to fully infuse within the preform. The time allotted for infusion is dependent on preform size and complexity. Once fully infused, the infusion channels are blocked off, and oven temperature is increase to final cure temperature. The steps of the Hot VARTM process are described below:

Mold preparation

A flat aluminum tool is used as a mold surface. The tool is cleaned with acetone, and release agent is applied. Once all coats of release agent are applied and allowed to cure, dry preform is placed onto the tool surface followed by peel ply, flow media, and spiral tubing used for infusion is installed.

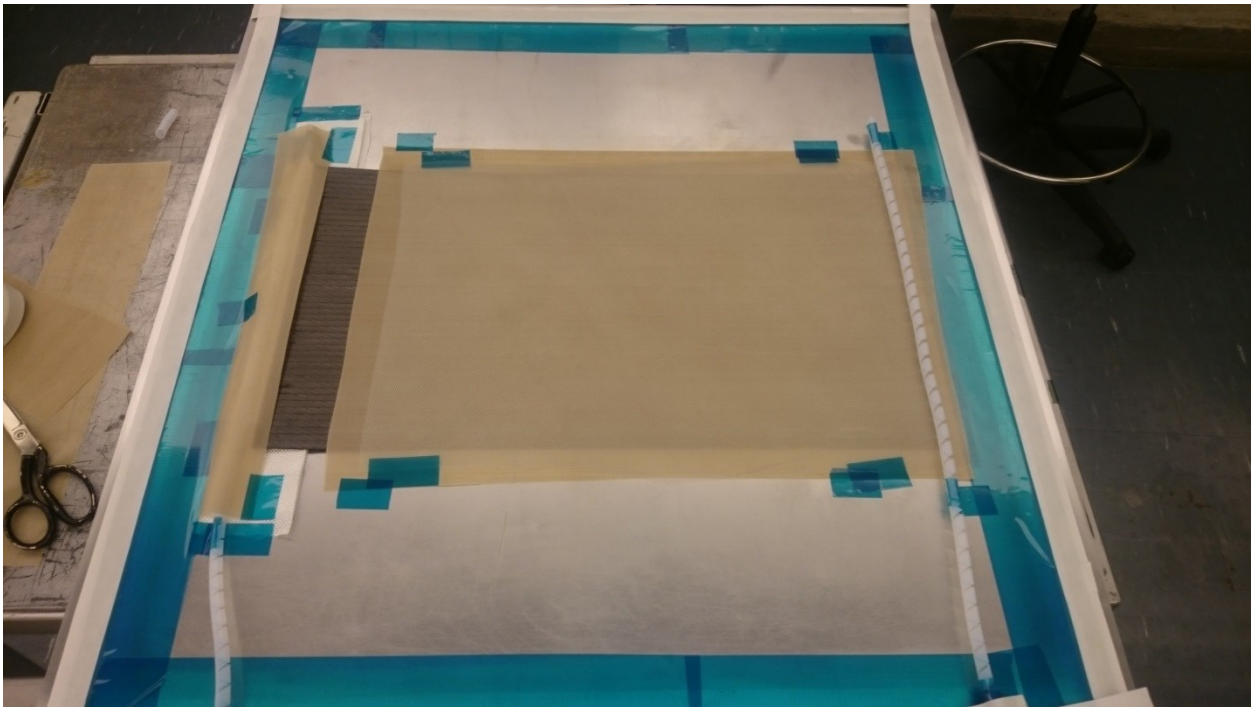

Figure 3.14: Prepared Preform for Infusion

Bagging

Placing sealant tape along the edges of the tool, vacuum bagging material is placed over the preform and material described in the mold preparation. Special attention is taken in order to insure a perfect bag with zero air leaks. Any leaks in the bag will result in air entering into the preform during the infusion, which would be disastrous to the final laminate quality.

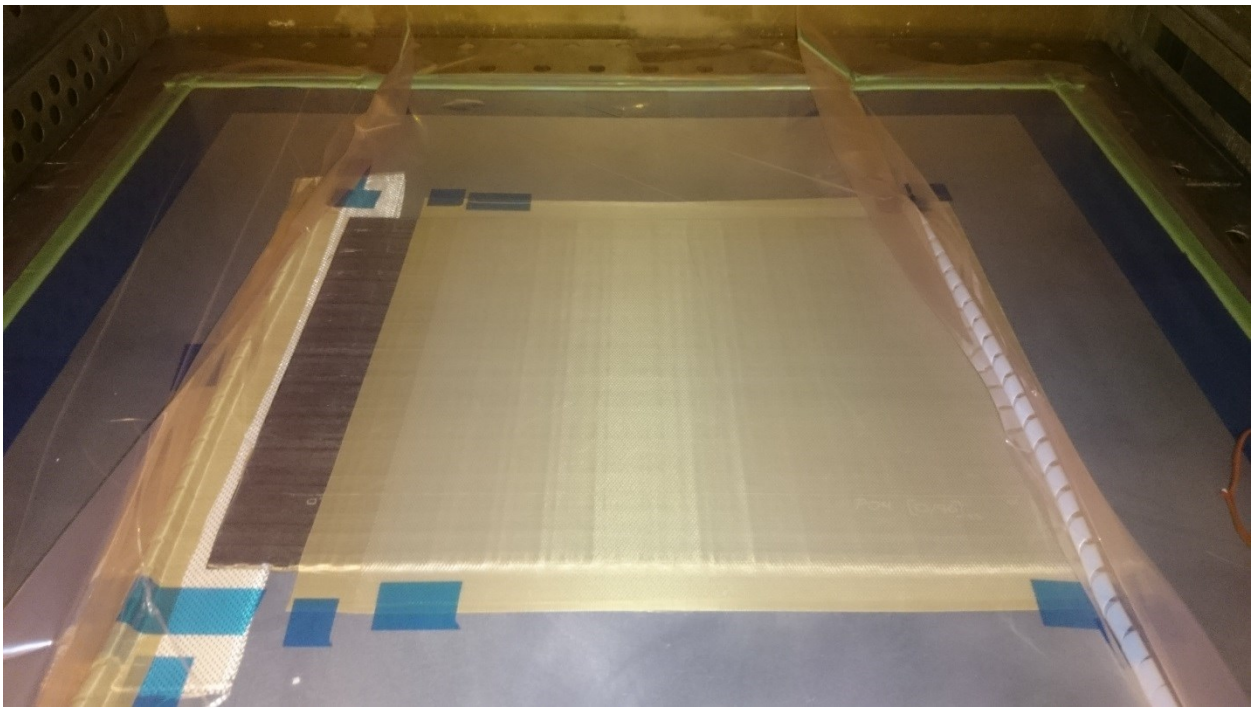

Figure 3.15: Laminate after Bagging and application of Vacuum

Degassing

This process can be started simultaneously when preparing the mold. A measured amount of resin that will be used for the infusion is placed into a container, and into the resin degassing system. It is important to weigh out the correct amount of resin for the infusion process to insure the proper amount. Too much resin could result in an uncontrollable exothermic reaction, too little would result a laminate not fully impregnated. Volumes of resin pots, resin inlet and preform weight are needed to determine amount of resin required to degas. The following equation is used as a guideline to determine resin amount by weight for infusion.

$$W_{resin} = \left(W_{preform} \times 0.5\right) + \rho_{resin}\left(D_{pot} \times h_{pot}\right) + \rho_{resin}\left(D_{tubing} \times L_{tubing}\right) \quad (2)$$

Where:
D_{pot} = Diameter of resin pot
D_{tubing} = Diameter of inlet and outlet tubing
H_{pot} = Height of resin pot
L_{tubing}= Total length of inlet and outlet tubing
ρ_{resin} = Density of resin

The equipment used to perform degassing is a Radius Engineering External Degassing System. A resin degasser is used to remove air that is entrapped in the resin. This process is crucial to ensuring low porosity in the manufactured laminate. The resin manufacturer suggests degassing at a temperature of 90°C for 30-45minutes [37]. Degassing system and example of resin in the process of degassing is shown in Figure 3.16.

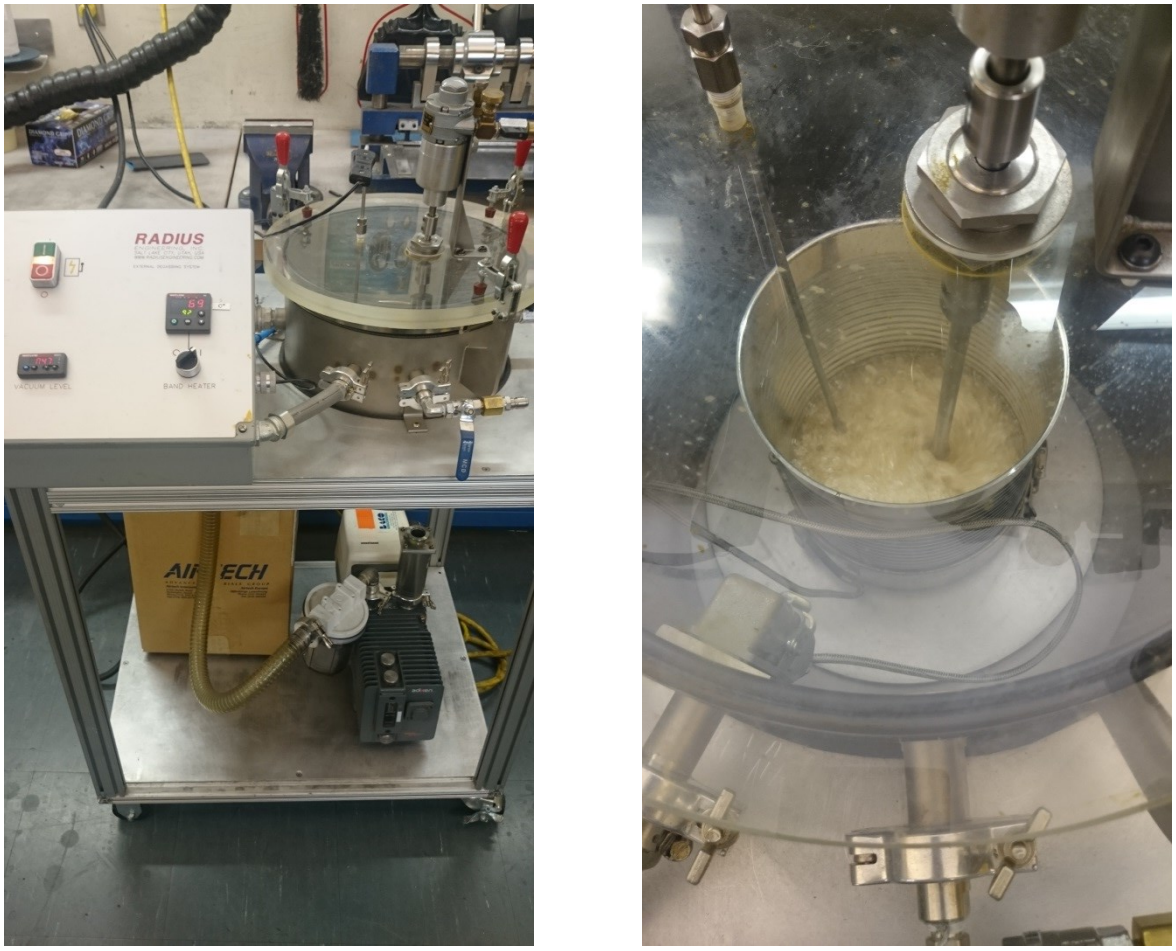

a) Resin degassing equipment

b) Resin in the process of degassing

Figure 3.16: Radius Engineering External Degassing System

Infusion

A list of material and equipment used to perform infusion is as follows:

- Oven
- High temperature plastic tubing
- Hose clamps
- Vise grip
- Resin Pot
- Resin Catch Can
- Vacuum
- Timer
- Marker

The catch can's purpose is to allow the resin to flow into the preform, and any excess resin to bleed into a reservoir without inhibiting the vacuum. The catch can is located at the end of the outlet port of the spiral tubing. A depiction of the VARTM process is shown in Figure 3.17.

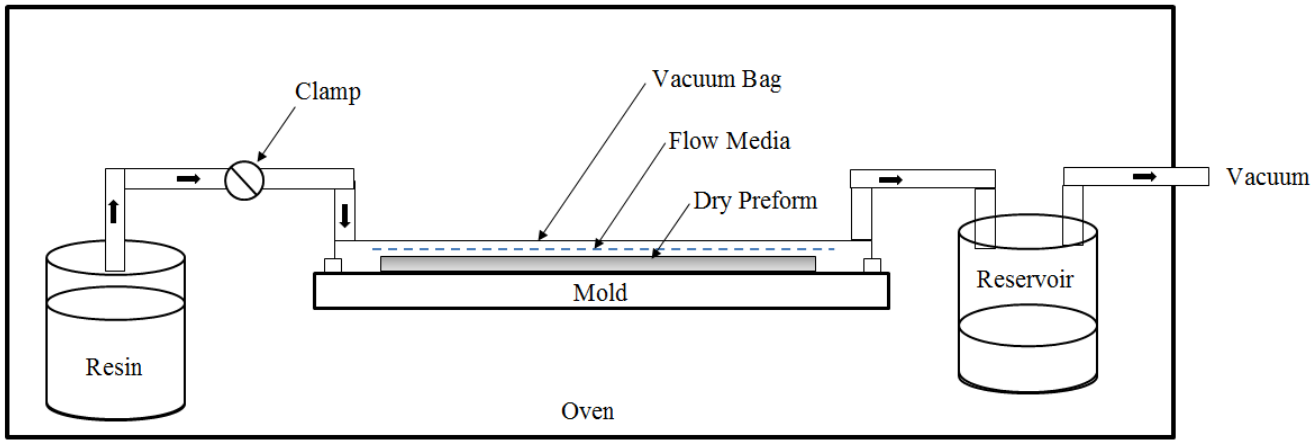

Figure 3.17: Schematic of the VARTM process

The following steps are used to infuse a preform:

1) Place mold, catch-can, and degassed resin into the oven.
2) Place inlet plastic tubing into the degassed resin, connect outlet tubing to catch can
3) Clamp inlet tubing using vise grip, and connect catch can to full vacuum

4) All air should be evacuated from bag, ensure the bagging material sets uniformly over preform surface and no air leaks are present
5) Set oven temperature to 180°F for 30min to allow resin and tool to reach temperature
6) Recheck vacuum bag and insure no leaks
7) After being assured that no leaks are present, release clamp from inlet tubing to commence infusion
8) At moment of releasing clamp, begin timer
9) Mark the location of the flow front with respect to time
10) Allow time for resin to flow through media and into entire preform
11) When preform has been entirely infused, re-clamp the inlet and ramp the oven to final cure temperature
12) Once cure cycle is completed, and sufficient time is allowed for oven to cool down, remove tool
13) Record distances of markings with respect to the inlet spiral tubing, and debag laminate

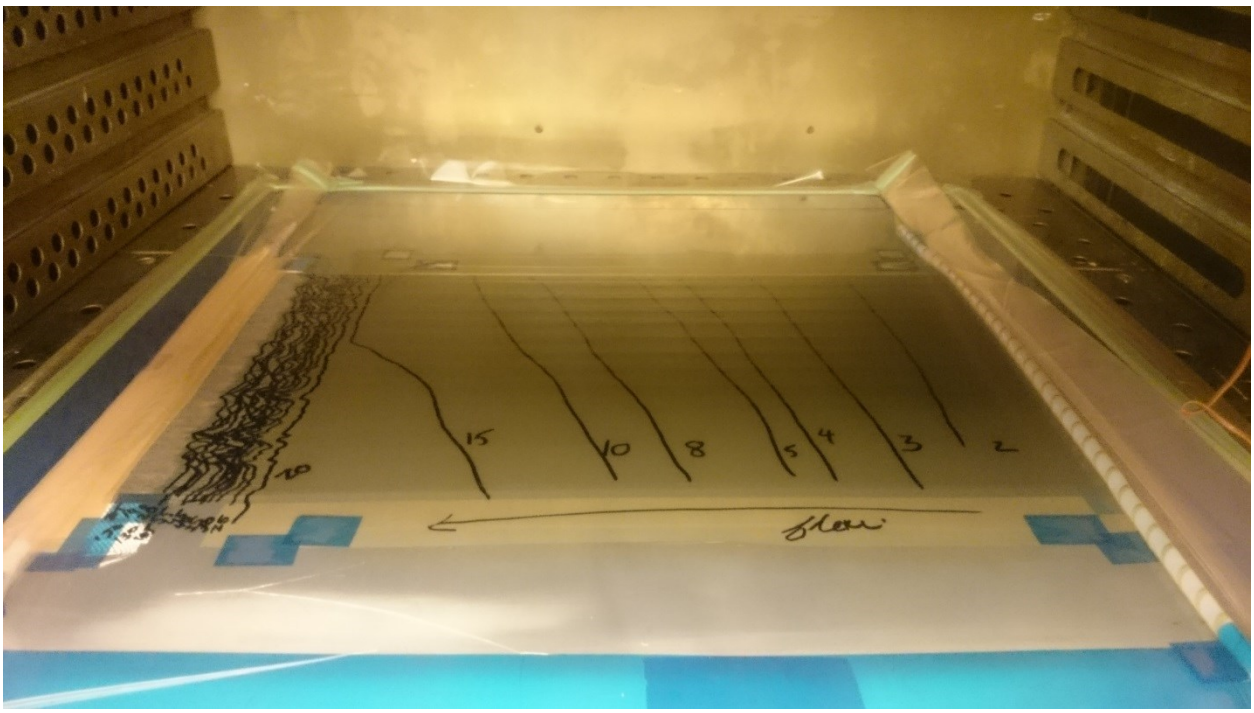

Figure 3.18: Example of Infusion Process completed before Ramping up to Final Cure

3.3. Quality Control

In order to quantify the quality of the laminates manufactured by DAFP VARTM, a series of tests are performed such as investigation of resin viscosity, determining glass transition temperature of cured laminate, as well as microscopic evaluation of laminate cross-sections to determine fiber volume content and porosity.

3.3.1. Resin Viscosity

In order to determine if the Cytec EP2400 resin system used for VARTM infusion is within its operating viscosity range of less than 100cP at temperatures between 100-120°C [37], as stated by the manufacturer, a resin viscosity test using the Brookfield CAP 2000+ Viscometer is performed. The technical data sheet of manufacture provides data of resin viscosity versus temperature, ranging from 60-140°C, shown in Figure 3.19. A best fit curve is added to this plot and shows to be a power trendline. This is confirmed by the R^2 value being very close to 1, showing good fit.

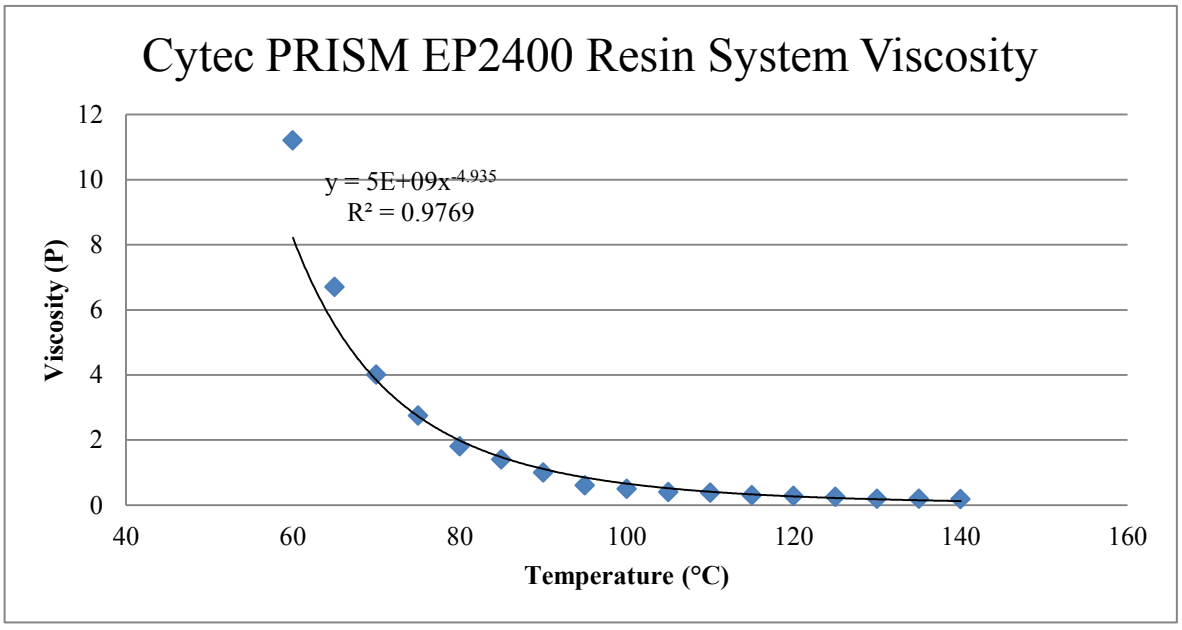

Figure 3.19: Cytec PRSIM EP2400 Viscosity versus Temperature Properties [37]

A Brookfield CAP 2000+ Viscometer, shown in Figure 3.20, is used to determine resin viscosity. The rotational viscometer is capable of determining a fluids' viscosity by measuring the amount of torque required to rotate a spindle against the fluid at a given speed. Rotational speed selection ranges are from 5 to 1000 RPM. Viscosity is selectively displayed in units of centipoise (cP). Temperature control of sample is possible between 5-75°C [38]. A sample of the batch of EP2400 resin system used for VARTM is tested, and results of resin viscosity versus temperature are plotted graphically.

a) Brookfield CAP 2000+ Viscometer

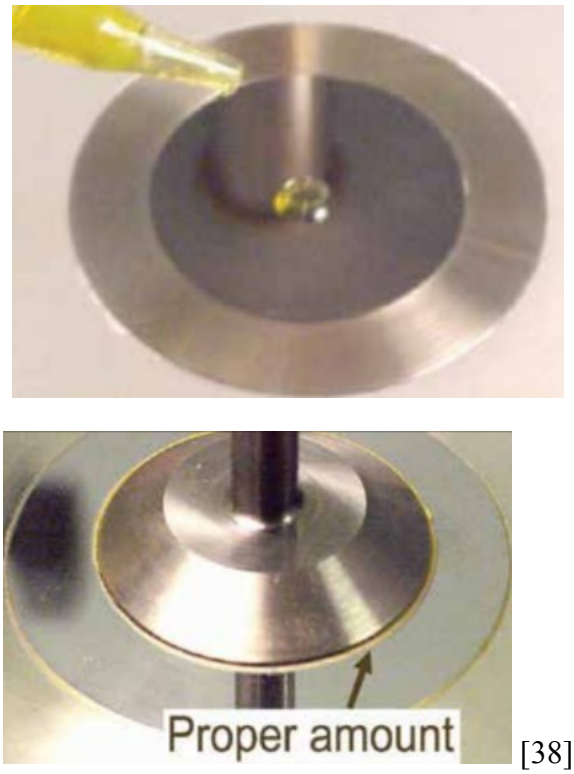

[38]

b) Example of fluid applied to surface for measuring viscosity

Figure 3.20: Brookfield Viscometer Used for Resin Viscosity Evaluation

The Brookfield instrument equipped hot plate capable of reaching a maximum of 75°C. This maximum temperature limit of the hot plate allows us only to experimentally determine viscosity up to 75°C. A sweep is performed from 60-75°C, and viscosity data is recorded. From Figure 3.19, we expect to have a similar slope with the recorded experimental data. Plotting a best fit

curve to the experimental data of 60-75°C, and evaluating R^2 value being almost exactly to 1, we are confident the experimental data follows a similar power trendline presented in Figure 3.19. In order to evaluate our current resin system beyond 75°C, the power trendline from the experimental data is extrapolated up to 120°C allowing to compare with the provided manufacturers resin viscosity data, shown in Figure 3.21.

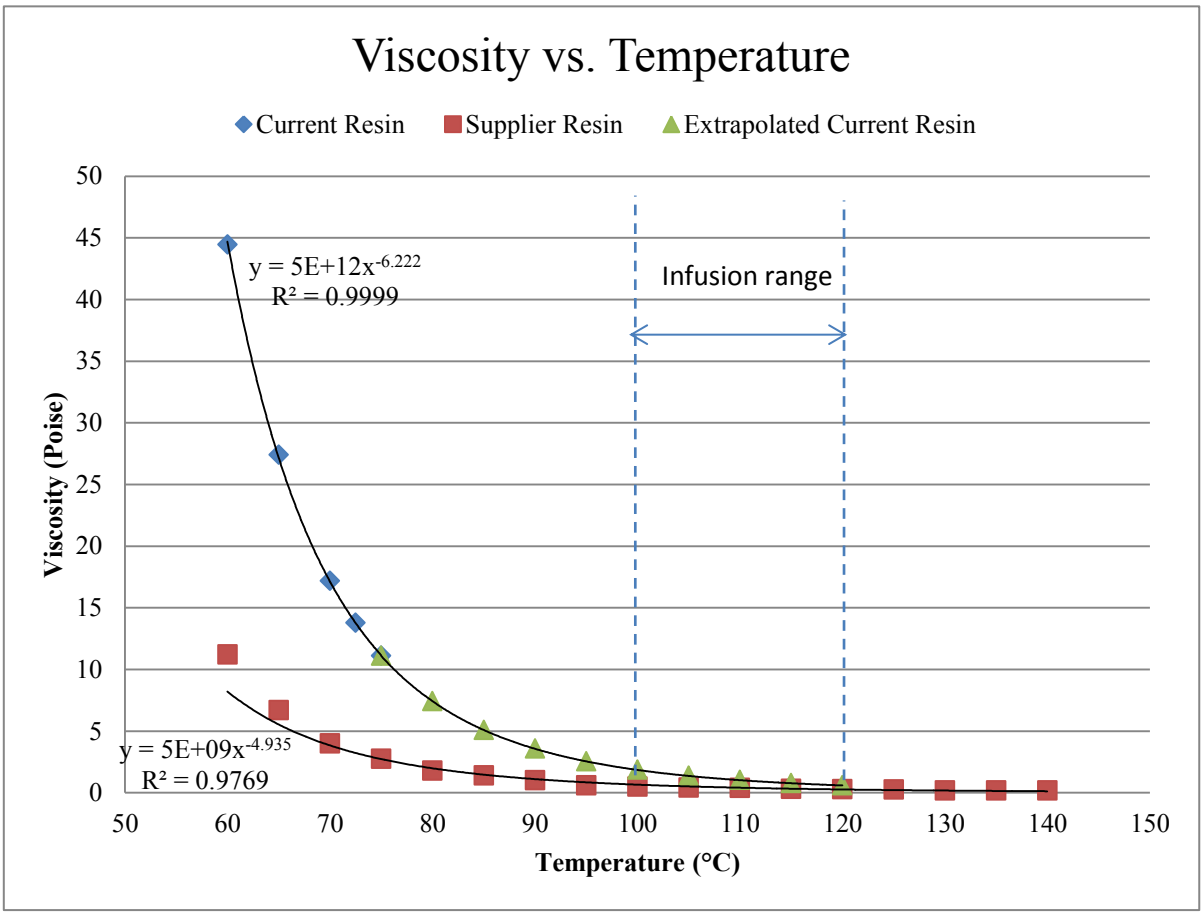

Figure 3.21: Comparison of Tested Resin Viscosity and Manufacture Resin Viscosity Data

The 'Current Resin' represents the experimental viscosity data recorded using the Brookfield viscometer of 60-75°C. The 'Extrapolated Current Resin' represents the extrapolated viscosity curve based on the power trendline equation from the experimentally recorded data. The 'Supplier Resin' represents the viscosity data provided by the technical data sheet of the manufacturer. It can be seen that the resin system used for this dissertation shows to be more

viscous at lower temperatures of the graph when comparing to fresh resin. However, at injection temperatures, is capable of reaching a less than 100cP viscosity as stated by the manufacturer. It is important that the resin system can attain viscosity range described by the manufacturer in order to achieve successful infusion, and wet out of all preform fibers.

Signs of higher viscosity can be an indication that the resin system has begun premature cross-linking. Premature can be associated to resin system that have passed their shelf life, or have been left out in room temperature/humid environment for an excessive amount of time. Excessively cross-linked resin prior to infusion may also affect the mechanical performance of laminate. With the data plotted in Figure 3.21, we have concluded that the resin system is within acceptable operational viscosities during infusion temperatures, the mechanical properties of the laminate are evaluated in Chapter 4.

3.3.2. Differential Scanning Calorimetry (DSC)

A DSC machine is an instrument that allows thermal properties of a given material to be analyzed. It is capable of recording heat flow change as a function of temperature or time. In the case of this study, a DSC machine is used in order to evaluate the materials degree of cure, as well as the glass transition temperature (Tg). The degree of cure represents the amount in which the laminate's resin system has reacted and cross-linked. The glass transition temperature is the temperature range in which thermosetting polymer changes from a hard, rigid state to a more compliant or 'rubbery' state [39]. A sample is taken from each laminate manufactured, and is analyzed using DSC.

Cytec, the manufacturer of the resin epoxy system indicates in their technical datasheet of the material an expected dry Tg of 179°C (354°F) using Dynamic Mechanical Analysis (DMA). DMA is an instrument which performs mechanical thermal analysis by applying a fixed sinusoidal force to a specimen and recording its change in stiffness during the process of heating the sample [40]. Like DSC, DMA is capable of determining the glass transition of a specimen, however its method is very different. DMA requires a sample of controlled geometry, in which would require computer aided machining to achieve. In addition, as multiple laminates are to be

analyzed with different thicknesses and layup orientations, DMA is not a feasible method to determine Tg of laminates.

For these reasons, DSC is the preferred method to determine Tg. However, it is not correct to compare Tg values obtained from DSC to DMA as they are two entirely different test methods, and are known to deviate in results. Published work has been performed by [41] using DSC to obtain Tg of the EP2400 resin epoxy system. The independent study preformed DSC testing one batch of 5 samples following ASTM D3418. Their obtained average results for Tg are 163.31°C, with a COV of 0.89%. The data from this published work is used as a comparison in order to confirm our experimental data using DSC.

Figure 3.22: Example of TA Instruments DSC Q200 machine

The ASTM D3418 standard is followed when operating the DSC machine. Approximately 10mg samples are placed into an aluminum pan and are processed using a Heat/Cool/Heat cycles. The first heat cycle involves heating the sample from 0°C to 225°C at a rate of 20°C/min. The initial heat cycle is performed in order to erase any previous thermal history of the material. The specimen is then quenched to 0°C (nitrogen purge rate of 50ml/m is used), which is referred to the cooling cycle. It is then finally reheated, for the second heat cycle, to 225°C at a rate of 20°C/min. The degree of cure is evaluated by observing the heat flow versus temperature of the first heat cycle to the second heat cycle. If both curves are similar, and/or overlap, this indicates that the samples have been fully cured. Should specimens not have been fully cured, the first heat

cycle would show any remaining thermal history, causing a deviation from the second heat cycle. In addition, comparing Tg of first and second heating cycles is another good indicator if the sample has been fully cured or not. A sample which has been properly cured should show similar Tg results for both first and second heating cycle. Figure 3.23 shows an example of Heat/Cool/Heat cycle performed from a sample taken from a DAFP VARTM Quasi 24ply laminate.

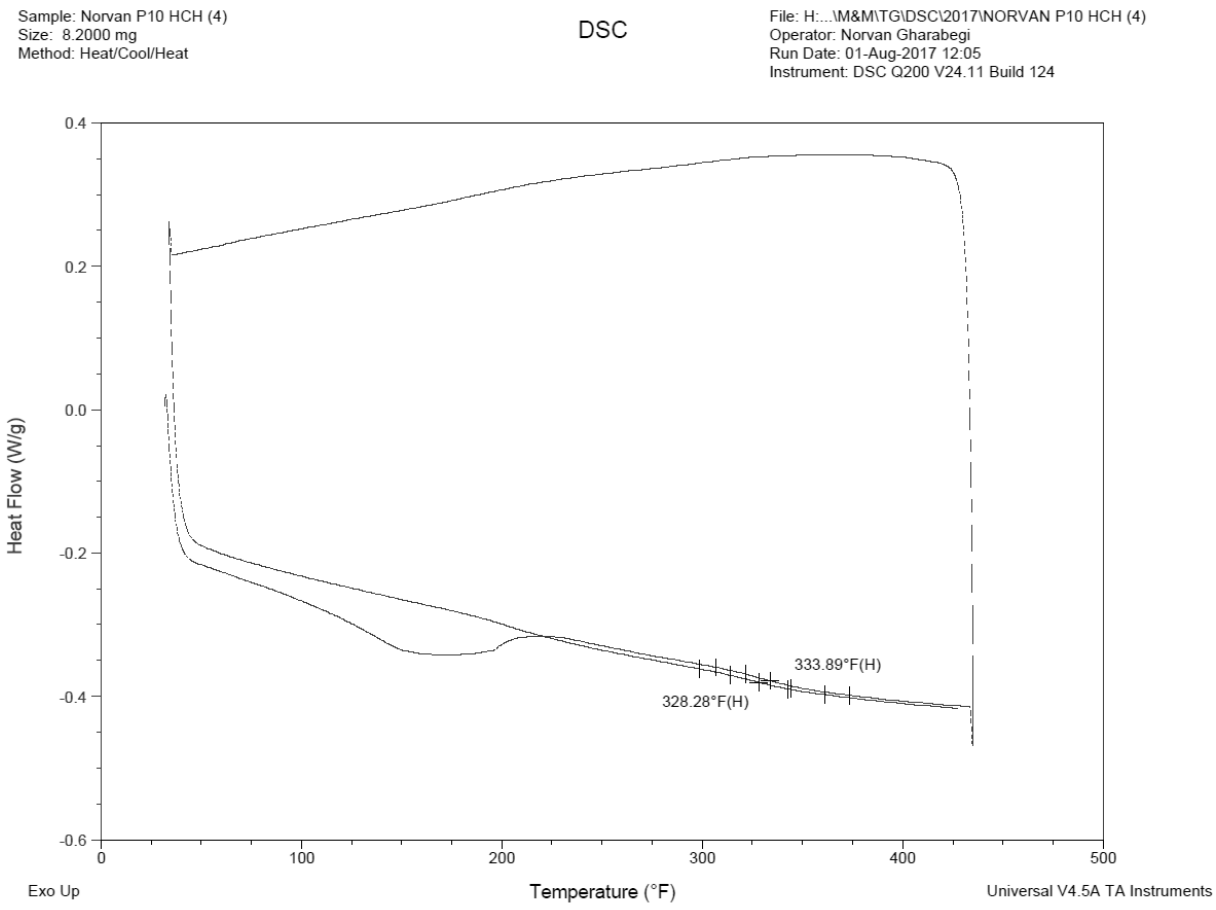

Figure 3.23: Heat Cool Heat cycle of Quasi 24ply laminate

It can be seen that both Tg values from first cycle to second cycle, 333.89°F (167.38°C) and 328.28° (164.60°C) respectively are nearly identical, and the trends of the heat flow curves are very similar. The initial deviation of the first heat flow cycle to the second, between 32-200°F (0-93°C), is associated to a factor known as an endothermic hook. The endothermic hook is an effect

seen at the beginning of programmed heating experiments and caused by differences in heat capacity of the sample and the reference pan, this effect is heightened by faster heating rates [42]. As our transition temperature is significantly past the region of the endothermic hook observed, it does not affect our results or interpretation of the degree of cure of the sample. A Heat/Cool/Heat cycle is performed on all manufactured laminates. Table 12 displays the obtained results of each laminate manufactured for mechanical testing.

Table 12: Tg Results from DSC

Layup Sequence	**Total Plies**	**Tg (°C)**
$[0]_8$	8	162.77
$[0]_{16}$	16	163.26
$[0/90]_{4S}$	16	161.89
$[0/90/45/-45]_{2S}$	16	167.08
$[0/90/45/-45]_{3S}$	24	164.60
	Average	163.92
	σ	2.02

The experimental results obtained agree with the independent published work by [41], with a 0.37% difference in average Tg results. This confirms that all the laminates used to manufacture specimens for mechanical testing have followed a proper cure cycle, and have been fully cured.

3.3.3. Microscopic Evaluation

Each laminate manufactured has samples inspected under digital microscope to evaluate the quality of the laminate in terms of fiber volume content, and porosity. This is performed evaluating cross-sections of 1” x 0.5” specimens taken from different locations of a manufactured laminate. Other methods of determining fiber volume content and porosity exist, such as ASTM D3171. Although this standard is commonly used in the industry to determine quality of composite laminates, it has its limitations. Accuracy of final results is highly dependent on precision of manufacturer technical information such as fiber and matrix density.

In addition this standard is a lengthy process, and requires handling of hazardous materials, such as nitric acid which is used to digest the epoxy matrix from carbon fibers.

Microscopic evaluation is chosen as the preferred method of analysis due to its suitable accuracy, simplicity, lower lead times, and does not require the use of costly and dangerous hazardous materials. A FeinOptic M50RT digital microscope is used for this evaluation, shown in Figure 3.24. Specimens are cut to size using diamond blade saw, then cured into a puck of resin which then is polished to a mirror finish.

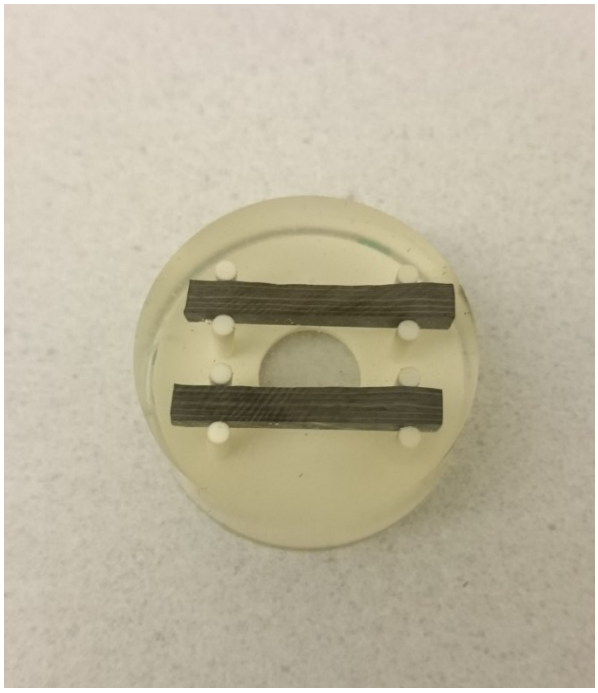

a) Polished specimens to be examined

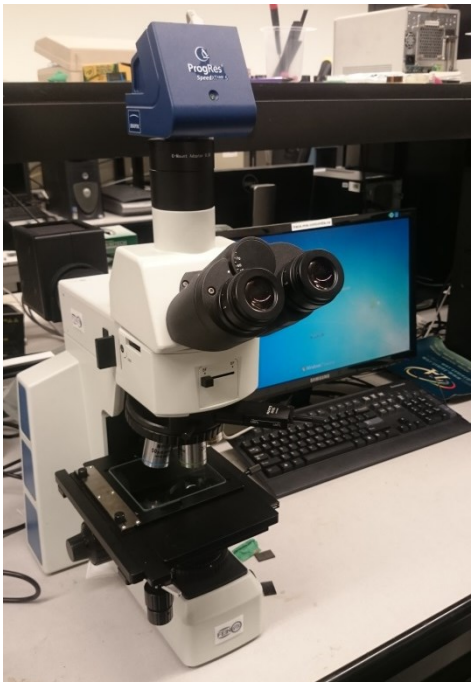

b) FeinOptic digital microscope

Figure 3.24: Specimen and Equipment used for Microscopic Analysis

Image processing software is used to determine the percent amount of fiber volume content and porosity. The software, ImageJ, is capable of stitching multiple high magnification captures together to create a seamless image of a specimen's cross-section. Secondly, it offers a feature that can distinguish between an image's grayscale, hence allowing us to differentiate between fibers, matrix, and voids in terms of percentage. For this purpose grayscale captures are used for this analysis. Fibers represents the lightest shade, matrix in the between, and voids as the darkest. Examples of captures that have been stitched to create one image for analysis of 5x and 10x

magnification can be seen in Figure 3.25 and Figure 3.26 respectively. It can be seen that the entire thickness of the sample can be captured using 5X magnification, however when increasing to 10X, the outermost plies do not fit in the envelope of the capture.

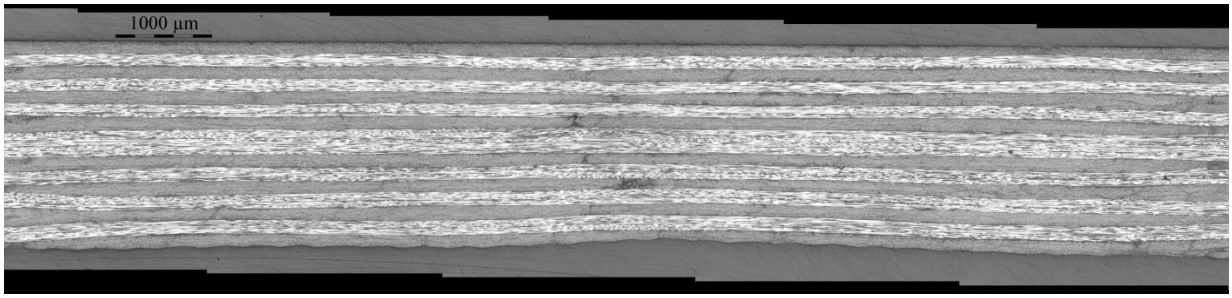

Figure 3.25: Stitched Image from [0/90]4S sample using 5X Magnification

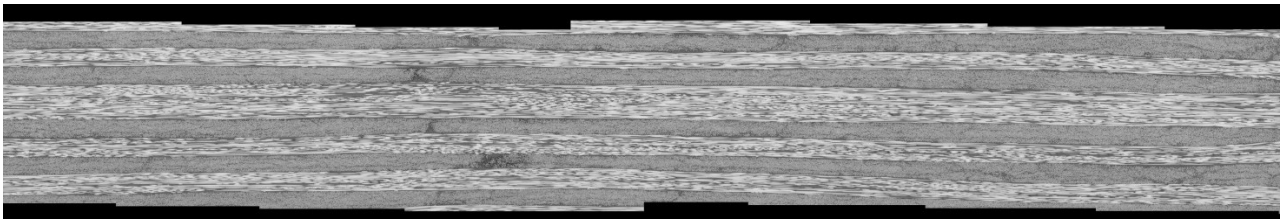

Figure 3.26: Stitched Image from [0/90]4S sample using 10X Magnification

An example of how the grayscale threshold is used to determine porosity is shown below. A capture of a cross-section is shown in Figure 3.27, in the middle regions of the capture shows there are pockets of resin rich areas, in these areas darker spots are seen which represent porosity. Using a trial an error method, setting the threshold to fixed values of 0-85 has shown to be the most consistent and representative method of distinguishing percentage of porosity found in the captures being analyzed. The software highlights the darker shades in red, which represents porosity, and determines its percentage area covered within the capture. Shown in Figure 3.28, the highlighted region that represents porosity is 0.32%. This method is used to determine the porosity of the entire specimen by stitching multiple images together to create a full capture. Three cross-sections of each manufacture laminate are evaluated in order to determine an average result of porosity. In reality, the cross-sections analyzed only represent a small section of the entire laminate. It would not be possible to analyze an entire laminate in this manner, as most of the laminate manufactured is intended to create specimens for mechanical

testing. However by analyzing multiple cross-sections at different locations of the laminate, we are able to determine a general overview of the laminates quality. Should there be any defects such as significant porosity, resin rich areas, or fiber washout, it is expected that these defects to be apparent throughout the panel as all laminates manufacture are flat and of uniform thickness.

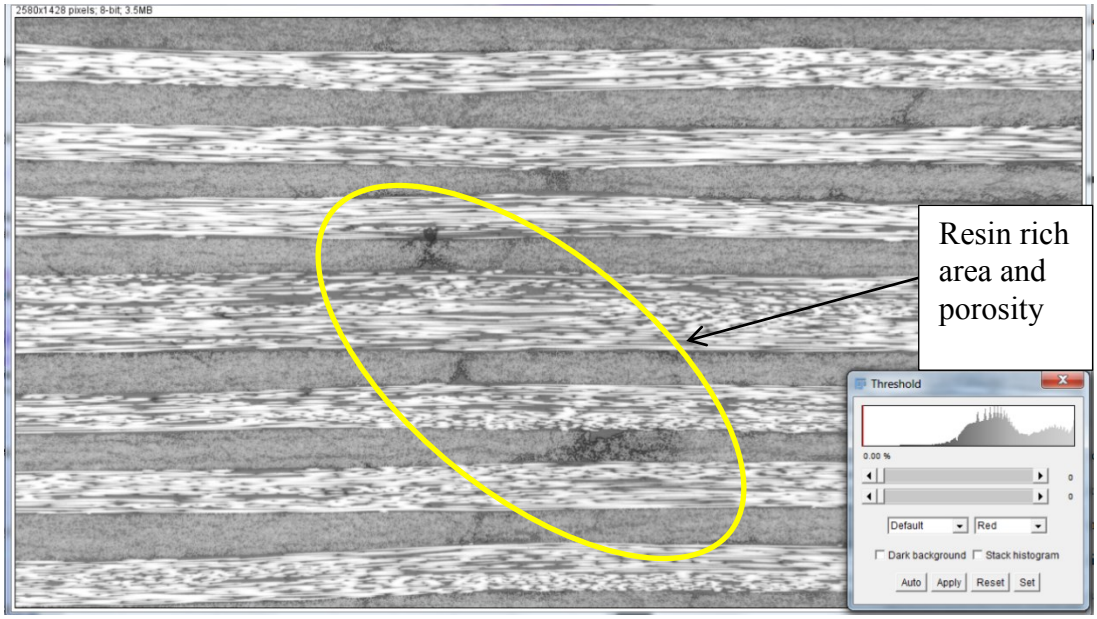

Figure 3.27: Image Capture Threshold set to Zero

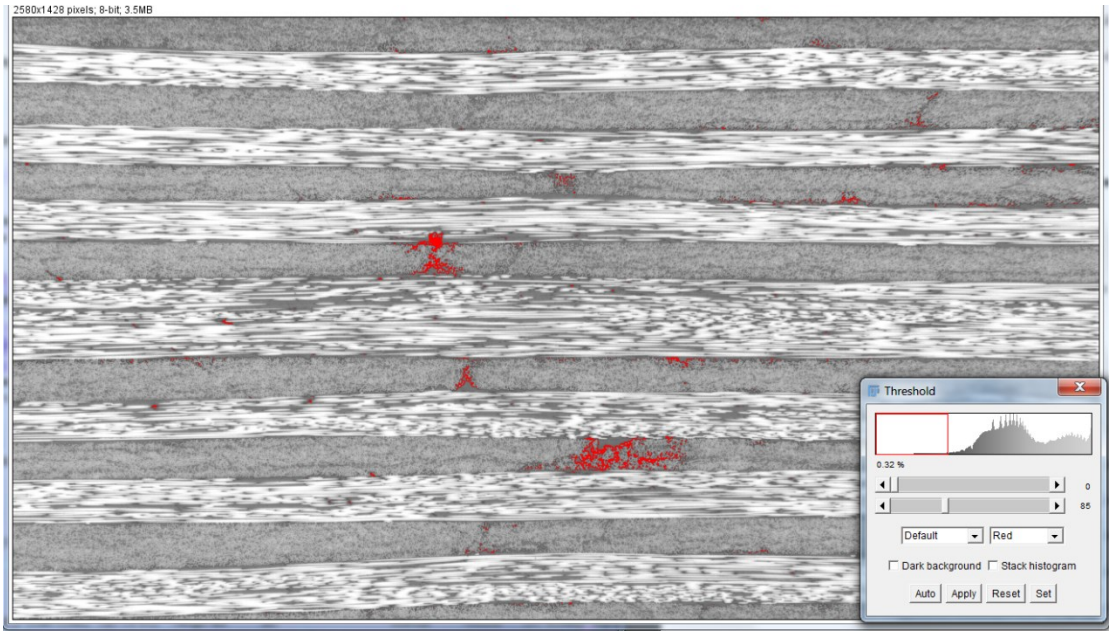

Figure 3.28: Image Capture Threshold set to 0-85, Porosity Highlighted in Red

The similar method of image analysis is used to evaluate fiber volume content, however the gray scale is inversed in order to capture the lighter shades, which in our case represents the fibers. Due to the diameters of the carbon fibers being 5.2µm [36], we are required to increase magnification to 20X in order to clearly distinguish fiber from matrix. The sections evaluated are limited to fibers facing normal to the laminate cross-section. Figure 3.29 shows an example of a magnified capture of a specimen's cross-section that has no thresholds defined.

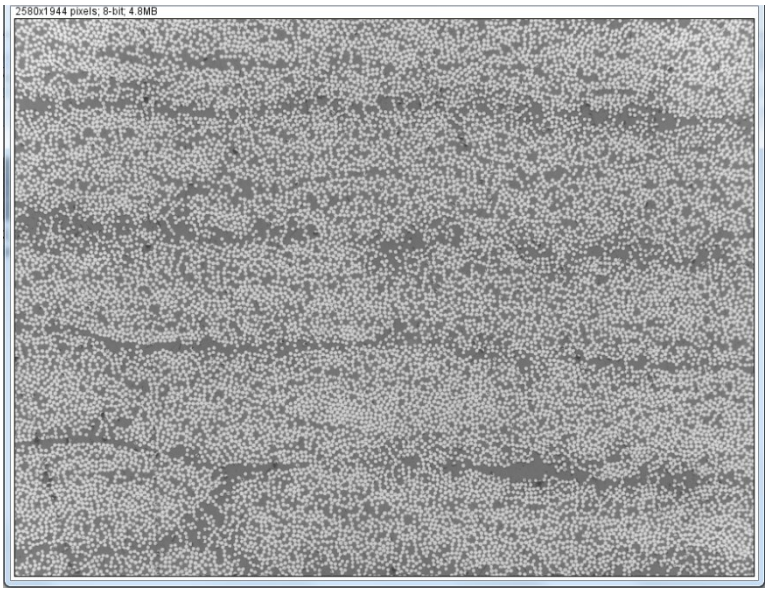

Figure 3.29: Image Capture of Fibers and Resin, default Threshold 0-255

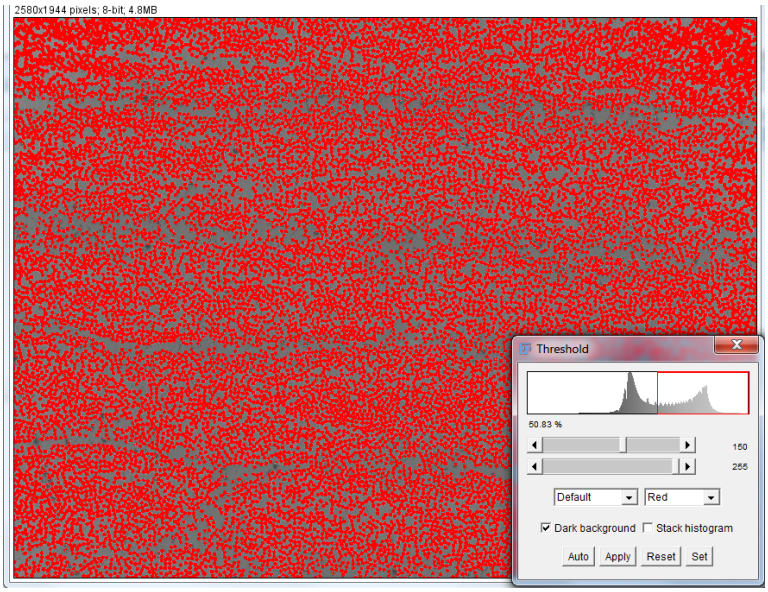

Figure 3.30: Image Capture of Fibers and Resin, Threshold set to 150-255

A set threshold of 150-255 has shown to be the most consistent and representative method of distinguishing fiber content of the images captured. With the predefined threshold, Figure 3.30 obtains a result of 50.83% fiber content. Similarly as done with porosity, multiple images are stitched together in order to evaluate the cross-section of each specimen being evaluated.

For each laminate three specimens are evaluated under microscope for porosity and fiber volume content. The samples are taken from the laminates in the following locations: near resin inlet, middle of laminate, and near resin outlet. This was performed to see if there was any effect in porosity or fiber volume content throughout laminate. Based on the evaluation, there were no notable changes or trends that suggested an effect on the laminates quality with respect to resin inlet or outlets from the VARTM infusion process. The summation of results from each laminate evaluated under microscopic image analysis is listed in Table 13.

Table 13: Results from Microscopic Evaluation of Fiber Volume Content, and Porosity

Layup Sequence	**Total Plies**	**Vf %**	**Porosity %**
$[0]_8$	8	52.1 ±0.34	0.16 ±0.04
$[0]_{16}$	16	51.1 ±0.34	0.79 ±0.03
$[0/90]_{2S}$	8	52.0 ±0.66	0.92 ±0.12
$[0/90]_{4S}$	16	50.4 ±0.46	0.61 ±0.04
$[45/-45/0/90]_{2S}$	16	52.0 ±0.61	0.29 ±0.03
$[45/-45/0/90]_{3S}$	24	51.8 ±0.93	0.51 ±0.02

Chapter 4 - Testing, Results and Discussion

This section describes methods of testing and evaluation. The subjects of evaluating VARTM flow front during infusion and mechanical characterization of DAFP VARTM laminates are discussed.

4.1. Evaluation of VARTM Flow Front

As part of the objectives set out for this dissertation, the effects of tailored gaps in DAFP manufactured preforms during the VARTM infusion process are investigated. The works presented in section 2.3 state that tailoring gaps in preforms have the potential to increase infusion by up to 65%. This statement however is based on infusing a preform alone, without materials such as peel ply or flow media conventionally used in the VARTM process. This information is practical for RTM techniques such as injection or compression molding, which utilize a top and bottom tool. However the objective is to evaluate the system using VARTM, and materials such as peel ply and flow media are essential to its process. In addition, they are typical materials which are used in the aerospace industry in order to meet production quality and demands.

The peel ply's role is to ensure good quality of surface, and to inhibit flow mesh or bagging material to adhere to the laminate when fully cured. The flow mesh's role is to aid the impregnation process and to reduce the infusion times. The flow mesh is significantly more permeable that the preform, causing the resin to flow through the flow mesh initially, and then impregnating the preform in the through-thickness direction. The flow front observed is the

combination of through thickness impregnation form flow mesh, and in-plane impregnation through preform. Therefore the flow front observed during the VARTM infusion process is similar to a cascading effect. The cascading effect during the impregnation of VARTM is depicted in Figure 4.1.

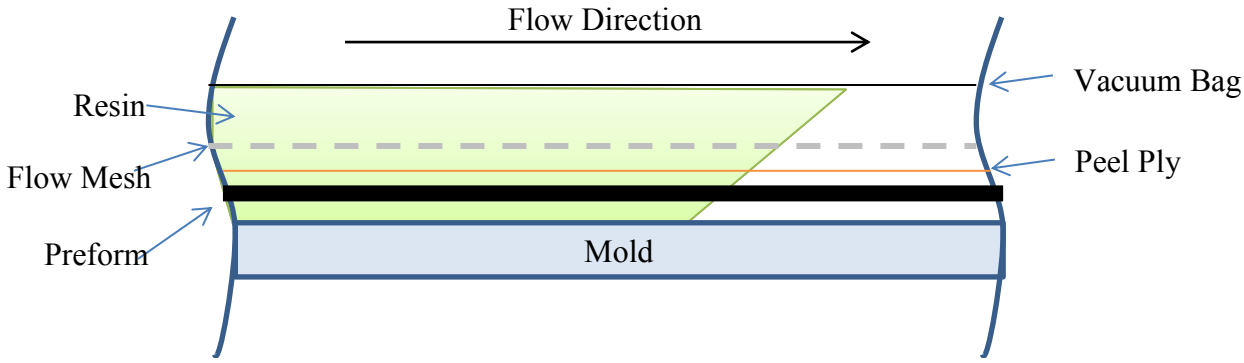

Figure 4.1: Cascading Effect during VARTM Infusion

During the course of VARTM infusion of all manufactured laminates, the flow front observed on the top bag-side of preform is monitored in terms of flow distance versus time. The first few moments of infusion are to allow flow front to stabilize once the resin inlet is opened. This is due to time 'zero' of the infusion commencing the moment when the resin inlet is opened. Once resin inlet is opened, the resin must flow into the vacant injection tubing and commence to flow into the flow mesh to begin wetting into preform.

4.1.1. Conventional Preforms

Conventional preforms refer to preforms with stacking sequences that are conventionally used in composite design such as unidirectional $[0]_n$, cross-ply $[0/90]_n$, and quasi-isotropic $[45/-45/0/90]_n$. An example of a preform that has had its flow front monitored during the VARTM infusion is shown in Figure 4.2. Each marked line represents the position of the flow front at a given moment during the infusion.

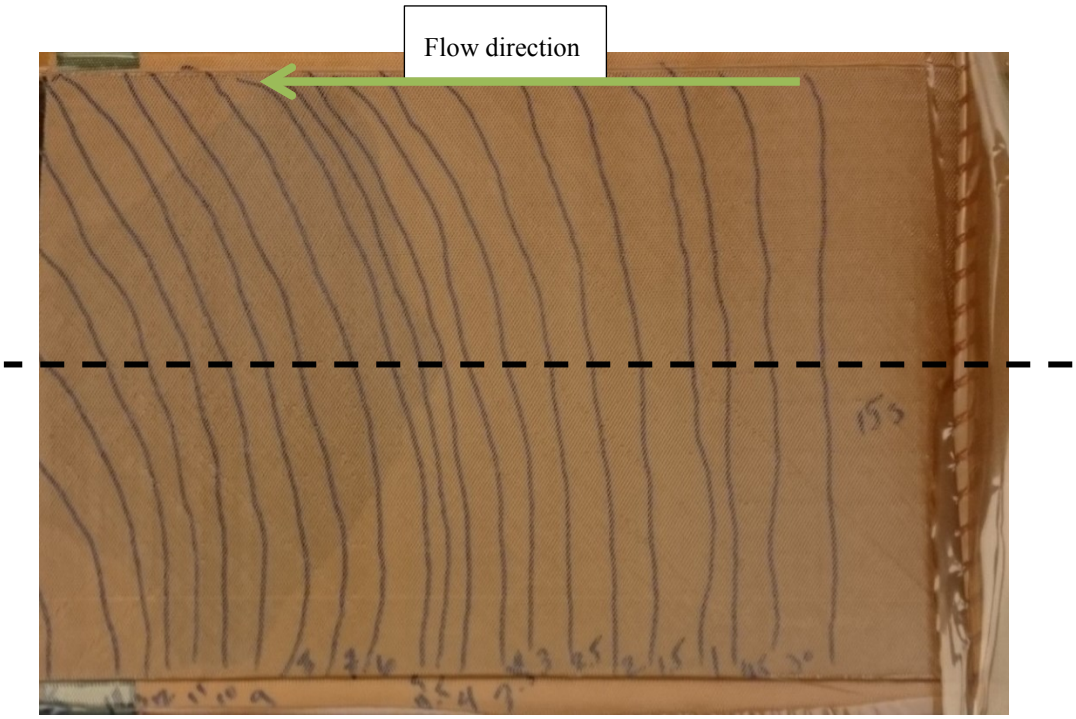

Figure 4.2: 16ply Quasi Preform after Infusion with Flow Front Markings

Each marked line is then measured in terms of distance from inlet and plotted with respect to time. For all preforms infusion, the flow front that develops is not perfectly tangential to the flow direction. This is due to the VARTM bagging resin inlet and outlet locations. For this reason during evaluation of flow front distance versus time, the middle section or the infused preform is evaluated depicted as the hashed line shown in Figure 4.2. When plotting the experimental data, it is observed that the best fit curve to the data is a power function shown in Figure 4.3.The value of R^2 shows to be very close to one, ensuring good fit.

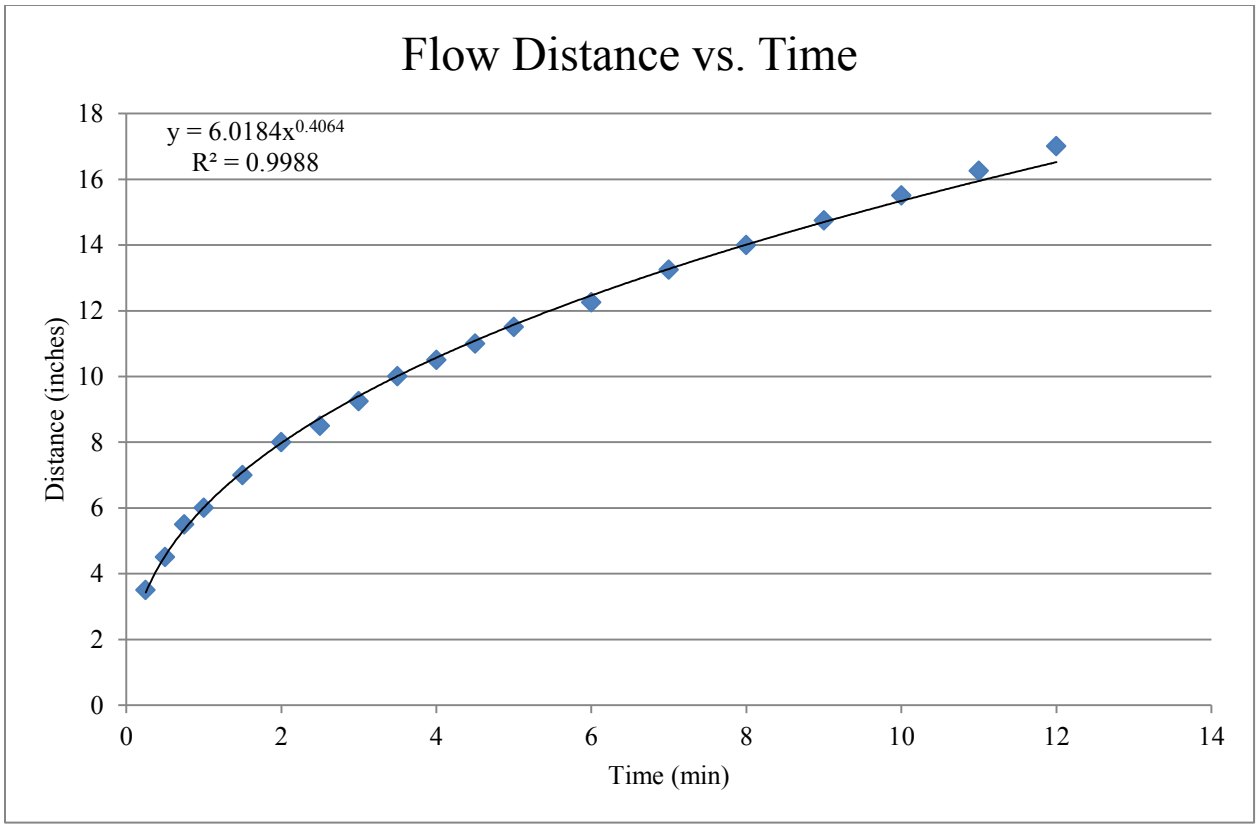

Figure 4.3: Flow Front Distance vs. Time plot for $[45/-45/0/90]_{2S}$ preform

The trend observed in Figure 4.3 for flow front versus time is the same for all conventional preforms evaluated. The results for all infused preforms are displayed in Figure 4.4. Each data set represents a preform of specific thickness and stacking sequence.

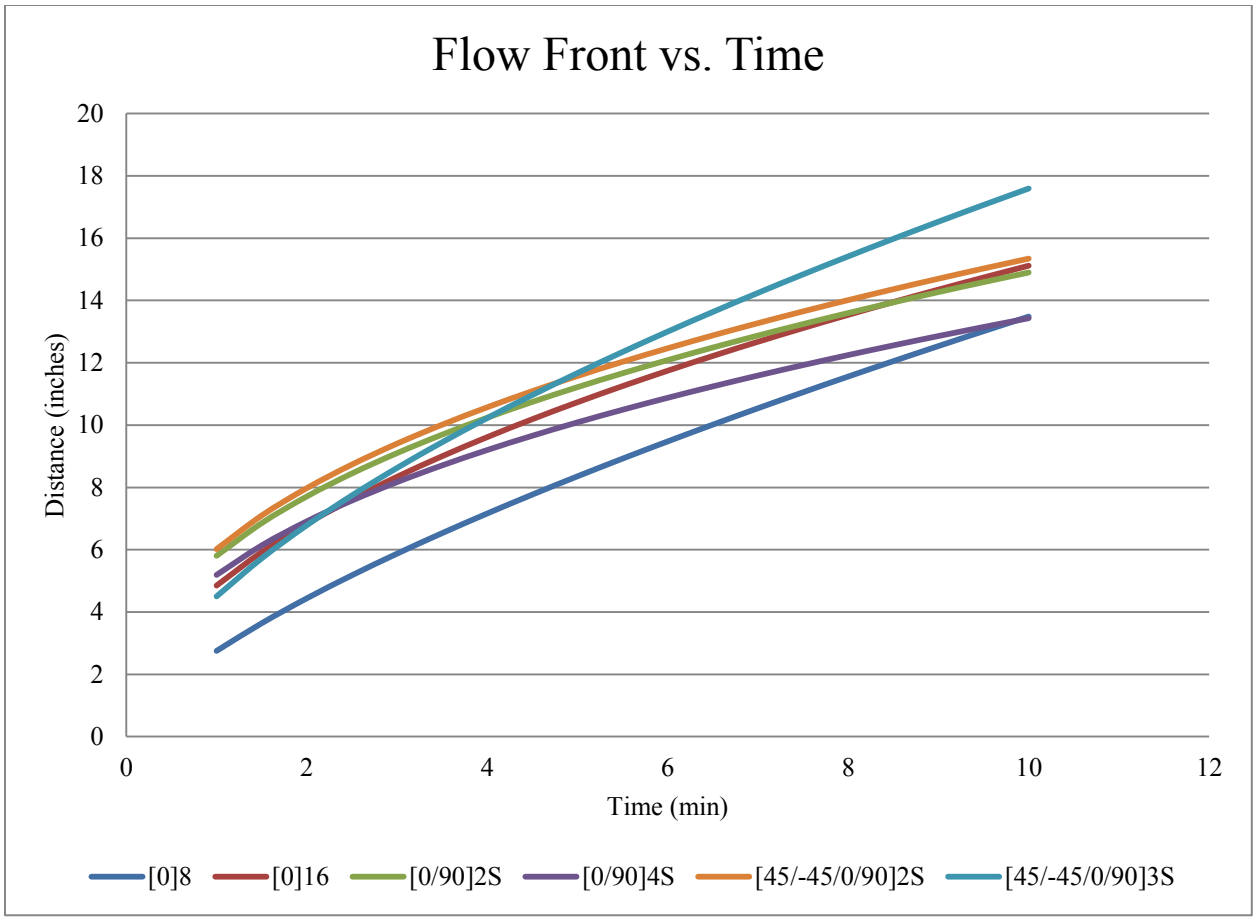

Figure 4.4: Flow Front vs. Time for all conventional preforms

4.1.2. Preforms with Gaps

The selection of gap frequency and sizing are all factors that can heavily influence the preforms permeability. Prior to the evaluation of infusion flow front of conventional preforms, preforms with induced gaps have not been evaluated. Following the initial test matrix presented in Table 11 of section 3.2.4, Scenario C is chosen to be the first to be evaluated. Scenario C represents the 'most extreme case' preform with largest gap sizing. The hypothesis is that the preform with larger gaps will result in greater preform permeability, hence quicker infusion time. Scenario C is a preform with a gap of 4mm spaced every 4 tows. Every 4 tows make one band (1 inch/25.4 mm). Both an 8 ply unidirectional and cross-ply preform is manufactured with the tailored gaps described, and infused.

During the course of the infusion of unidirectional 8 ply preform with 4mm gaps, it was visually confirmed that as the flow front progressed locations within the preform where gaps were present created visible ‘resin highways’ where the flow was more advanced. This phenomenon was only observed after the flow front completed half of the infusion process. Figure 4.5 shows an image of the preform after it has completed the VARTM infusion and cure. The lines marked over the bag represent the flow front that was monitored at different time intervals of the infusion process. Peaks in the flow front, referred to as resin highways, can be observed at the locations where gaps within the preform are present.

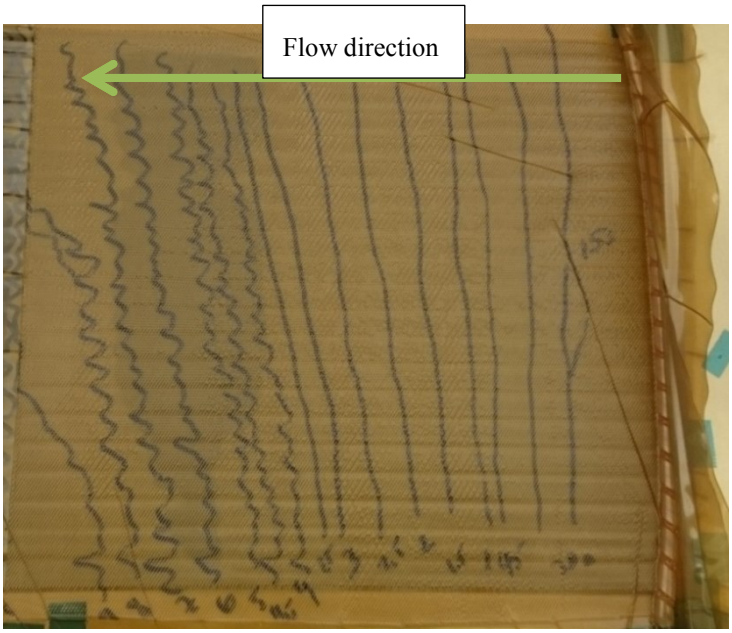

Figure 4.5: Flow front observed of 8ply unidirectional preform with 4mm gaps

However, resin highways were not visually detected when infusing the 8 ply cross-ply preform with 4mm gaps shown in Figure 4.6. This may be due to the transverse gaps aiding flow in the tangential direction of the flow front, negating the effect of highways as was observed in the 8 ply unidirectional preform.

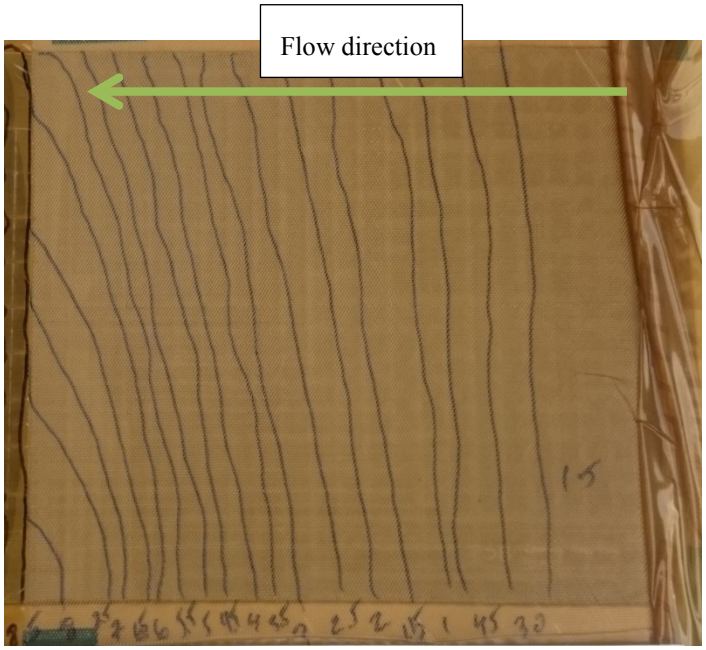

Figure 4.6: Flow front observed of 8ply cross-ply preform with 4mm gaps

As performed for all conventional preforms, flow fronts are monitored with respect to time and distance. Results of preforms with gaps are plotted and overlaid on top of conventional preform results for comparison.

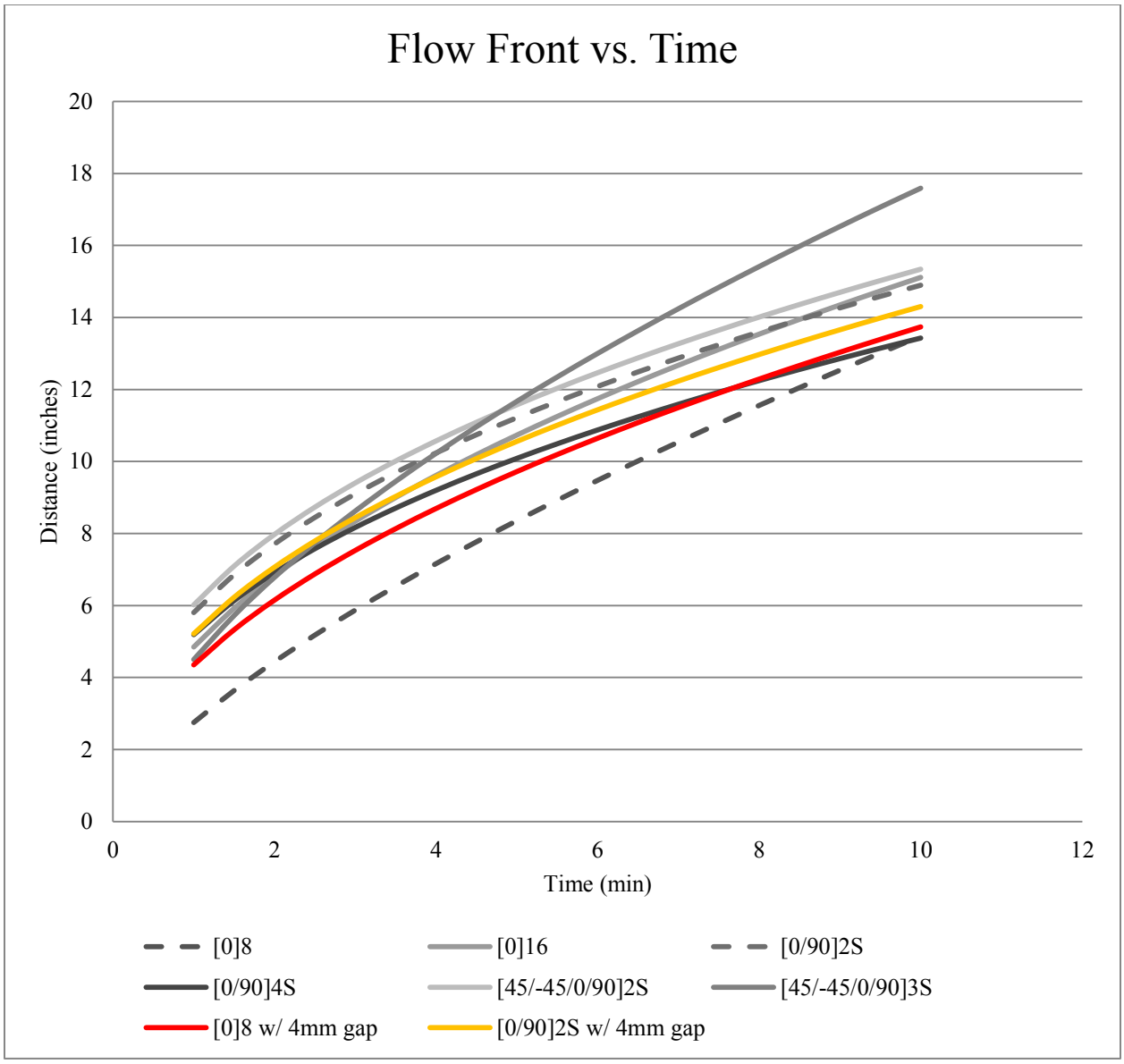

Figure 4.7: Comparison of Flow Front vs. Time between Conventional and Gapped Preforms

Observing the progression of flow front during infusion of both 8ply unidirectional and cross-ply preforms, the curves fall within the ranges observed in conventional preforms. The results of 8ply conventional preforms are highlighted by dashed curves. This suggests that there is no significant change of the overall infusion cycle time with preforms with gaps.

From the results observed in the Figure 4.7, the remaining scenarios A and B for gapped preforms to be evaluated presented in the test matrix of Table 10 were halted. The reasoning is

that the remaining scenarios to investigate involved creating preforms with smaller sized gaps (1mm and 2mm), and it was observed that 4mm gapped preforms showed similar overall results observed when compared with conventional preforms.

4.1.3. Discussion

The observation of flow front progression in the 8ply unidirectional preform, shown in Figure 4.7, demonstrates that the tailored gaps do have an effect on the flow front. It is likely that permeability of a preform is affected when gaps are introduced between bands or tows, as was described in [30]. However, when examining the effects of gaps in preforms as a whole system with peel ply and flow mesh included, the overall flow front progression and infusion times show no significant changes between preform thickness, layup, or introduced gaps.

The hypothesis behind the observed results is that as the flow mesh is inherently very porous, it is the predominant driver of the permeability of the system (preform, peel ply and flow mesh). For the permeability of the system to significantly change, the preform would have to reach permeability values as high as the flow mesh.

4.2. Mechanical Characterization

In order to evaluate the mechanical performance of laminates manufactured by DAFP and VARTM; tensile, compressive, short beam shear, Open Hole Tension (OHT) and Open Hole Compression (OHC) tests have been performed to determine their respective properties. These sets of tests and results are intended to provide basic composite properties essential to most methods of analysis for composite laminates [43]. All tests and methods performed adhere to American Society for Testing and Materials (ASTM) standards. Table 14 describes in further details the test, ASTM standards, stacking sequences, specimen thicknesses and properties that are being evaluated. It should be noted for are laminates manufactured for mechanical evaluation, the same fiber batch and resin system is used for all. Each laminate was infused and cured independently.

Table 14: Summary of Tests Performed and their Details

Test	**ASTM Standard**	**Property Evaluated**	**Stacking Sequence**	**Avg. Specimen thickness**
Tensile (0°)	ASTM D3039	Strength & Modulus	$[0]_8$	0.044”
Tensile (90°)	ASTM D3039	Strength & Modulus	$[90]_{16}$	0.088”
Compression (0°)	ASTM D6641	Strength & Modulus	$[0/90]_{4S}$	0.086”
Short Beam Shear (0°)	ASTM D2344	Strength	$[0]_{16}$	0.088”
OHT	ASTM D5766	Strength	$[45/-45/0/90]_{2S}$	0.083”
OHC	ASTM D6484	Strength	$[45/-45/0/90]_{3S}$	0.123”

4.2.1. Tensile Testing (0°)

Mechanical tensile tests in the 0° orientation were performed following the standard test method of ASTM D3039. A laminate of sequence $[0]_8$ was manufactured. A total of 5 specimens from the laminate were cut using diamond blade saw to 10 inches in length and 0.5 inches in width. The overall average thickness of specimens was 0.044 inches. All specimens were tabbed using fiberglass cross-ply laminate of 0.063 inches in thickness; bevel angle of 7° was used. Tabs were bonded using Cytec FM300 film adhesive. The gauge length of specimen is 5.5 inches. The test was performed using a hydraulic MTS machine. Specimens were clamped in the tabbed areas, and force is applied at a rate of 0.05 inches/min until failure. During the course of the load application, an MTS extensometer is installed on the specimen and records strain up to 6000με. Once reached, the test in stopped momentarily in order to remove extensometer. The extensometer is removed to not cause damage to the instrument, as the nature of the failure of tensile specimens is explosive. Test is then resumed until failure. All specimens exhibited explosive failure mode in the gauge length area.

a) Specimen with extensometer b) Specimen after failure

Figure 4.8: Tensile 0° Specimen

The method used in order to determine mechanical tensile strength and modulus in the 0° specimens is as follows:

$$\sigma_{1UT} = \frac{P_{max}}{A} \quad (3)$$

Where:
σ_{1UT}= Tensile strength, MPa
P_{max}= Maximum force before failure, N
A= Average cross-sectional area, mm^2

The average cross-sectional area is determined by measuring 3 locations of the specimen in the width and thickness directions, and multiplying them together.

$$E_1 = \frac{\Delta\sigma}{\Delta\varepsilon} \quad (4)$$

Where:
E_1= Tensile modulus, GPa
$\Delta\sigma$= difference in applied stress between 3000με and 1000με, MPa
$\Delta\varepsilon$= 3000με minus 1000με

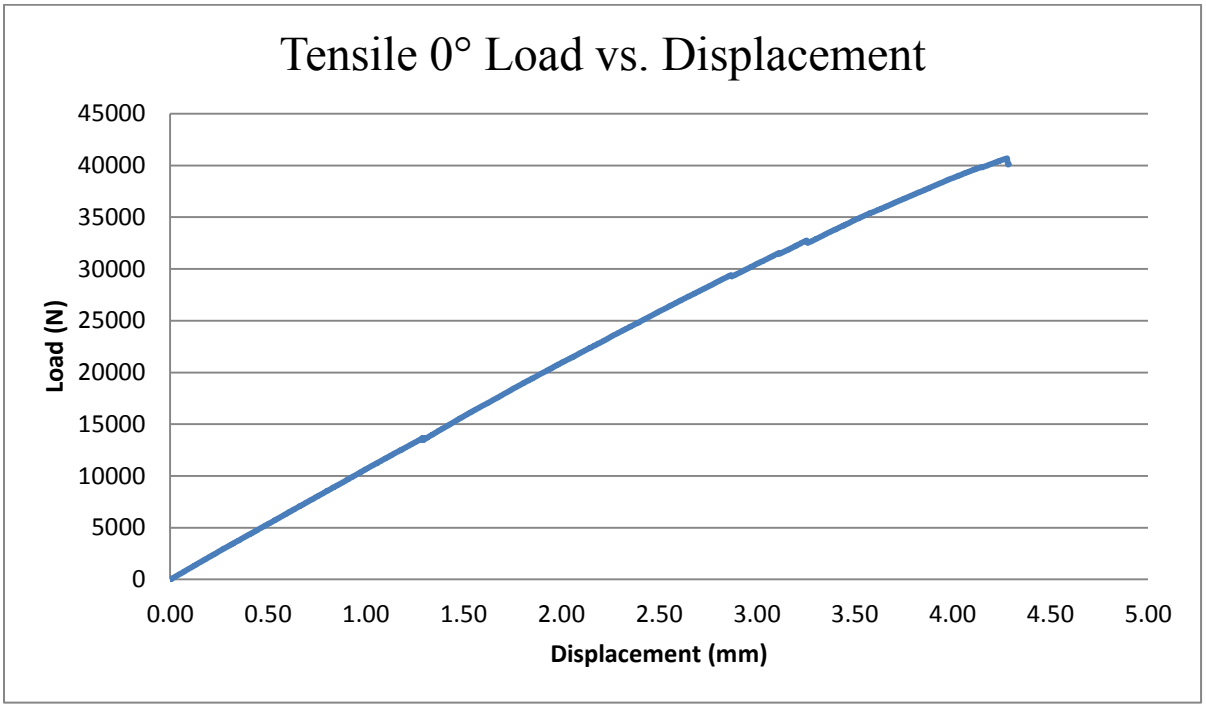

Figure 4.9: Example of Load vs. Displacement for Tensile 0° Specimen

4.2.2. Tensile Testing (90°)

Mechanical tensile tests in the 90° orientation were performed following the standard test method of ASTM D3039. A laminate of sequence $[90]_{16}$ was manufactured. A total of 5 specimens were cut from the laminate using diamond blade saw to 7.0 inches in length and 1.0 inches in width. The overall average thickness of specimens was 0.088 inches. All specimens were tabbed using fiberglass cross-ply laminate of 0.063 inches in thickness; bevel angle of 90° was used. Tabs were bonded using Cytec FM300 film adhesive. Specimens were tested using hydraulic MTS machine with 100kN load cell. Specimen is clamped in the tabbed areas, and force is applied at a rate of 0.05 inches/min until failure. During the course of the load application, stress and strain values are recorded with the use of load cell and unidirectional strain gauge (model CEA-06-125UW-350 from Micro Measurements) applied in the center location of each specimen. With the recorded data plotted, both modulus and strength of the laminate in the 90° orientation was determined. All specimens exhibited lateral failure mode in gauge length area near the tabs.

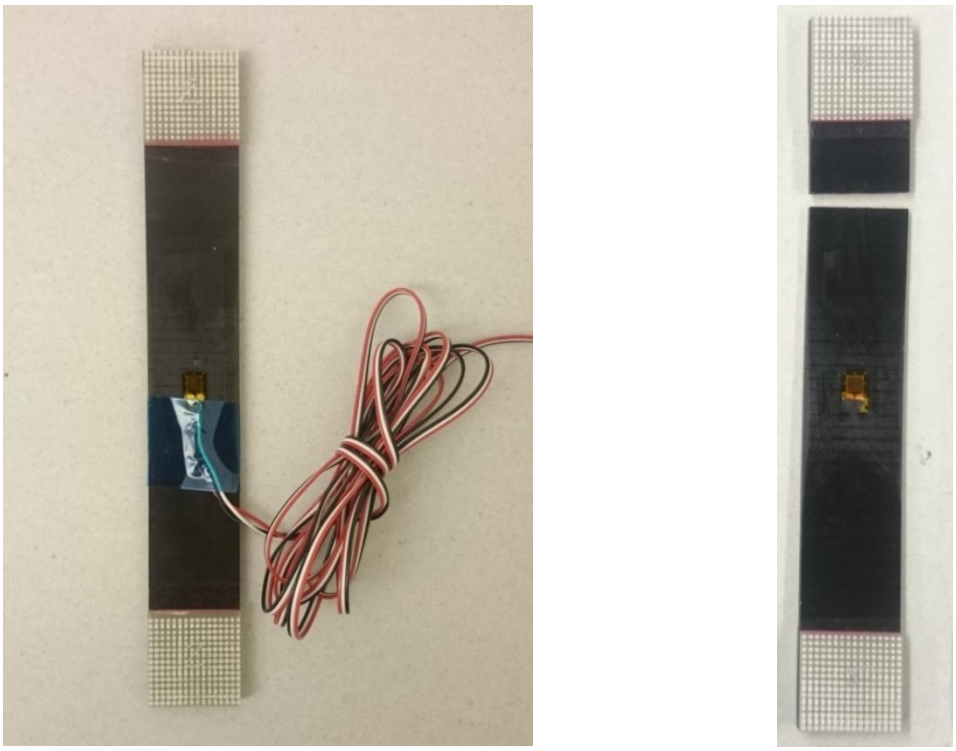

a) Specimen with strain gauge b) Specimen failure

Figure 4.10: Tensile 90° Specimen

The method used in order to determine mechanical tensile strength and modulus in the 90° specimens is as follows:

$$\sigma_{2UT} = \frac{P_{max}}{A} \tag{5}$$

Where:
σ_{2UT}= Tensile strength, MPa
Pmax= Maximum force before failure, N
A= Average cross-sectional area, mm^2

The average cross-sectional area is determined by measuring 3 locations of the specimen in the width and thickness directions, and multiplying them together.

$$E_2 = \frac{\Delta\sigma}{\Delta\varepsilon} \tag{6}$$

Where:
E_2= Tensile modulus, GPa
$\Delta\sigma$= difference in applied stress between 3000με and 1000με
$\Delta\varepsilon$= 3000με minus 1000με

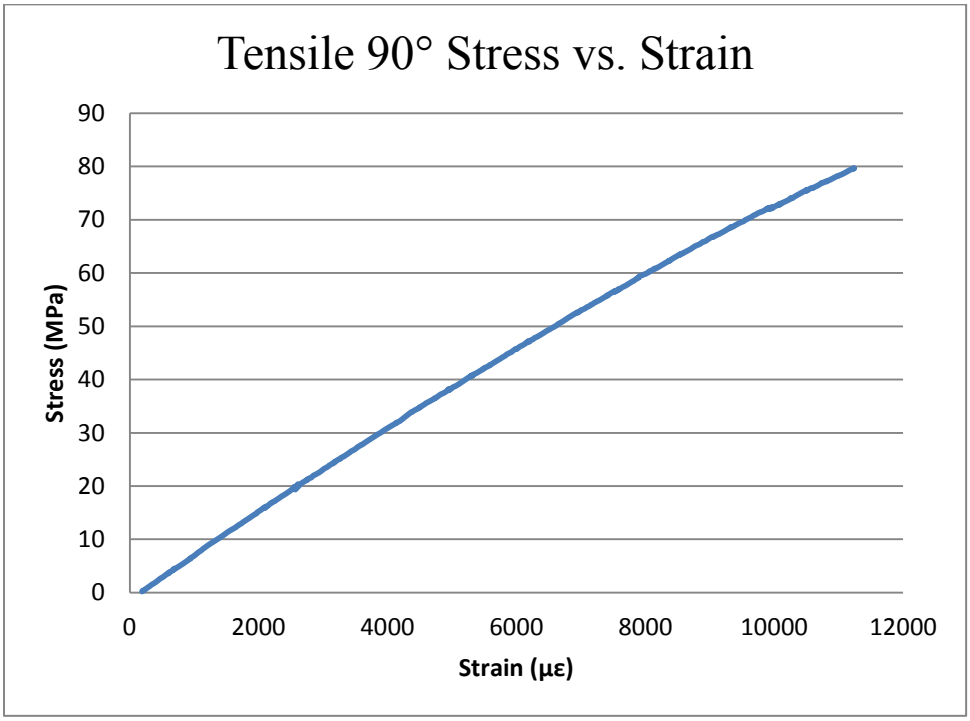

Figure 4.11: Example of Stress vs. Strain Curve of Tensile 90° Sample

4.2.3. Short Beam Shear (0°)

Mechanical short beam shear tests in the 0° orientation were performed following the standard test method of ASTM D2344. A laminate of sequence $[0]_{16}$ was manufactured. A total of 5 specimens were cut from the laminate using diamond blade saw to 0.55 inches in length and 0.17 inches in width. The overall average thickness of specimens was 0.088 inches. Specimens were tested using a Hoskin Scientific Tensile Tester with a 5 kN load cell. The specimen is placed in a 3-point bending fixture as per standard, and load is applied until 30% load drop off or crushing of specimen is observed, whichever comes first. During the course of the load application, force and displacement values are recorded. With the recorded data, the Interlaminar Short beam Shear (ILSS) strength of the laminate in the 0° orientation was determined. All specimens exhibited lateral failure mode in inelastic deformation.

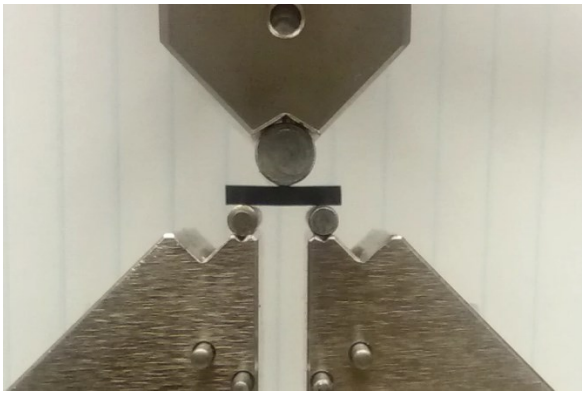

a) Specimen installed on 3-point flexure support

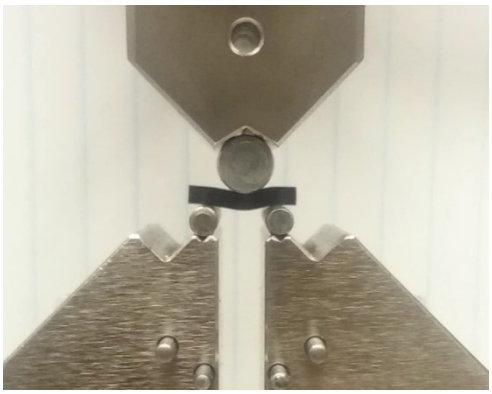

b) Specimen at failure

Figure 4.12: Short Beam Shear 0° Specimen

The short beam strength is determined by the following equation:

$$F^{sbs} = 0.75 * \left(\frac{P_m}{b_{avg} * h_{avg}} \right) \quad (7)$$

Where:

F_{sbs}= Short beam strength, MPa
Pm= Maximum load observed, N
b_{avg}= average of 3 measurements of specimen width, mm
h_{avg}= average of 3 measurements of specimen thickness, mm

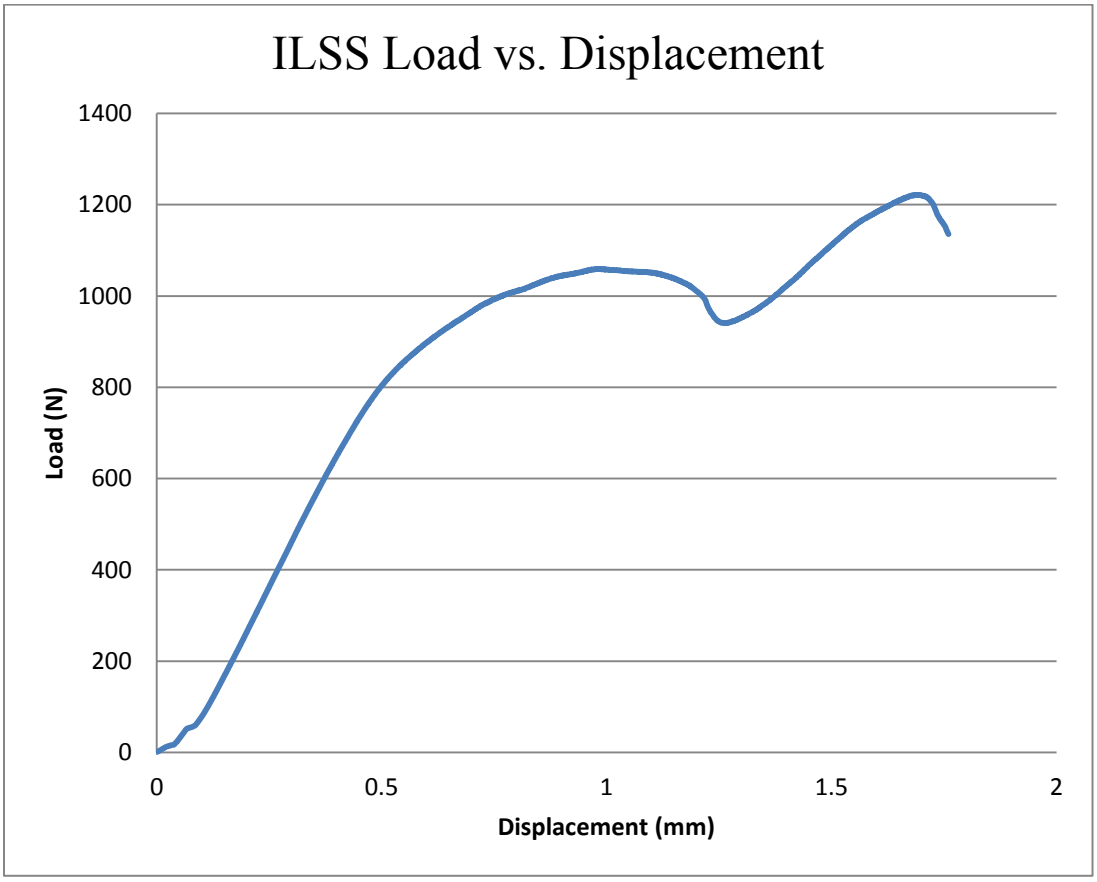

Figure 4.13: Example of Load vs. Displacement of ILSS 0° Specimen

It is important to discuss the peaks observed in the load versus displacement data of Figure 4.13. This occurrence is seen in all ILSS tests. In order to understand which peak should be used to determine the short beam shear strength, the following definition is stated per ASTM D2344:

Continue loading of specimen until either of the following occurs:

- Load drop-off of 30%
- Two-piece specimen failure, or
- Head travel exceeds specimen thickness

As none of the specimens exhibited a load drop-off of 30% after the first peak, did not show two-piece failure, and head travel did not exceed specimen thickness, the second peak is deemed as the ultimate load observed and is therefore used to calculate short beam shear strength.

4.2.4. Compression Testing (0°)

Mechanical compression tests were performed following the Combined Loading Compression (CLC) standard test method of ASTM D6641. A laminate of sequence $[0/90]_{4S}$ was manufactured. A total of 5 specimens were cut from the laminate using diamond blade saw to 5.5 inches in length and 0.5 inches in width. The overall average thickness of specimens was 0.086 inches. Specimens were tested using hydraulic MTS machine with 100kN load cell. Specimen is clamped, and force is applied at a rate of 0.05 inches/min until failure. During the course of the load application, stress and strain values are recorded from the load cell and uni-directional strain gauge (model C2A-06-250LW-350 from Micro Measurements) applied in the center location of each specimen. With the recorded data plotted, both modulus and strength of the laminate in the 0° orientation was determined.

The first sample tested had two strain gauges installed, one on each side of the specimen, to determine if excessive bending would cause premature failure. The test determined 6.94% bending at the 2000με checkpoint, which is below the maximum allowable of 10% as per standard; remaining samples were tested with only one strain gauge installed.

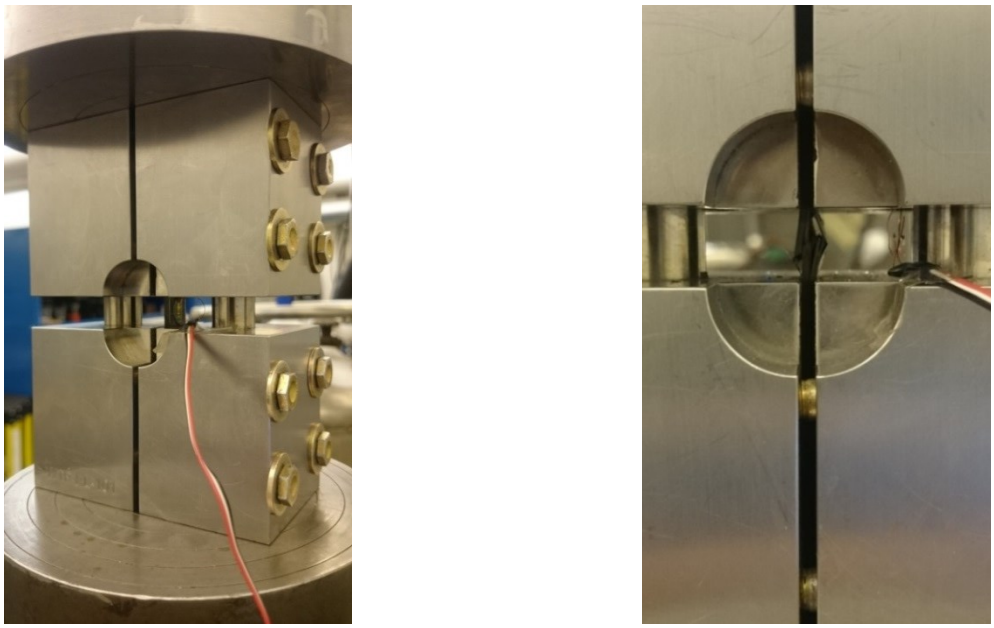

a) CLC fixture with specimen installed

b) Specimen failure in middle of gauge section

Figure 4.14: Specimen in ASTM D6641 CLC Fixture

Compression testing is performed on cross-ply specimens using ASTM D6641, and compression result of the 0° laminate is derived using a method known as the Back-out Factor (BF). This is a common method used by most suppliers in order to obtain more valid and reproducible results. The equations used to determine specimen strength and modulus, as well as derivation of 0° strength properties using BF is as follows [44]:

$$BF = \frac{E_1[V_0E_2 + (1 - V_0)E_1] - (v_{12}E_2)^2}{[V_oE_1 + (1 - V_oE_2)][V_0E_2 + (1 - V_0)E_1] - (v_{12}E_2)^2} \quad (8)$$

Where:
E_1= Axial Modulus
E_2= Tangential Modulus
V_0= Percentage of zero degree plies
V_{12}= Poisson's ratio

In the case of cross-ply laminates, we may simplify equation (8). As the Poisson's ratio is always less than 1, the term $(\nu_{12}E_2)^2$ is negligible compared to both the numerator and denominator, and therefore can be removed. Additionally, as the percentage of zero degree plies used is 50%, the equation is simplified to the following:

$$BF = \frac{2E_1}{(E_1 + E_2)} \quad (9)$$

The following equation is used to determine specimen strength and modulus:

$$\sigma_{2UC,[0/90]} = \frac{P_{max}}{A} \quad (10)$$

Where:
$\sigma_{2UC,[0/90]}$ = Compression strength of Cross-ply laminate, MPa
Pmax= Maximum force before failure, N
A= Average cross-sectional area, mm^2

The average cross-sectional area is determined by measuring 3 locations of the specimen in the width and thickness directions, and multiplying them together.

$$\sigma_{2UC,0^\circ} = BF \times \sigma_{2UC,[0/90]} \quad (11)$$

Where:
$\sigma_{2UC,0^\circ}$= Compression strength of 0° laminate, MPa
BF= Back-out factor, unit less
$\sigma_{2UC,[0/90]}$= Compression strength of Cross-ply laminate, MPa

$$E_{1C} = \frac{\Delta\sigma}{\Delta\varepsilon} \quad (12)$$

Where:
E_2= Tensile modulus, GPa
$\Delta\sigma$= difference in applied stress between 3000με and 1000με
$\Delta\varepsilon$= 3000με minus 1000με

The following equation is used to determine the percent bending of specimen during loading when ε_{ave}= 2000με per standard:

$$B_y = \frac{\varepsilon_1 - \varepsilon_2}{\varepsilon_1 + \varepsilon_2} \times 100 \quad (13)$$

Where:
ε_1= Indicated strain at Gauge 1
ε_2= Indicated strain at Gauge 2
ε_{ave}= Average longitudinal strain $(\varepsilon_1 + \varepsilon_2)/2$ at data point closest to checkpoint for bending

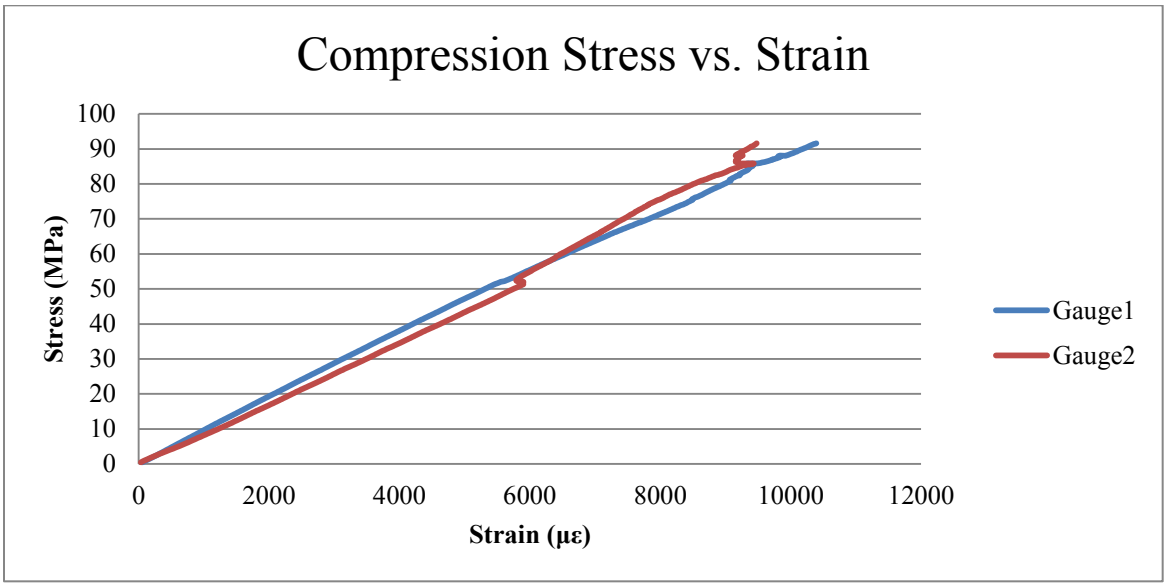

Figure 4.15: Example of Stress vs. Strain Curve of Compression $[0/90]_{4S}$ Specimen

4.2.5. Open Hole Tensile Testing

Mechanical Open Hole Tensile (OHT) tests were performed following the standard test method of ASTM D5766. A laminate of sequence $[45/-45/0/90]_{2S}$ was manufactured. A total of 5 specimens were cut from the laminate using diamond blade saw to 12 inches in length and 1.5 inches in width. A hole of 0.25 inches is machined in the center location of each specimen. The overall average thickness of specimens was 0.083inches. Specimens were tested using hydraulic MTS machine with 100kN load cell. Specimen is clamped, and force is applied at a rate of 0.05 inches/min until failure. During the course of the load application, load and displacement values are recorded. With the recorded data plotted, ultimate OHT strength of the laminate was determined. All specimens exhibited explosive failure mode in the gauge length area.

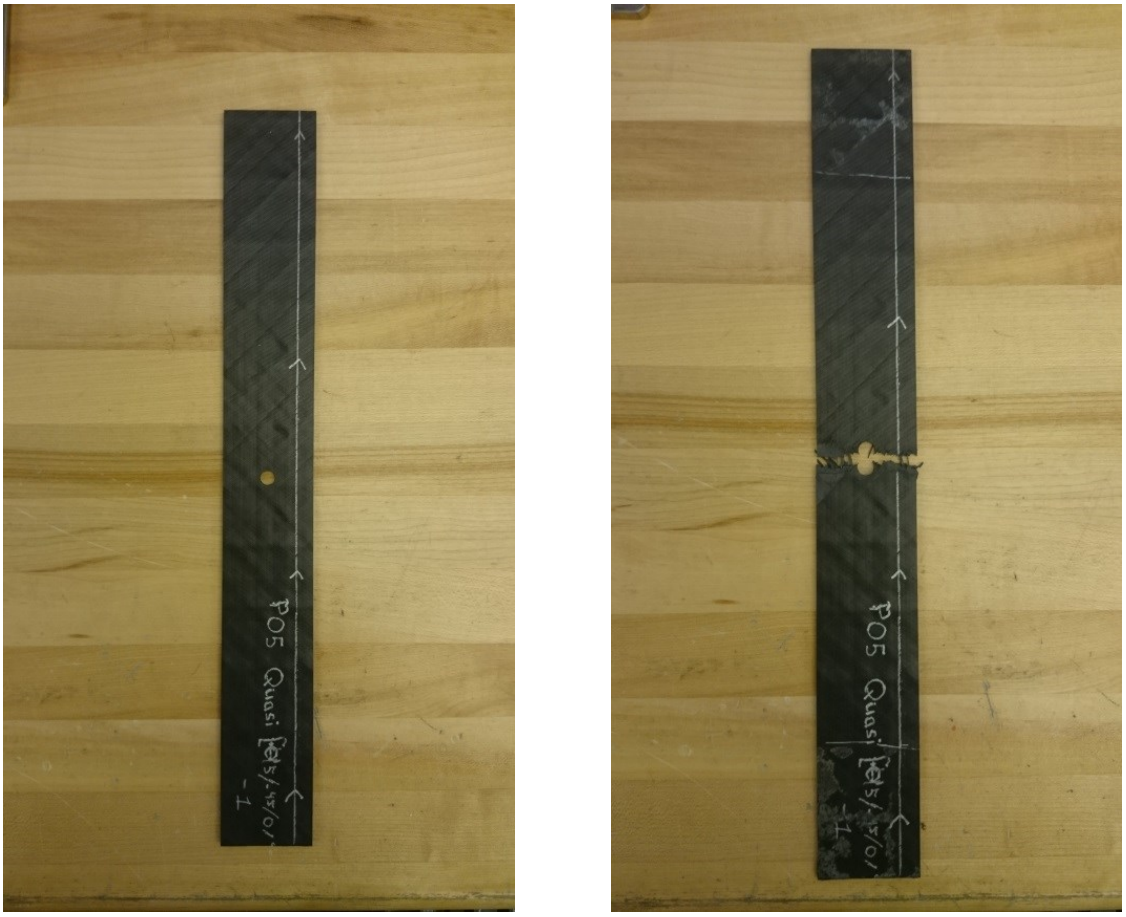

a) Specimen prior loading b) Specimen after failure

Figure 4.16: Open Hole Tensile Test Specimen

The following equation is used in order to determine the OHT strength of the specimens:

$$F_x^{OHTu} = \frac{P_{max}}{A} \tag{14}$$

Where:

F_x^{OHTu}= The ultimate open-hole tensile strength, MPa
P_{max}= Maximum tensile force prior to failure, N
A= Gross average cross-sectional area of specimen (disregarding hole), mm^2

The average cross-sectional area is determined by measuring 3 locations of the specimen in the width and thickness directions, and multiplying them together.

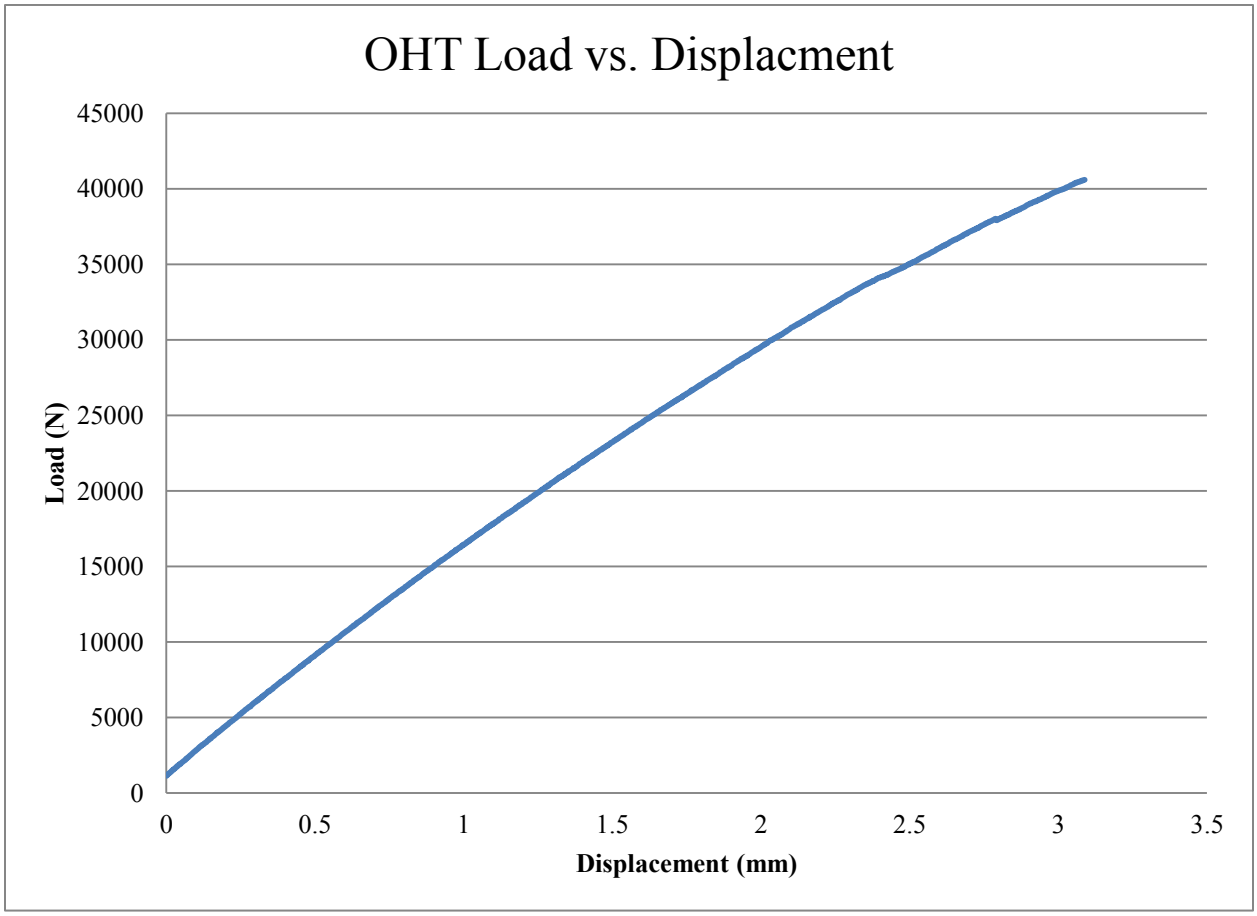

Figure 4.17: Example of Load vs. Displacement of OHT Specimen

4.2.6. Open Hole Compression Testing

Mechanical Open Hole Compression (OHC) tests were performed following the standard test method of ASTM D6484. A laminate of sequence $[45/-45/0/90]_{3S}$ was manufactured. A total of 5 specimens were cut from the laminate using diamond blade saw to 12 inches in length and 1.5 inches in width. A hole of 0.25 inches is machined in the center location of each specimen. The overall average thickness of specimens was 0.123 inches. Specimens were tested using hydraulic MTS machine with 100kN load cell. Specimen is installed in specific support fixture as per ASTM D6484 testing prior to placing into MTS machine, and force is applied at a rate of 0.05 inches/min until failure. During the course of the load application, load and displacement values are recorded. With the recorded data plotted, ultimate OHC strength of the laminate was determined. All specimens exhibited compressive failure laterally across the center of the hole, denoted as LGM as per ASTM D6484.

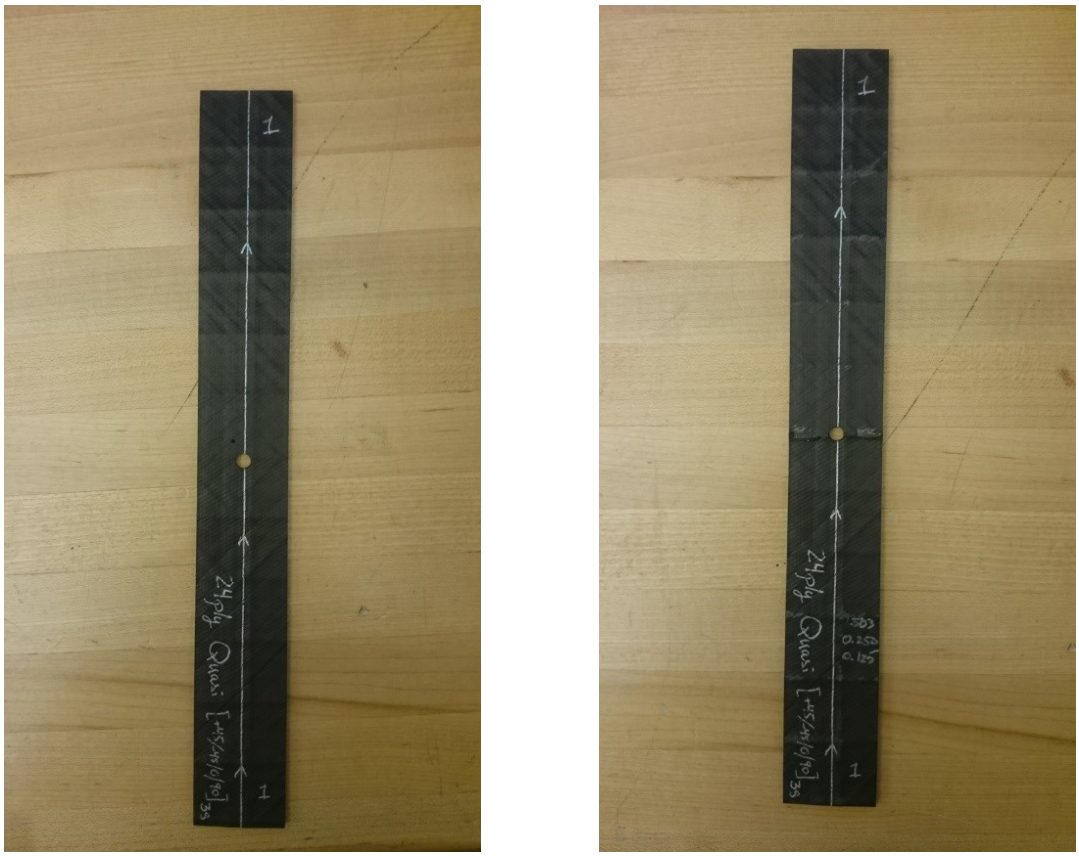

a) Specimen prior loading b) Specimen failure

Figure 4.18: Open Hole Compression Specimen

The following equation is used in order to determine the OHT strength of the specimens:

$$F_x^{OHCu} = \frac{P_{max}}{A} \tag{15}$$

Where:

F_x^{OHCu}= The ultimate open-hole compressive strength, MPa
P_{max}= Maximum tensile force prior to failure, N
A= Gross cross-sectional area of specimen (disregarding hole). mm^2

The average cross-sectional area is determined by measuring 3 locations of the specimen in the width and thickness directions, and multiplying them together.

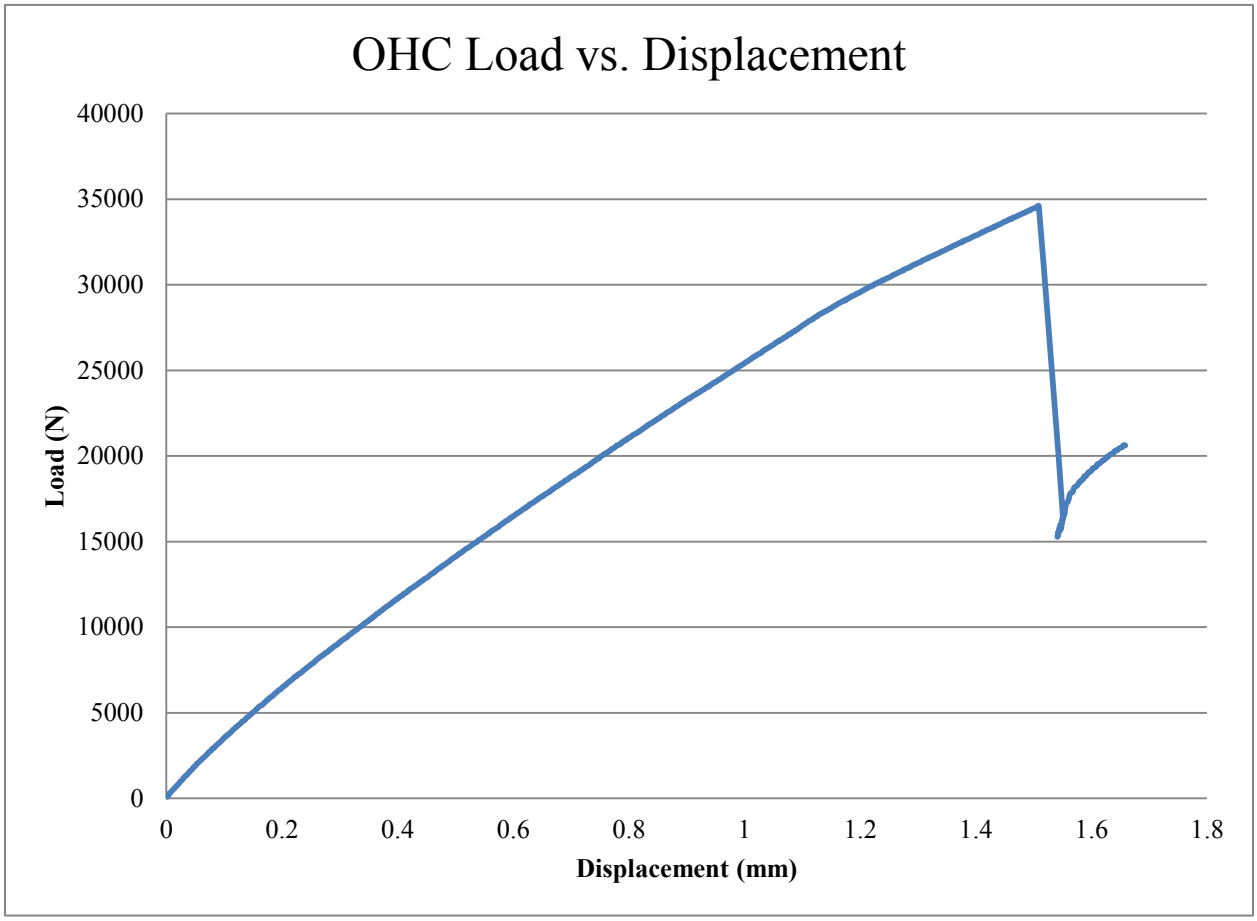

Figure 4.19: Example of Load vs. Displacement of OHC Specimen

4.2.7. Summary of Mechanical Test Results

Performing the described mechanical tests following ASTM standards, an overview of mechanical properties of DAFP VARTM laminates is shown in Table 15.

Table 15: Summary of all Mechanical Testing Data

Test	Property Evaluated	Avg. Result	COV (%)
Tensile (0°)	Strength	2882.7 MPa (418.1 ksi)	1.03
	Modulus	159.1 GPa (23.1 Msi)	4.40
Tensile (90°)	Strength	77.4 MPa (11.2 ksi)	5.38
	Modulus	8.1 GPa (1.2 Msi)	1.36
Compression (0°)	Strength[2]	1113.8 MPa (161.5ksi)	6.18
	Modulus	140.0 GPa (20.3 Msi)	5.71
Short Beam Shear (0°)	Strength	109.4 MPa (15.9 ksi)	3.36
OHT	Strength	493.7 MPa (71.6 ksi)	2.08
OHC	Strength	281.3 MPa (40.8 ksi)	5.29

[2] Derived from 0/90 strength result using Back-out Factor

4.3. Mechanical Performance Compared to Conventional Aerospace Material Systems

The most notable composite material suppliers in today's aerospace market are Cytec (now named Solvay Group), Hexcel, Toray and TenCate. Each supplier manufacturers a large selection of thermoset, and thermoplastic systems geared towards the aerospace industry, and works along with aerospace manufacturers to develop new products.

In order to gain an understanding of the mechanical performance of DAFP VARTM laminates, it was chosen to compare the obtained mechanical results with different carbon/epoxy systems intended for primary structural applications currently used by aerospace OEMs.

4.3.1. Selection of Carbon/Epoxy System Baselines

When comparing and baselining against other materials, it is important to select materials that are in the same class, and designed to be used in similar applications. Materials must have carbon fibers of the same grade, comparable matrix epoxy systems, as well as similar curing and service temperatures. In addition, in order to compare between different manufacturing processes of carbon/epoxy systems a conventional autoclave curing prepreg system and an OOA curing prepreg system is selected as a baseline.

The first material chosen is Hexcel's HexPly IM7 8552. This is an amine cured, toughened epoxy system with unidirectional carbon fibers and is recommended for structural applications requiring high strength and damage tolerance. It is a 350°F curing prepreg with a service temperature of up to 250°F [45]. The HexPly IM7 8552 material represents a conventional autoclave curing prepreg that is qualified for primary structural aerospace structures. The second material chosen to compare with is Cytec's IM7 5320-1 for OOA carbon/epoxy prepreg system. This toughened epoxy resin prepreg system is designed for OOA manufacturing of primary

structural applications. This is a 350°F curing prepreg with a service temperature of up to 320°F [46].

Both of these baseline material systems are made up of unidirectional intermediate modulus (IM7) carbon fibers, and are 350°F curing toughened epoxy systems designed for primary structural applications.

It is notable to mention Hexcel's HexPly IM7 8552 prepreg has been extensively evaluated in terms of mechanical properties for the purpose of material qualification. Data has been published and made available by the National Center for Advanced Materials Performance (NCAMP). NCAMP is an organization within the National Institute for Aviation Research (NIAR) at Wichita State University which works with the Federal Aviation Administration (FAA) and industry partners to qualify material systems in a shared effort. It is interesting to note that in general, mechanical properties published by NCAMP show slightly lower properties than that published by the material supplier. As NCAMP is a third party evaluating the materials performance, and has no affiliations with the material manufacturers, it is chosen to compare DAFP VARTM results to that of NCAMP's published HexPly 8552 IM7 autoclave prepreg.

Cytec's IM7 5320-1 OOA prepreg has not been evaluated by NCAMP. A similar version of Cytec's material using standard modulus fibers T650 has been evaluated and published by NCAMP. As this is not the same fiber system, it is not used as a comparison. The data of Cytec's IM7 5320-1 is published by the manufacturer and is used to compare DAFP VARTM results.

There exist differences between methods of determining mechanical properties of Hexcel and Cytec systems to the DAFP VARTM laminates. The most notable is the Hexcel system qualified by NCAMP evaluates 3 batches of prepreg, 2 panels per batch, and 3 specimens per panel (18 specimens total) for each mechanical property. This is to ensure that data reproduced takes into account all types of variability between supplier batches, and manufacturing methods. Cytec does not mention to use this method, however we assume they do as it is a common method for qualification within the industry. Due to limited time and batch, only one fiber and resin batch were evaluated for each test for DAFP VARTM laminates

A figure with normalized comparison of DAFP VARTM mechanical performance can be seen with both Hexcel and Cytec systems in Figure 4.20 and Figure 4.21 respectively.

4.3.2. DAFP VARTM vs. Autoclave Prepreg

From the comparative Figure 4.20, DAFP VARTM laminates show areas of decreased, as well as areas of increased performance compared to the baseline autoclave curing prepreg. In all forms of modulus testing DAFP VARTM laminates show comparable results to Hexcel's HexPly 8552 prepreg. The largest variation in modulus observed is a decrease of 10% in 90° Tensile testing. An increase in performance of 13% in Tensile 0° Strength, 21% in Tensile 90° Strength, and 22% in OHT Strength is observed. ILSS shows a small decrease of 7%. Finally a significant decrease is seen in all forms of compression strength tests, 17% for OHC Strength and 35% in Compression 0° Strength.

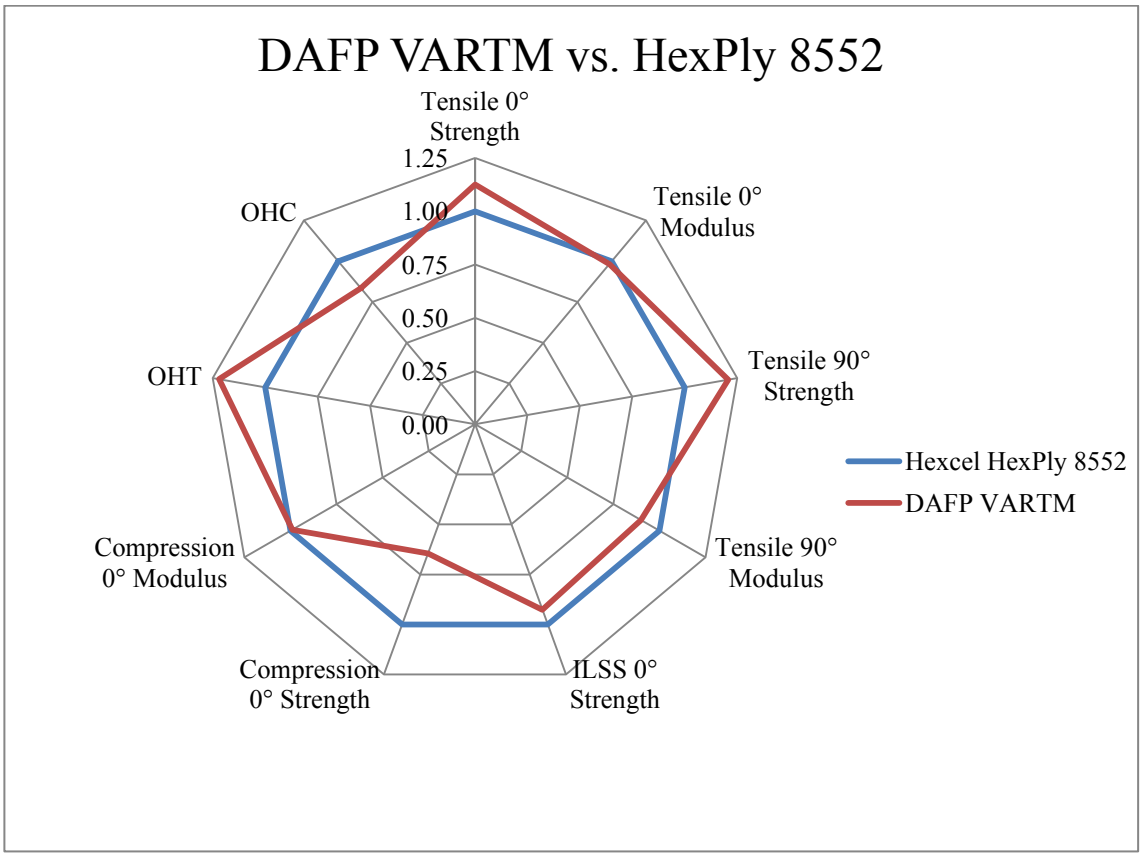

Figure 4.20: Normalized Mechanical Data Comparison of DAFP VARTM to Hexply 8552 Autoclave Prepreg

4.3.3. DAFP VARTM vs. OOA Prepreg

From the comparative Figure 4.21, DAFP VARTM laminates show areas of decreased, as well as areas of increased performance when compared the baseline OOA prepreg. Modulus results are comparable in 0° tensile and 0° compression testing. As similarly seen in autoclave prepreg comparison, a decrease in 90° tensile modulus is seen, in this case 14%. An increase in performance of 15% in Tensile 0° Strength is observed. Comparable performance is seen in both Tensile 90° Strength, and OHT Strength. ILSS shows a decrease of 18%. Finally a significant decrease is seen in all forms of compression tests, 24% for OHC Strength and 46% in Compression 0° Strength.

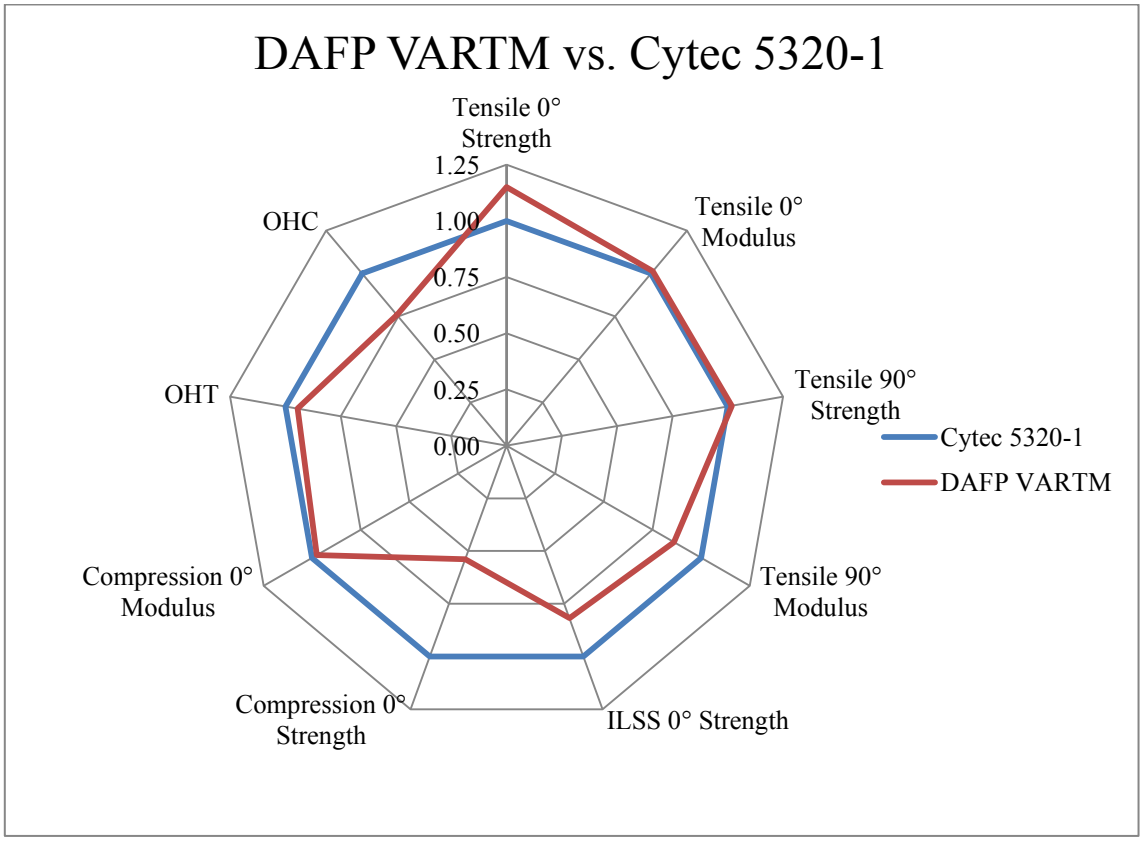

Figure 4.21: Normalized Mechanical Data Comparison of DAFP VARTM to Cytec's 5320-1 OOA Prepreg

4.3.4. Discussion

In the comparison of mechanical performance presented in both Figure 4.20 and Figure 4.21, DAFP VARTM laminates show properties in the realms of conventional autoclave prepreg and OOA prepreg materials. The largest knockdowns in performance are seen in compression strengths. Mechanical performance in compression is heavily influenced by the performance of the resin matrix. This could suggest weaker fiber/matrix interaction in the DAFP VARTM laminates, causing premature failure.

The evaluation of the PRISM EP2400 resin system rheology presented in section 3.3.1 showed resin viscosity to be slightly higher than the manufacturer's suggested range. This could imply that the resin system had begun premature cross-linking which has the possibility to affect the mechanical properties of the laminate. The resin system was donated as part of this research dissertation and its historical freezer in/out times was not available. Should the resin system have been left out for long durations of time exceeding its room temperature handling life, its mechanical properties have potential to be decreased. As mechanical performance in compression of laminates is significantly influenced by the resin matrix, any reduction of resin properties and its effect its interaction with the dry fibers would be highlighted in reduced compressive properties.

Another possible cause of knockdown seen in compression strengths is due to the manufacturing technique of the dry preforms. The dry fibers are only held together with the aid of powdered thermoplastic binder veils. The dry tows are not imbedded with resin compared to traditional prepregs, and are freer to move during AFP deposition. Dry fiber preforms manufactured as part of the material characterization have shown an observable waviness seen in the laid tows, seen in Figure 4.22.

Figure 4.22: Example of Waviness Observed in Dry Preform Tows

This phenomenon is not observed when processing conventional prepreg slit tapes using AFP, and could be a cause to have minor fiber misaligned throughout the ply's direction. Fiber alignment in the desired orientation is crucial to laminate mechanical properties. As stated in the CHM-17 Handbook, unidirectional specimen fiber misalignment can reduce strength as much as up to 30% due to 1° misalignment [47].

Lastly, 0° degree compressive strength was determined from specimens oriented in $[0/90]_{4S}$ without the use of bonded tabs. CHM-17 suggests that works in progress indicate that $[90/0]_{ns}$ laminates yield higher mean values in compression strength tests. Factors such as the outer 90° plies protect load bearing 0° plies from damage during manufacturing or testing in addition to enhance stability, as well as 0° outer plies increase stress concentrations at gage areas [47].

Chapter 5 - Cost Analysis

The study published by [6] investigates the economic and environmental impacts of multiple different types of composite manufacturing methods. The case study evaluates conventional hand-layup of autoclave curing prepreg manufacturing to OOA methods of manufacturing such as oven curing prepregs, microwave curing prepregs, oven curing infusion of NCF, as well as microwave curing infusion of NCF. The study uses a 400mm x 400mm x 4mm laminate as a representative panel for aerospace. The cost model evaluates material costs, consumables, equipment, tooling, energy, and labour associated to each method of fabrication. The oven cured infused panels was shown to have the lowest production cost with a 14% reduction against the conventional autoclave prepreg baseline.

5.1. Cost modeling

Similarly to the case study mentioned above, a cost analysis is performed to compare current methods of automated composite manufacturing methods to DAFP VARTM manufacturing. The cost analysis preformed in this dissertation attempts to encompass all relevant processes, equipment, and labour associated with three different types of automated composite manufacturing scenarios:

1. AFP of autoclave prepregs
2. AFP of OOA prepregs
3. DAFP and Hot VARTM

5.1.1. Assumptions

Geometry:

Geometry of the panel has significant impact on the overall costs associated with manufacturing and labour. The geometry of panel investigated is 12" x 24" with a 24 ply with stacking sequence of $[0/90/45/-45]_{4S}$. This geometry was used to manufacture panels used for mechanical characterisation of DAFP VARTM and therefore processing variables related to DAFP manufacturing and VARTM infusion are well understood.

Costs:

Material costs are estimated to be $75/lb for slit autoclave prepreg, $105/lb for slit OOA prepreg, $90/lb for dry fiber tape and $30/lb for resin used for infusion. The estimates of raw material cost are obtained from published case study [6] and Concordia University's CONCOM research group's experience from ordering and purchasing such materials from suppliers. The labour costs associated to employing trained technicians for AFP machine and autoclave or oven operations is assumed to be $75/hr. Material wastage for all prepregs and dry fiber are assumed to be 10%, and resin wastage for infusion is assumed to be 30%.

The overhead costs associated with ownership of equipment is determined by averaging the cost of the equipment over the expected lifetime of the equipment divided by the expected amount of hours the equipment is to be operational per year. Operational hours for all equipment are assumed to be a standard single shift of 8 hours a day in 250 working day year. Table 16 describes the assumed costs of each equipment and its determined hourly cost of operation. As geometry of laminates evaluated in the study is simple and flat, a flat aluminum tool is assumed to be used in all three scenarios. It should be mentioned that the autoclave and oven assumed to be used in this case study are of comparable volume.

Table 16: Equipment Overhead Costs

Equipment	Cost	Lifetime (yrs)	Cost ($/hr)
AFP Machine	$2,000,000.00	15	$66.67
Autoclave	$250,000.00	15	$8.33
Oven	$10,000.00	10	$0.75
VARTM Equipment	$1,000.00	10	$0.07
Tooling	$500.00	10	$0.03

AFP machine and autoclave costs are determined from the amount Concordia University's CONCOM group invested to purchase and install such equipment. Cost of oven of comparable volume and VARTM equipment (resin catch-can, and vacuum pump) are determine from [48] and [49] respectively. The cost for flat aluminum tooling used for all scenarios is assumed to be $500.

Costs associated with all types of consumables used throughout the manufacturing process are obtained from [49] assuming bulk pricing. The costs of each consumable are listed in Table 17.

Table 17: Consumable Costs

Material	Cost ($)	Unit
Sealant Tape	0.016667	$/inch
Flow Media	0.002134	$/inch^2
Spiral tubing	0.044167	$/inch
Peel Ply	0.001302	$/inch^2
Vacuum Bag	0.001775	$/inch^2
Release Film	0.000509	$/inch^2
Breather	0.000903	$/inch^2
Perforated Release Film	0.000972	$/inch^2
High temp Tubing	0.0375	$/inch
High temp Tube Fittings	1.19	Each

AFP Processing and Bagging:

Table 18 shows AFP processing times of all scenarios of manufacturing. The processing times are determined form experience with Concordia University's ADC AFP machine, and includes machine stoppage and in between ply inspections. AFP setup time of 30 minutes is constant to all scenarios. The average laydown speed is assumed to be 4 inches/sec using 4 tows placement. The processing times are assumed to be the same for autoclave prepreg and OOA prepreg, an additional 10 minutes is given laydown of DAFP preform as it requires a laydown speed of 1inch/sec for its first ply. Autoclave and OOA prepregs have very similar bagging techniques and therefore take the same amount of time. VARTM bagging is more unique and requires more time to setup due to injection lines and tubing.

Table 18: AFP Processing and Bagging Times

Scenario	Autoclave PP	OOA PP	DAFP
AFP Setup	30	30	30
Laydown	95	95	105
Bagging	15	15	30
Total (min)	140	140	165

Curing:

Curing cycles and methods of each scenario are described in Table 19. Hexcel's HexPly 8552, Cytec's 5320-1 and Cytec's PRISM EP2400 resin systems supplier recommended curing cycles are followed for autoclave, OOA prepregs, and VARTM infusion respectively. Both the autoclave curing and hot VARTM infusion curing cycles require two dwell temperatures, whereas the OOA cure requires a third dwell for a post-cure. Unique to the VARTM cure cycle, resin requires 30 minutes of degassing prior to infusion, and is taken into consideration.

Table 19: Cure Cycle Times

Scenario	Autoclave PP	OOA PP	DAFP VARTM
Resin Degassing (min)	-	-	30
Ramp 1 (°F/min)	4	2	5
Dwell 1 (min)	60	120	80
Dwell 1 (°F)	225	140	195
Ramp 2 (°F/min)	4	2	4
Dwell 2 (min)	120	120	120
Dwell 2 (°F)	350	250	356
Ramp 3 (°F/min)	-	3	-
Dwell 3 (min)	-	120	-
Dwell 3 (°F)	-	350	-
Ramp Down (°F/min)	3.5	8	7
Total Time (min)	306	507	309

Energy:

Energy consumption for AFP processing was not monitored, however as all scenarios have the same processing time energy consumption is assumed to be the same, and is not considered in this evaluation. Works from [6] determined energy consumption of autoclave and oven operation. Autoclave energy costs showed to be 2%, and oven infusion to be 0.7% of total part cost. These findings are used to determine costs associated to energy consummation.

5.1.2. Overall Costs

With the information and assumptions stated, an analysis is performed in order to evaluate the cost of a single laminate manufactured by three different types of automated manufacturing techniques. The evaluation takes into consideration raw material costs, consumables, equipment, tooling, energy, and labour associated to each method of fabrication and Table 20 breaks down the overall costs to each variable.

Table 20: Cost Breakdown

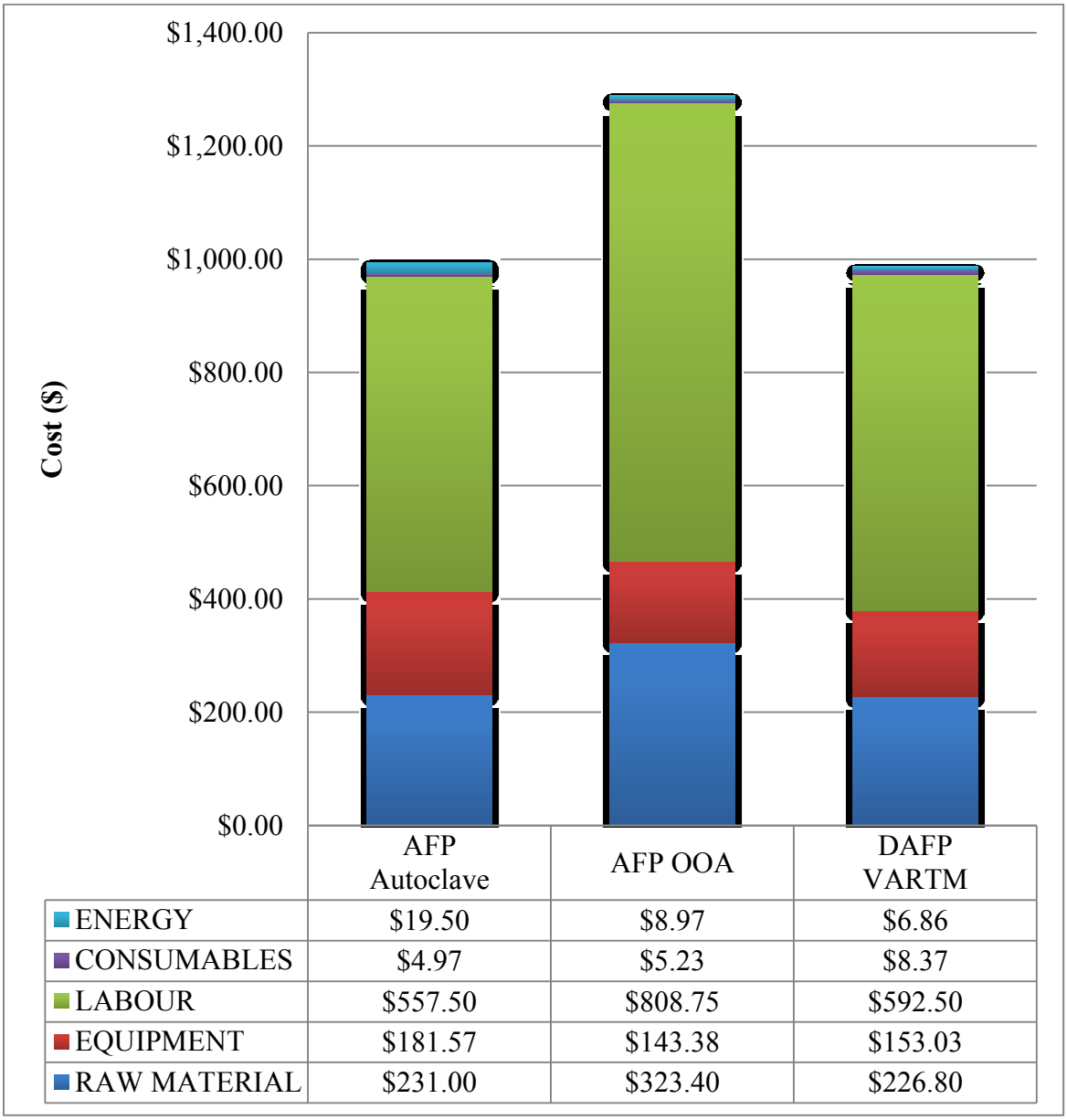

	AFP Autoclave	AFP OOA	DAFP VARTM
ENERGY	$19.50	$8.97	$6.86
CONSUMABLES	$4.97	$5.23	$8.37
LABOUR	$557.50	$808.75	$592.50
EQUIPMENT	$181.57	$143.38	$153.03
RAW MATERIAL	$231.00	$323.40	$226.80

The total sum of manufacturing costs is $994.54, $1,289.73, and $987.57 for AFP of autoclave prepreg, AFP of OOA prepreg, and DAFP VARTM respectively. Subsequent post processing such as trimming, finishing, or non-destructive inspection for all three scenarios is not evaluated as they are assumed to be the same.

5.2. Cost Comparison

In the presented evaluation the outcome shows a reduction of overall cost is for DAFP VARTM of 0.70% and 23.42% compared to AFP manufacturing of autoclave prepreg and OOA prepreg respectively. Both OOA methods of manufacturing show reduction of costs associated with equipment and energy. However these cost reductions seen in OOA prepreg manufacturing is quickly offset by higher raw material costs, and significant increase in labour costs due to longer cure cycle time making it the most costly method of production in this study. As expected in infusion manufacturing, DAFP VARTM shows an increase in costs associated to labour and consumables compared to autoclave prepreg manufacturing. However the lesser costs associated with raw materials, equipment and energy allow DAFP VARTM manufacturing to be comparable in costs with autoclave prepreg.

A significant variable that could not be evaluated in this study is cost savings in tooling associated to OOA manufacturing. The example laminates evaluated in the study simple in geometry and flat. Therefore a same flat aluminum tool is used for all three scenarios. OOA manufacturing has significant benefits as tooling is not required to withstand high pressures (up to 100 psi) in autoclave curing. As OOA manufacturing does not require any external pressure, cost associated to tool manufacturing is significantly reduced as it they do not need to be made of stronger materials or have additional reinforcements. This also results is reduced weight of tooling, which eases transportation of tools within shop floor environments. This would have a large impact on aerospace structures such as fuselages or wing skins, building a stronger business case for OOA prepreg and DAFP VARTM manufacturing.

Lastly, it is previously mentioned that the AFP heat source and laydown speeds in this evaluation are assumed to be constant throughout all manufacturing scenarios. The ADC AFP machine at Concordia University is normally operated between 3-4 inches/sec, as it is not designed or used for mass production. AFP machines in industry are known to be able to operate at laydown speeds of 6.5-13 inches/sec [7]. Evaluation of automated dry fiber preform manufacturing studied in [34] successfully deposit using a laser heat source at a speed of 400 mm/sec (15.75 inches/sec). Recent development in light pulse source heating technology by Heraeus Noblelight

Limited claim to be capable of AFP processing dry fiber tape in excess of 1 meter/sec (39.37 inches/sec) [50]. Advancements in automated dry fiber processing, and utilising heat sources such as laser or light pulse, show to achieve higher deposition speeds when compared to conventional prepreg systems. If these benefits are factored into account, DAFP VARTM manufacturing may show additional reduction in costs due to quicker processing times, which in turn results in reduced labour costs.

Chapter 6 - Conclusion & Outlook

This final chapter concludes the overall works presented in this dissertation. In addition future areas of interest that would merit future examination are proposed.

6.1. Conclusion

The aerospace industry is always on the lookout for new innovations or advancements in materials and manufacturing methods that can increase performance and reliability of their aircrafts. At the same time these new technologies must be capable of demonstrating feasible integration in design and manufacturing, whilst a competitive business case that has potential to bring added value to multiple ranges of products in a cost effective manner.

The works of this dissertation focused on the evaluation of flat carbon/epoxy laminates manufactured by DAFP VARTM throughout its multiple stages. Automated preform manufacturing using HGT as heat source, resin infusion of preforms using hot VARTM, inspection of manufactured laminate quality, evaluation of effects of tailored gaps on the VARTM process, baselining mechanical laminate properties against industry qualified primary structural prepreg materials, as well as a comparative cost analysis have been investigated and discussed.

The presented experimental trials of automated preform manufacturing described the unique challenges of processing dry fiber tapes using AFP with HGT as a heat source. Traditionally dry fiber tapes manufactured by suppliers are intended to be processed using laser as means of heat

source, as thermoplastic veil requires high processing temperatures in order to activate. Prior to this study, no works has been published regarding process window for DAFP utilizing HGT. A trial and error based approach addressed each of these challenges and proved that minor modifications to equipment and tuning processing controls can result in successful automated preform manufacturing of large multi-layered and multi-oriented preforms consistently. As a result a process window for automated dry fiber manufacturing was created using an ADC AFP machine equipped with thermoset head and HGT.

Laminate infusion using hot VARTM technique showed to successfully impregnate laminates of multiple different stacking orientations of up to 24 plies, and with low void content (less than 1%). A conventional for VARTM and bagging technique was used during the impregnation of dry fiber preforms and proved to be satisfactory to manufacture good quality flat laminates.

Mechanical evaluations performed allowed to gain a better understanding of the laminates properties, and their performances were baselined against qualified autoclave prepreg and OOA prepreg systems which have been adopted by aerospace OEM in applications of automated composite manufacturing. DAFP VARTM manufactured panels have shown mechanical properties comparable and in some cases superior to that of the qualified systems. However, mechanical properties that show considerable knockdown in performance are those associated to compression strength. Knockdown in compression properties, such as 0° compression strength or OHC strength could be attributed possible premature cross-linking of resin system, or factors inherit to the DAFP preform manufacturing process.

Lastly, a cost analysis evaluating material costs, consumables, equipment, tooling, energy, and labour associated to DAFP VARTM manufacturing showed to be cost effective manufacturing technique when compared to automated manufacturing of autoclave prepreg and OOA prepreg systems. In addition, DAFP VARTM suggests more potential to reduce costs associated tooling of large composite structures that was not able to be captured evaluating relatively small flat laminates.

6.2. Outlook

The completion of this dissertation has laid out the processing requirements of dry fiber tape and infusion technique for flat carbon/epoxy laminates. The mechanical properties achieved as a result of the processes developed have also been evaluated. The outcome of manufacturing processes, part quality, mechanical properties, and overall costs associate have shown that DAFP VARTM manufacturing is a contender to traditional automated manufacturing of autoclave prepreg and OOA prepreg systems currently adopted by industry. Advancements in academic research, in collaboration with industry partners, will allow for further development and understanding of the technology.

Future work can further investigate the root causes of reduced compression strengths observed in this dissertation. Improvements in preform manufacturing, test specimen layup orientations as well as bagging techniques could be evaluated.

Evaluation of automated manufacturing of more complex shapes and structures such as curved or tubular geometry, as well as sandwich structures using dry fiber preforms and infusion. Core materials such as honeycomb Nomex, or high temperature resistance foams would be of interest.

DAFP of preforms also give the opportunity to infuse with multiple different types of resin systems other than that presented in this dissertation. Resins with faster curing cycles, or without the need for oven cure could be of interest, particularly to industries other than aerospace such as automotive or recreational sports.

Last potential suggested to investigate is other sources of heat source for automated dry fiber processing. An example of light pulse heat technology claims to be capable of processing dry fiber tapes at speed in excess of 1m/sec (39.37 inches/sec) [50]. This would be of great interest to aerospace, automotive and other industries interested in automated manufacturing of composite structures.

Chapter 7 - Contributions

Building Process Window

- For the first time, a process window is developed to successfully manufacture dry fiber carbon preforms using an ADC AFP machine equipped with thermoset head and HGT.
    - Challenges faced with processing dry fiber tapes are outlined and mitigations to each issue are presented.
    - With the parameters and techniques developed large multi-layered (up to 24 plies) and multi-oriented preforms are manufactured successfully without fault.
    - AFP processing speeds and productivity is matched to conventional autoclave prepreg or OOA prepreg systems.

Resin Infusion

- Hot VARTM processing of dry fiber preforms manufactured using AFP has shown to be successful. Preform and resin system show good compatibility, and do not require special processing or bagging techniques for flat laminates.
- Evaluation of effects of tailored gaps of 4mm in dry fiber preforms on the VARTM infusion process show no significant difference between infusions of conventional preforms.

Evaluation of Quality

- Investigation of laminate quality in terms of porosity show to be less than 1%, and fiber volume fraction to be greater than 50% for all manufactured test panels. These are within the desirable ranges of the aerospace industry.

Mechanical Results

- A series of mechanical tests of DAFP VARTM laminates result in mechanical properties that are in the realms of qualified material systems currently used for primary structural applications in the aerospace industry.

Cost Analysis

- A cost analysis evaluating material costs, consumables, equipment, tooling, energy, and labour associated to DAFP VARTM manufacturing showed to be cost effective manufacturing technique when compared to automated manufacturing of autoclave prepreg and OOA prepreg systems.

References

[1] S. V. Hoa, "Automated composites manufacturing," *Science and Engineering of Composite Materials,* p. 113, March 2015.

[2] Composites World, "A350 XWB update: Smart manufacturing," 1 September 2011. [Online]. Available: http://www.compositesworld.com/articles/a350-xwb-update-smart-manufacturing. [Accessed 1 March 2017].

[3] Seattle Times, "Massive, speedy robots ready to build composite wings for Boeing 777X," 5 February 2016. [Online]. Available: http://www.seattletimes.com/business/boeing-aerospace/massive-speedy-robots-ready-to-build-composite-wings-for-boeing-777x/. [Accessed 1 March 2017].

[4] Composites World, "The market for OOA aerocomposites," 4 March 2014. [Online]. Available: http://www.compositesworld.com/articles/the-market-for-ooa-aerocomposites-2013-2022. [Accessed 2 March 2017].

[5] R. Tong, S.V. Hoa, M. Chen, "Cost Analysis on L-shape Composite Component Manufacturing," in *Proceedings of 18th International Conference on composite materials*, 2011.

[6] R.A. Witik et al., "Assessing the economic and environmental potential of out of autoclave processing," in *Proceedings of 18th International Conference on composite materials*, Jeju Island, 2011.

[7] D. Lukaszewicz. C. Ward, K. Potter, "The engineering aspects of automated prepreg layup: History, present and future," *Composites Part B: Engineering,* vol. 43, no. 3, pp. 997-1009, 2011.

[8] Compostes World, "The Markets: Aerospace (2015)," 12 1 2015. [Online]. Available: http://www.compositesworld.com/articles/the-markets-aerospace-2015. [Accessed 1 April 2017].

[9] J. Sloan, "ATL and AFP: Defining the megatrends in composite aerostructures," Composites World, 30 June 2008. [Online]. Available: http://www.compositesworld.com/articles/atl-and-afp-defining-the-megatrends-in-composite-aerostructures. [Accessed 25 August 2017].

[10] Electroimpact, "Composite Manufacturing," Electroimpact Inc., 2017. [Online]. Available: https://www.electroimpact.com/Products/Composites/Overview.aspx. [Accessed 28 August 2017].

[11] Automated Dynamics, "Automation Equipment: Media Galleries," 2017. [Online]. Available: http://www.automateddynamics.com/automation-equipment. [Accessed 28 August 2017].

[12] K. K. Subramanian, "Why carbon fiber is preferred for aircraft bodies?," Quora, 9 March 2017. [Online]. Available: https://www.quora.com/Why-carbon-fiber-is-preferred-for-aircraft-bodies. [Accessed 28 August 2017].

[13] D. Dawson, "Automation: Robots taking off in commercial aircraft," Composites World, 26 February 2016. [Online]. Available: http://www.compositesworld.com/articles/automation-robots-taking-off-in-commercial-aircraft. [Accessed 28 August 2017].

[14] G. Gardiner, "Out-of-Autoclave prepregs: Hype or Revolution?," Composites World, 1 Jan 2011. [Online]. Available: http://www.compositesworld.com/articles/out-of-autoclave-prepregs-hype-or-revolution. [Accessed 22 August 2017].

[15] T. Centea, L.K. Grunenfelder, S.R. Nutt, "A review of out-of-autocalve prepregs - Material properties, process phenomena, and manufacturing considerations," *Composites Part A: Applied Science and Manufacturing,* vol. 70, no. 2015, pp. 123-154, 2015.

[16] S. V. Hoa, Principles of the Manufacturing of Composite Materials, Montreal: DEStech Publications, 2017.

[17] Owens Corning, "Multiaxial Non-Crimp Fabric (NFC) Reinforcements," February 2014. [Online]. Available: https://dcpd6wotaa0mb.cloudfront.net/mdms/dms/CSB/10018955/10018955-%E2%80%93-Multiaxial-NCF-brochure.pdf. [Accessed 23 August 2017].

[18] S. V. Lomov, Non-Crimp Fabric Composites: Manufacturing, Properties and Application, Cambridge: Woodhead Publishing Limited, 2011.

[19] G.A. Bibo, P.J. Hogg, M. Kemp, "Mechanical Characterization of Glass and Carbon Fiber Reinforced Composite made with Non-Crimp Fabrics," *Composite Science and Technology,* vol. PII, no. 57, pp. 1221-1241, 1997.

[20] G. Gardiner, "CSeries Composite Wing," Composites World, 14 October 2013. [Online]. Available: http://www.compositesworld.com/blog/post/cseries-composite-wing. [Accessed 23 August 2017].

[21] Bombardier Aerospace, *CSeries - Transonic Wing,* Belfast: YouTube, 2013.

[22] G. Marsh, "Bombardier throws down the gauntlet with CSeries airliner," *Reinforced Plastics,* vol. 55, no. 6, pp. 22-26, 2011.

[23] X. Song, "Vacuum Assisted Resin Transfer Molding (VARTM): Model Development and Verification," Ph.D. dissertation, Virginia Polytechnic Institute and State University, Blacksburg, 2003.

[24] L. Aktas, D.P. Bauman, S.T. Bowen, M. Saha, M.C. Altan, "Effect of Distribution Media Length and Multiwalled Carbon Nanotubes on the Formation of Voids in VARTM Composites," *Journal of Engineering Materials and Technology,* vol. 133, no. 4, pp. 1-9, 14 October 2011.

[25] Mitsubishi Heavy Industies Ltd., "Research in the Application of the VaRTM Technique to the Fabrication of Primary Aircraft Composite Structures," *Mitsubishi Heavy Industies Technical Review,* vol. 42, no. 5, 2005.

[26] NLR, "NLR wins award for new fiber placement processes," 30 January 2012. [Online]. Available: http://www.nlr.org/news/nlr-wins-award-for-new-fibre-placement-processes/. [Accessed 13 September 2017].

[27] NLR Aerospace, "AUTOW: Automated Preform Fabrication by Dry Tow Placement," January 2009. [Online]. Available: https://trimis.ec.europa.eu/sites/default/files/project/documents/20120519_102727_52292_autow.pdf. [Accessed 15 Dec 2017].

[28] European Commission, "Community Research and Development Information Service," 25 May 2017. [Online]. Available: http://cordis.europa.eu/project/rcn/91195_en.html. [Accessed 14 September 2017].

[29] M. Belhaj et al., "Dry fiber automated placement of carbon fibrous preforms," *Elsevier,* vol. Composites: Part B, pp. 107-111, 2013.

[30] R. Graupner, "Presentations: LCC-symposium," 24 October 2014. [Online]. Available: http://www.lcc.mw.tum.de/en/5th-anniversary-of-lcc/symposium/presentations/. [Accessed 1 November 2017].

[31] O. Rimmer, D. Becker, P. Mitschang, "Maximizing the out-of-plane-permeability of preforms manufactured by dry fiber placement," *Polymer & Composite Science,* vol. 2, no. 3-4, pp. 93-102, 2016.

[32] Hexcel, "HiTape: A new efficient composite solution for Primary Aircraft Structures," 2018. [Online]. Available: http://www.hexcel.com/user_area/content_media/raw/HiTape.pdf. [Accessed 26 February 2018].

[33] G. Dell'Anno et al., "Automated manufacture of 3D reinforced aerospace composite structures," *International Journal of Structural Integrity,* vol. 3, no. 1, pp. 22-40, 2012.

[34] L. Veldenz et al., "Characteristics and Processability of Bindered Dry Fiber Material for Automated Fiber Placement," in *17th European Conference on Composite Materials*, Munich, 2016.

[35] R. L. Pinckney, "Fabrication of the V-22 composite aft fuselage using automated fiber placement," 1993. [Online]. Available: https://ntrs.nasa.gov/archive/nasa/casi.ntrs.nasa.gov/19930021254.pdf. [Accessed 24 August 2017].

[36] Hexcel, "HexTow IM7 Carbon Fiber," Hexcel, 2016. [Online]. Available: http://www.hexcel.com/user_area/content_media/raw/IM7_HexTow_DataSheet.pdf. [Accessed 1 September 2017].

[37] Cytec Industries, "PRISM™ EP2400 RESIN SYSTEM," 12 March 2012. [Online]. Available: https://www.cytec.com/sites/default/files/datasheets/PRISM_EP2400_031912.pdf. [Accessed 1 January 2017].

[38] Brookfield Ametek, "Brookfield CAP 2000+ Operating Instructions," [Online]. Available: http://www.brookfieldengineering.com/-/media/ametekbrookfield/manuals/lab%20viscometers/cap2000%20instructions.pdf?la=en. [Accessed 15 July 2017].

[39] Epoxy Technology Inc., "Tg-Glass Transition Temperature for Epoxies," 2012. [Online]. Available: http://www.epotek.com/site/files/Techtips/pdfs/tip23.pdf. [Accessed 27 July 2017].

[40] PerkinElmer, "Dynamic MEchanical Analysis (DMA): A Beginner's Guide," 2013. [Online]. Available: http://www.perkinelmer.ca/CMSResources/Images/44-74546GDE_IntroductionToDMA.pdf. [Accessed 5 August 2017].

[41] C.F. Bandeira et al., "Comparison of Glass Transition Temperature Values of Composite Polymer Obtained by TMA and DSC," *Applied Mechanics and Materials,* Vols. 719-720, pp. 91-95, 2015.

[42] TA Instruments, "Interpreting Unexpected Events and Transitions in DSC Results," [Online]. Available: http://www.tainstruments.com/pdf/literature/TA039.pdf. [Accessed 1 August 2017].

[43] National Institute for Aviation Research, "Hexcel 8552 IM& Unidirectional Prepreg," Wichita State University, Wichita, 2011.

[44] M. Scafè et al., "Experimental determination of compressive strength of an unidirectional composite lamina: indirect estimate by Using Back-out Factor (BF)," in *Convegno Nazionale IGF XXII*, Rome, 2013.

[45] HEXCEL, "HexPly 8552 Epoxy Matrix," Hexcel, 2014.

[46] Cytec Industies, "CYCOM 5320-1 Epoxy Resin System," October 2015. [Online]. Available: https://www.cytec.com/sites/default/files/datasheets/CYCOM%205320-1%20Rev%20CR5.pdf. [Accessed 8 August 2017].

[47] CHM-17, COMPOSITE MATERIALS HANDBOOK: VOLUME 1 POLYMER MATRIX COMPOSITES GUIDELINES FOR CHARACTERIZATION OF STRUCTURAL MATERIALS, SAE International, 2012.

[48] Control Panels Incorporated, "Blue M Lo-850 Lab Oven, 30 cu. ft.," 2018. [Online]. Available: http://www.cpiheat.com/Blue-M-Lab-Ovens-p/881011.htm. [Accessed 11 February 2018].

[49] Fiberglass Supply, "Carbon Fiber and Composite Supplies," [Online]. Available: http://www.fiberglasssupply.com/Product_Catalog/Vacuum_Bagging/vacuum_bagging.html. [Accessed 9 January 2018].

[50] Heraeus, "Intelligent heat for Automated Fibre Placement," in *proceedings of International Symposium on Automated Composites Manufacturing (ACM4)*, Montreal, 2017.